

Aus dem Dr. von Haunerschen Kinderspital
Klinik der Universität München

Vorstand: Prof. Dr. Dr. Christoph Klein

Induction of T-cell attack against ALL through a TIM-3-CD28 fusion receptor

Dissertation zum Erwerb des Doktorgrades der
Medizin an der Medizinischen Fakultät der
Ludwig-Maximilians-Universität zu München

vorgelegt von Eva Kristina Ortner

aus
München

Jahr

2023

**Mit Genehmigung der Medizinischen Fakultät
der Universität München**

Berichterstatter: Prof. Dr. Tobias Feuchtinger

Mitberichterstatter: Prof. Dr. Andreas Humpe

Prof. Dr. Sebastian Kobold

Prof. Dr. Louisa von Baumgarten

Mitbetreuung durch den

promovierten Mitarbeiter: Dr. med. Franziska Blaeschke, PhD

Dekan: Prof. Dr. med. Thomas Gudermann

Tag der mündlichen Prüfung: 19.01.2023

Eidesstaatliche Versicherung / Affidavit

Hiermit versichere ich an Eides statt, dass ich die vorliegende Dissertation „Induction of T-cell attack against ALL through a TIM-3-CD28 fusion receptor“ selbstständig angefertigt habe, mich außer der angegebenen keiner weiteren Hilfsmittel bedient und alle Erkenntnisse, die aus dem Schrifttum ganz oder annähernd übernommen sind, als solche kenntlich gemacht und nach ihrer Herkunft unter Bezeichnung der Fundstelle einzeln nachgewiesen habe.

Ich erkläre des Weiteren, dass die hier vorgelegte Dissertation nicht in gleicher oder in ähnlicher Form bei einer anderen Stelle zur Erlangung eines akademischen Grades eingereicht wurde.

I hereby confirm that the dissertation “Induction of T-cell attack against ALL through a TIM-3-CD28 fusion receptor“ is the result of my own work and that I have only used sources or materials listed and specified in the dissertation.

München / Munich, 23.01.2023

Ort, Datum / Place, Date

Eva Ortner

Unterschrift / Signature

Danksagung

An dieser Stelle möchte ich mich bei nachstehenden Personen bedanken, die mich bei dieser Arbeit maßgeblich unterstützt haben.

Insbesondere danke ich meinem Doktorvater Herrn Prof. Dr. med. Tobias Feuchtinger, für die Möglichkeit, diese Promotion unter seiner Aufsicht durchführen zu können sowie für seine exzellente Betreuung und herausragende Förderung.

Frau Dr. med. Franziska Blaeschke danke ich für ihre hervorragende Mitbetreuung, ihre Hilfsbereitschaft und wissenschaftliche Unterstützung, ohne die die Fertigstellung der Promotion nicht möglich gewesen wäre. Auch für die Durchsicht und Mitkorrektur dieser Arbeit möchte ich mich bedanken.

Ich möchte mich bei meiner gesamten Arbeitsgruppe für die freundschaftliche Arbeitsatmosphäre bedanken. Mein besonderer Dank gilt Frau Dana Stenger für ihre enorme Hilfsbereitschaft und Geduld sowie die Mitkorrektur dieser Arbeit.

Während meiner Promotion erhielt ich ein Promotionsstipendium der Kind-Philipp-Stiftung für pädiatrisch-onkologische Forschung. Ich danke der Stiftung für die finanzielle Unterstützung, die es mir ermöglichte, mich vollkommen auf mein Forschungsvorhaben zu konzentrieren.

Meinem Freund Christoph Clement danke ich für seine liebevolle und bedingungslose Unterstützung.

Mein besonderer Dank gilt meinen Eltern, Petra und Peter Ortner, sowie meinen Großeltern, Rose-Marie Ulmer und Gertrud Ortner, welche mir meinen bisherigen Lebensweg ermöglicht haben und denen ich diese Arbeit widme.

Table of Contents

1	Abbreviations.....	7
2	Introduction.....	9
2.1	Acute lymphoblastic leukemia.....	9
2.1.1	Risk stratification	9
2.1.2	Therapy	10
2.2	CAR T-cell therapy for B-cell precursor ALL	11
2.2.1	CAR T-cell engineering.....	11
2.2.2	Challenges of CAR T-cell therapy.....	13
2.2.3	Resistance to CAR T-cell therapy.....	14
2.3	Role of inhibitory molecule TIM-3.....	15
3	Aim of the study.....	17
4	Material.....	18
4.1	Equipment and software	18
4.2	Solutions, media, and sera for cell culture	19
4.3	Consumables	21
4.4	Antibodies.....	22
5	Methods.....	24
5.1	CAR T-cell generation	24
5.1.1	PBMC isolation and T-cell activation.....	24
5.1.2	Virus generation	24
5.1.3	Retroviral CAR T-cell transduction.....	24
5.1.4	Functionality assays	25
5.1.5	Cytotoxicity assay.....	25
5.1.6	Intracellular cytokine stain (ICS)	26
5.1.7	Activation assay.....	26
5.1.8	Proliferation assay	26
5.1.9	Phenotype assays	26
5.1.10	CD3 coating assays.....	26

5.2	Transduction of cell lines	27
5.3	General cell culture.....	27
5.4	Flow cytometry	28
5.5	Statistical analysis	28
6	Results	29
6.1	Retroviral transduction enables stable overexpression of TIM-3 in CAR T cells.....	29
6.2	CAR T-cell killing capacity is scarcely influenced by TIM-3 expression but is diminished in presence of TIM-3 ligand CEACAM.....	33
6.3	TIM-3 expression is associated with reduced CAR T-cell functionality in vitro	35
6.4	Retroviral transduction of T cells with TIM-3/CD28 fusion receptor constructs.....	39
6.5	TIM-3/CD28 fusion receptor-transduced T cells exhibit similar expansion rates, viability and phenotype	42
6.6	Functional comparison of TIM-3/CD28 fusion receptor-transduced T cells reveals high activation potential in accordance with CD28 proportion in the construct.....	44
6.7	Generation of CD19 CAR T cells incorporating TIM-3/CD28 fusion receptor constructs with superior activation potential.....	47
6.8	CAR T cells with a TIM-3/CD28 fusion receptor show comparable expansion rates and viability	49
6.9	TIM-3/CD28 fusion receptor CAR T cells undergo comparable differentiation of phenotype upon contact with CD19-positive target cells	51
6.10	Combination of first generation CAR T cells with a TIM-3/CD28 fusion receptor leads to augmented functionality against CEACAM-positive cell line	53
6.11	Second generation CAR T cells with a TIM-3/CD28 fusion receptor show marginal functional advantages over conventional CAR T cells	56
7	Discussion	60
7.1	TIM-3 expression coincides with CAR T-cell exhaustion.....	60
7.2	TIM-3 is associated with impaired CAR T-cell functionality	61
7.3	Overcoming TIM-3-mediated CAR T-cell suppression	62
7.4	Identification of a superior TIM-3/CD28 fusion receptor	62
7.5	TIM-3/CD28 fusion receptors restore CAR T-cell functionality	63
7.6	Clinical application of CAR T cells with a TIM-3/CD28 fusion receptor.....	65
8	Summary	66

9	Zusammenfassung	67
10	Literature	69
11	Supplements.....	74
11.1	Primer sequences.....	74
11.2	T-cell sequences	74
11.2.1	Sequence of 19_3z CAR	74
11.2.2	Sequence of 19_3z_28-TM2 CAR	75
11.2.3	Sequence of 19_3z_28-TM3 CAR	76
11.2.4	Sequence of 19_3z_TIM-3 CAR	77
11.2.5	Sequence of 19_BB_3z CAR.....	78
11.2.6	Sequence of 19_BB_3z_28-TM2 CAR	79
11.2.7	Sequence of 19_BB_3z_28-TM3 CAR	80
11.2.8	Sequence of 19_BB_3z_TIM-3 CAR	81
11.2.9	Sequence of 19t CAR	82
11.2.10	Sequence of 28-TM1 fusion receptor.....	83
11.2.11	Sequence of 28-TM2 fusion receptor.....	83
11.2.12	Sequence of 28-TM3 fusion receptor.....	84
11.2.13	Sequence of 8-TM fusion receptor.....	84
11.2.14	Sequence of TIM3t construct.....	85
11.2.15	Sequence of TIM3-TM1 fusion receptor.....	85
11.2.16	Sequence of TIM3-TM2 fusion receptor.....	85
11.3	Vector maps	86
11.3.1	Vector map of pMP71	86
11.3.2	Vector map of gag/pol (pcDNA3.1-MLV-g/p).....	87
12	Appendix	88
12.1	Publications	88

1 Abbreviations

Abbreviation	Name
ALL	Acute lymphoblastic leukemia
19_3z	First generation CAR with intracellular CD3 ζ stimulatory domain
19_3z_28-TM2	First generation CAR with 28-TM2 fusion receptor
19_3z_28-TM3	First generation CAR with 28-TM3 fusion receptor
19_3z_TIM-3	First generation CAR with intracellular CD3 ζ stimulatory domain and TIM-3
19_BB_3z	Second generation CAR with intracellular CD3 ζ stimulatory domain and 4-1BB costimulatory domain
19_BB_3z_28-TM2	Second generation CAR with 28-TM2 fusion receptor
19_BB_3z_28-TM3	Second generation CAR with 28-TM3 fusion receptor
19_BB_3z_TIM-3	Second generation CAR with intracellular CD3 ζ stimulatory domain, 4-1BB costimulatory domain and TIM-3
19t	Control CAR without the CD3 ζ stimulatory domain
28-TM1	TIM-3/CD28 fusion receptor with CD28 transmembrane domain
28-TM2	TIM-3/CD28 fusion receptor with CD28 transmembrane domain
28-TM3	TIM-3/CD28 fusion receptor with CD28 transmembrane domain
8-TM	TIM-3/CD28 fusion receptor with CD8 transmembrane domain
AML	Acute myeloid leukemia
B-ALL	B-cell precursor ALL
Bcl-2	B-cell lymphoma 2
Bcl-xL	B-cell lymphoma-extra large
CAR	Chimeric antigen receptor
CD	Cluster of differentiation
CEACAM	Carcinoembryonic antigen cell adhesion molecule 1
CLL	Chronic lymphocytic leukemia
CR	Complete remission
CRS	Cytokine-release syndrome
DMSO	Dimethyl sulfoxide
DNA	Deoxyribonucleic acid
E: T	Effector to target
EC	Extracellular
EMA	European Medicines Agency
FBS	Fetal bovine serum
FC	Fold change
FDA	U.S. Food and Drug Administration
GMP	Good manufacturing practice
HMGB1	High-mobility group box 1
HSA	Human serum albumin
HSCT	Hematopoietic stem-cell transplantation
IC	intracellular
ICS	Intracellular cytokine stain
IFN- γ	Interferon γ

IKZF1	Ikaros family zinc finger protein 1
IL	Interleukin
KMT2A	Histone-lysine N-methyltransferase 2A
LAG-3	Lymphocyte-activation gene 3
MFI	Mean fluorescence intensity
MRD	Minimal residual disease
NK cells	Natural killer cells
NKT cells	Natural killer T cells
PBMC	Peripheral blood mononuclear cell
PBS	Phosphate buffer saline
PCR	Polymerase-chain-reaction
PD-1	Programmed death-ligand 1
PD-L1	Programmed cell death protein 1
scFv	Single-chain variable fragment
SD	Standard deviation
SEB	Staphylococcus enterotoxin B
T _{CM}	Central memory T cells
T _{EFF}	Effector T cells
T _{EM}	Effector memory T cells
TET2	Tet methylcytosine dioxygenase 2
TIM-3	T cell immunoglobulin and mucin domain 3
TIM3t	truncated TIM-3 construct without the intracellular signaling domain
TIM3-TM1	TIM-3/CD28 fusion receptor with TIM-3 transmembrane domain
TIM3-TM2	TIM-3/CD28 fusion receptor with TIM-3 transmembrane domain
TM	Transmembrane
T _N	Naive T cells
TNF- α	Tumor necrosis factor α
T _{SCM}	Stem cell-like memory T cells

2 Introduction

2.1 Acute lymphoblastic leukemia

Malignant neoplasms represent the third leading cause of death for children and adolescents in developed countries.¹ Most frequently, death from cancer is caused by acute lymphoblastic leukemia (ALL). In the United States, ALL has an approximate incidence of 30 cases per million children aged 0-14, thus rendering it the most common pediatric malignancy.²

Children suffering from ALL often show clinical signs of anemia, thrombocytopenia, and neutropenia that result from bone marrow infiltration of leukemic blasts. Additional symptoms such as hepatosplenomegaly may develop from infiltration of other organs.³

Although certain genetic and environmental factors are associated with an increased risk for ALL, the cause for development of leukemia remains unknown in most patients.³ On a molecular level, several genetic mutations in lymphoid progenitor cells have been identified as a cause of ALL. Most commonly, genetic alterations arise in genes involved in RAS signaling, lineage development, epigenetic regulation, and the p53/cell-cycle pathway.⁴ Depending on the origin of the malignant clone and respective lineage marker expression, leukemic blasts derive from B-cell or T-cell progenitor cells. 85% of patients suffer from B-cell precursor ALL (B-ALL), which is characterized through expression of B-cell lineage markers.³

2.1.1 Risk stratification

Clinical presentation, genetic mutations, and treatment response can stratify patients into different risk groups, thus allowing for individual prognosis and adequate intensity of therapy. Patients are considered to be at high risk when they have high white blood-cell count $\geq 50 \times 10^9/l$, show lymphoblastic infiltration of the central nervous system, and are over 10 years of age at diagnosis.⁵ Adverse cytogenetics include KMT2A rearrangement and mutations of IKZF1, as well as hypodiploidy with less than 44 chromosomes.⁶ However, previous studies have shown that level of minimal residual disease (MRD) after induction therapy is the most significant variable in risk stratification.⁷ Level of MRD is measured via polymerase-chain-reaction (PCR) amplification of altered genes or assessed by flow-cytometric detection of leukemia-specific markers on blasts.³ Newer methods include multidimensional flow cytometry as well as high-throughput sequencing and enable detection of one leukemic blast in 1×10^5 cells.⁸

2.1.2 Therapy

Over the past 50 years, survival rates of pediatric ALL have improved dramatically (Figure 1). In 1968, combination chemotherapy achieved high initial response rates of 87% but relapses occurred frequently and median survival was only 2.6 years during a follow-up time of 3 years.⁹ In contrast, recent clinical studies have shown overall survival rates of up to 95% for pediatric B-ALL.³

The immense improvement of outcome for children suffering from ALL was realized through advances in therapy. Most patients are enrolled in clinical trials and treated according to similar protocols, based on four phases of chemotherapy.³ Induction phase includes administration of a glucocorticoid, vincristine, and asparaginase during a period of 4 to 6 weeks. Induction therapy achieves remission in 98% of patients, but consolidation therapy is obligatory to attain sustainable remission.¹⁰ Therefore, patients receive intensive chemotherapy consisting of repeated methotrexate infusions, followed by administration of folinic acid. Consolidation phase typically lasts 4 to 12 weeks. Finally, maintenance therapy aims at continuous remission and is applied over an extended period (months to years). Maintenance therapy involves oral application of low-intensity therapeutics, usually anti-metabolites such as mercaptopurine. Although highly effective, chemotherapy causes a variety of toxicities and must, therefore, be supplemented with adequate supportive care in all stages of therapy. Cranial radiation remains a therapeutic option for children with overt CNS disease, whereas hematopoietic stem-cell transplantation (HSCT) is used as primary therapy for few high-risk patients or, more commonly, after relapse.^{3,11} In addition, immunotherapy is becoming increasingly established in treatment protocols for relapsed patients, as both monoclonal antibodies and the CD19/CD3-bispecific T-cell engager Blinatumomab have shown promising results in patients with relapsed or refractory ALL.^{3,12}

While survival rates for standard-risk patients have been approaching 90%, survival remains poor for children with relapsed or refractory ALL. 10-15% of patients relapse and an additional 2% remain refractory after induction therapy.^{10,13} As recently demonstrated by the group of Sun et al., chances of achieving complete remission (CR) diminish with every relapse, from 51% CR rates after a second treatment attempt down to 31% after the fourth.¹⁴ The 2-year event-free survival ranged from 13% to 41% in patients after multiple therapy attempts, portraying a dismal prognosis.¹⁴ Another meta-analysis estimated 10-year survival rates of 32% in refractory ALL patients.¹⁰ Thus, the need to provide a cure for these children sparked the search for new concepts in treatment of ALL.

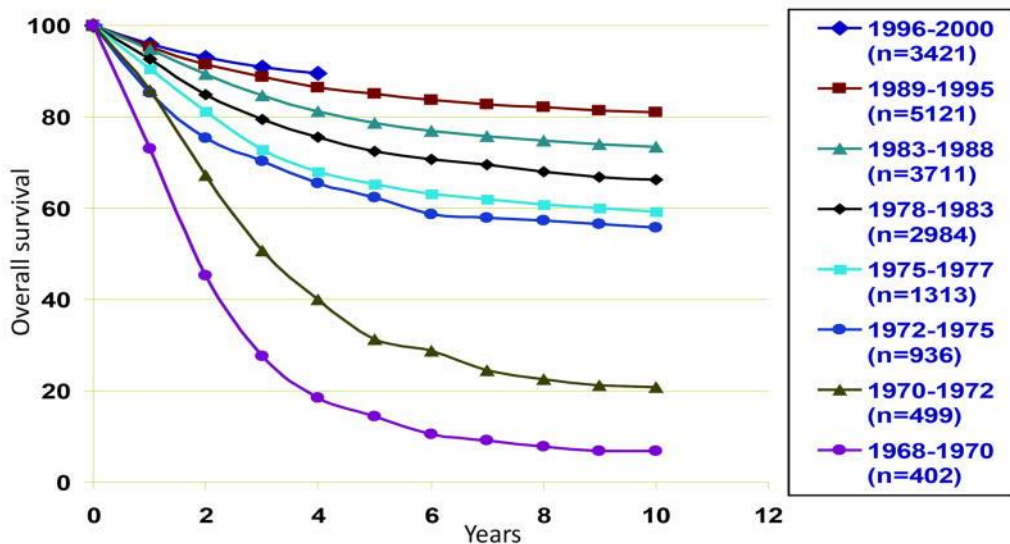


Figure 1: Outcome of pediatric ALL in clinical trials. Over the past 50 years, 10-year survival rates for pediatric ALL have improved from a mere 10% in 1968 to over 90% in 2000 (Figure adapted from Cooper et al., *Pediatr Clin North Am*, 2015).

2.2 CAR T-cell therapy for B-cell precursor ALL

Adoptive transfer of chimeric antigen receptor (CAR) redirected T cells has shown unprecedented success in treatment of relapsed pediatric B-ALL.

A recently published, multi-center phase II trial observed an overall remission rate of 81% and an overall survival rate of 76% at 12 months after CAR T-cell infusion.¹⁵ Previous studies showed 93% of children achieving CR following CAR T-cell therapy.¹⁶ In light of the tremendous results, the FDA (U.S. Food and Drug Administration) and later EMA (European Medicines Agency) approved the anti-CD19 CAR T-cell therapy Tisagenlecleucel for treatment of children with relapsed or refractory B-ALL.¹⁷

2.2.1 CAR T-cell engineering

CARs are synthetically engineered receptors that redirect specificity of a cell by targeting surface molecules.¹⁸ CARs recognize targets via an antibody-derived single-chain variable fragment (scFv), which allows for HLA-independent engagement of the receptor. Upon antigen recognition, CARs provide a stimulatory signal by intracellular signaling domains, which differ in their composition depending on the generation of the CAR (Figure 2) First generation CARs incorporate a single CD3 ζ -derived intracellular domain, whereas second generation CARs contain an additional co-stimulatory domain, usually derived from 4-1BB or CD28. Clinical studies commonly use second generation CAR constructs as they have been associated with greater T-cell persistence.¹⁹ Third and fourth generation CARs are designed with two or three co-stimulatory signaling domains,

respectively. Additional variables in CAR design are the transmembrane and hinge region, which are usually derived from CD28 or CD8 α .²⁰

Clinical manufacturing of CAR T cells is accomplished by integration of the genetically engineered CAR into patient-derived T cells in vitro, subsequent expansion, and finally, re-infusion of the T-cell product into the patient (Figure 3).²¹ Application of allogenic, donor-derived CAR T cells is currently investigated.²² The CAR is usually introduced into previously activated T cells by lentiviral or γ -retroviral transduction.

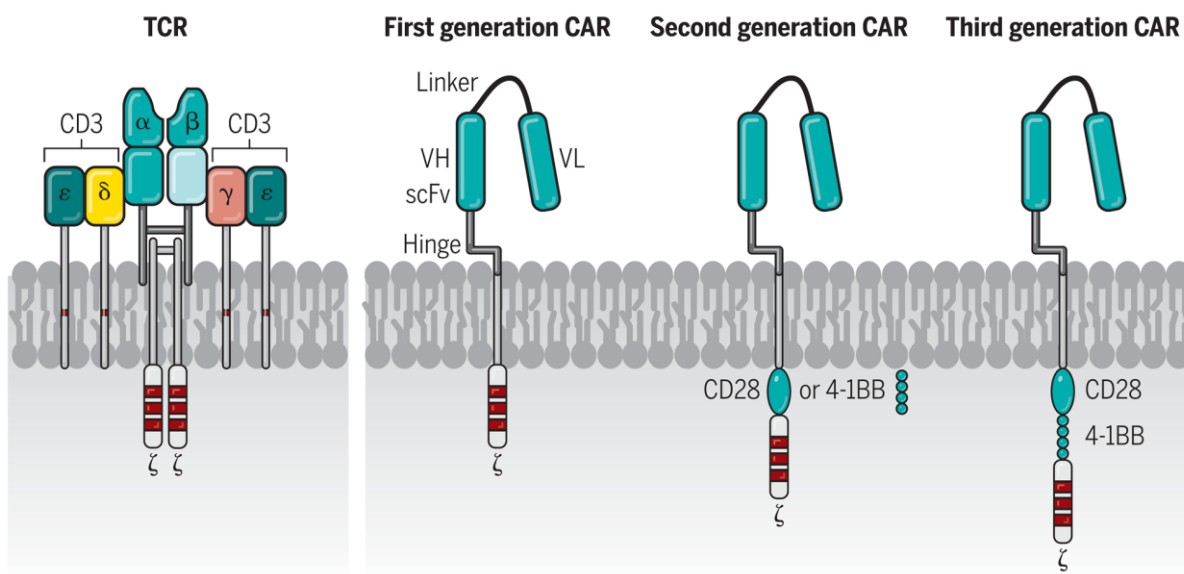


Figure 2: Structure of the T-cell receptor (TCR) in comparison to different CAR designs. The TCR is a heterodimeric molecule that is associated with the invariant CD3 complex and recognizes targets via HLA-bound peptides. In contrast, CARs engage targets independent from HLA and transfer an activating signal via a CD3 ζ intracellular domain and optional co-stimulatory domains (Figure adapted from June et al., Science, 2018).

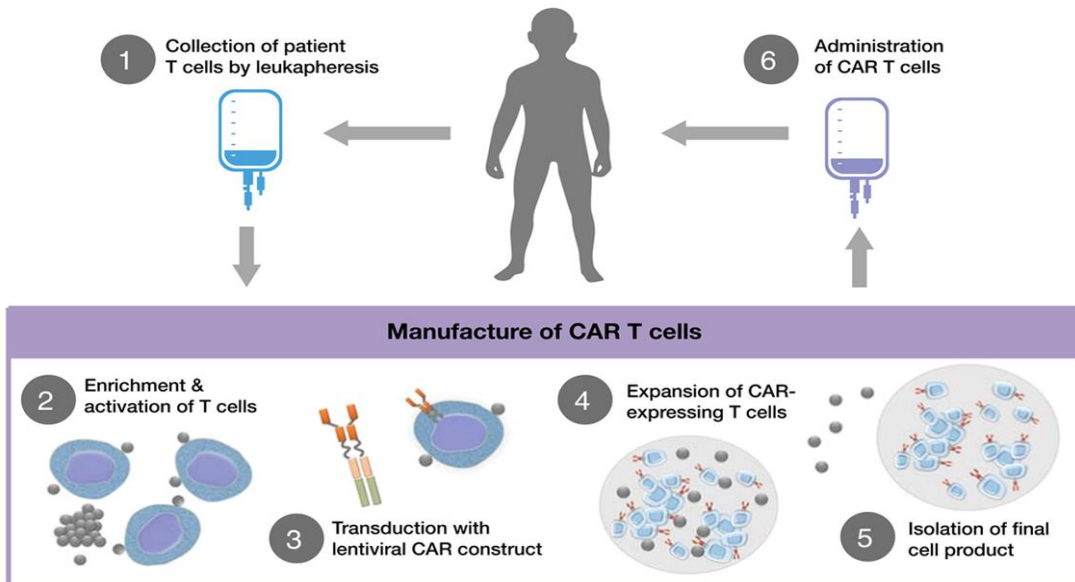


Figure 3: Clinical manufacturing of CAR T cells. T cells are isolated from the patient's leukapheresis product, retrovirally or lentivirally transduced with the CAR and subsequently expanded in vitro. CAR T cells are then reinfused into the patient (Figure adapted from Hucks and Rheingold, Blood Cancer J, 2019).

2.2.2 Challenges of CAR T-cell therapy

Therapy with genetically modified T cells imposes the risk of insertional mutagenesis. In a recently reported case, insertion of the CAR caused disruption of the *TET2* gene and subsequent clonal expansion of *TET2*-deficient CAR T cells.²³ Although *TET2*-disrupted CAR T cells ultimately showed a favorable phenotype and provoked CR in the patient, the study emphasized the possibility of CAR insertion into various, potential oncogenetic loci and subsequent expansion of malignant CAR T-cell clones. Furthermore, safety of CAR T-cell therapy heavily depends on transduction process, as recently demonstrated by the group of Ruella et al. They reported a case, where a single leukemic B cell was unintentionally transduced during CAR T-cell manufacturing, ultimately resulting in the patient relapsing from CAR-expressing leukemia that had gained resistance through masking of the CD19 epitope.²⁴

Notably, CAR T-cell therapy may impose various side effects on patients. As CD19 is uniformly expressed on B cells, infusion of anti-CD19 CAR T cells causes B-cell aplasia in patients, thus rendering them more susceptible to opportunistic infections. Moreover, cytokine-release syndrome (CRS) and neurotoxicity are common side effects of CAR T-cell therapy. Often developing within days after infusion, CRS is a systemic inflammatory response with varying symptoms, which is caused by predominantly monocyte-derived IL-1 and IL-6 secretion.²⁵ In their phase II study, Maude et al. reported CRS in 77% of patients and another 40% of patients experienced late-onset neurotoxicity, typically appearing days after CRS.¹⁵ Treatment of CRS involves IL-6 blockade via Tocilizumab, although a recent model suggests that the IL-1 receptor antagonist Anakinra might be able to abolish both CRS and neurotoxicity.^{25,26}

2.2.3 Resistance to CAR T-cell therapy

Despite high initial response rates, approximately 50% of ALL patients relapse after CAR T-cell therapy.¹⁵ Therefore, new approaches in CAR T-cell therapy focus on investigating the mechanisms behind resistance and attaining more durable remission.

Analyzes of CD19 expression on blasts at the time of relapse revealed that relapse may result from a CD19-negative status and therefore, antigen escape of the tumor.¹⁷ Recently published data suggest various mechanisms responsible for CD19-negative relapse. Sotillo et al. reported cases of alternative splice variants of CD19, leading to lack of recognition by commonly used scFvs FMC63 and SJ25C1 or loss of surface expression.²⁷ Another group observed lineage switching with acquisition of a CD19-negative myeloid phenotype in blasts following CAR T-cell therapy.²⁸ As recent publications introduced an equally successful anti-CD22 CAR construct as well as CD19/CD20-bispecific CAR T cells, combinatorial targeting of multiple antigens could potentially overcome relapses due to single-antigen loss.^{29–31} Yet, the exact incidence of CD19-negative relapse has not been sufficiently assessed and seems to vary in different clinical trials, depending on patient population, CAR construct, and follow-up time.^{15,16,28,32–37}

Furthermore, the results of Maude et al. underline the importance of CAR T-cell persistence for clinical response and sustained remission.¹⁵ Consequently, current efforts aim at improving CAR design in order to achieve prolonged persistence of CAR T cells.^{38,39} Since clinically used CARs contain murine scFvs, immune-mediated rejection of the CAR may promote loss of CAR T cells. Therefore, development of a novel, fully humanized anti-CD19 scFv could enhance CAR T-cell persistence and is currently under clinical investigation.⁴⁰

Moreover, resistance to CAR T-cell therapy may evolve from intrinsic T-cell dysfunction, characterized by phenotypical differentiation and expression of exhaustion markers (Figure 4). Intrinsic fitness of T cells was identified as the most significant factor for response to CAR T-cell treatment in chronic lymphocytic leukemia (CLL), as CAR T cells from responding patients exhibited a memory-like phenotype and gene signature.⁴¹ A similar analysis in ALL patients receiving CAR T-cell therapy revealed that early treatment failure is associated with a dysfunctional phenotype and, importantly, with the expression of co-inhibitory molecules PD-1, LAG3, and TIM-3.⁴²

Our group could equally demonstrate increased expression of PD-1 and TIM-3 in T cells upon treatment with Blinatumomab, a CD19/CD3-bispecific T-cell engager.⁴³ Since PD-L1 was simultaneously elevated in leukemic blasts and antibody-based blockade of the PD-1/PD-L1 axis could restore anti-leukemic effects, this underlines the benefit of checkpoint blockade in combination with anti-CD19-based immunotherapy. Investigation on the role of PD-1 in CAR T-cell functionality confirmed increased anti-tumor responses in PD-1 deficient CAR T cells, further emphasizing the importance of exhaustion on CAR T-cell functionality.⁴⁴ Notably, combination of checkpoint blockade

with anti-CD19 CAR T-cell therapy showed promising results in recent publications.^{45,46} In patients with poor initial response, PD-1 blockade could re-initiate anti-leukemic effects of CAR T-cells, ultimately resulting in improved outcome. Hence, there is an increasing rationale for targeting other co-inhibitory molecules to improve CAR T-cell functionality against pediatric B-ALL.

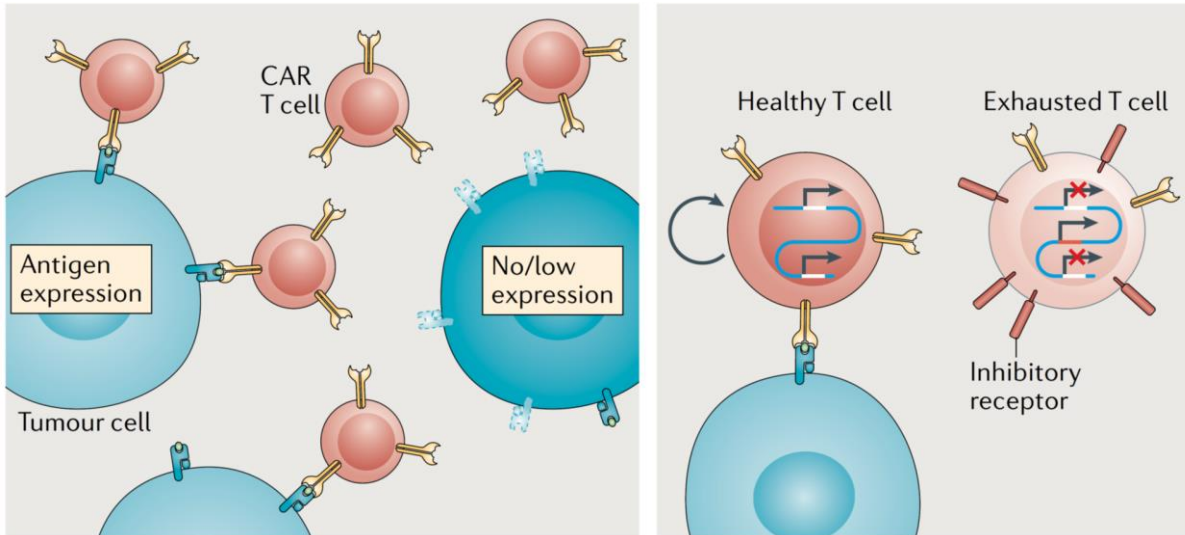


Figure 4: Mechanisms of resistance to CAR T-cell therapy. Malignant cells may evade CAR T cells by altering expression of the target gene, resulting in antigen-low or antigen-negative tumors. Alternatively, CAR T-cell exhaustion leads to intrinsic dysfunction and, subsequently, lack of anti-tumor response (Figure adapted from Brown and Mackall, *Nat Rev Immunol*, 2019).

2.3 Role of inhibitory molecule TIM-3

T-cell immunoglobulin and mucin domain 3 (TIM-3) is a transmembrane protein that is expressed on various cells of the immune system and mediates cell-type dependent immune modulation.⁴⁷

In T cells, TIM-3 expression is associated with chronic exhaustion and correlates with T-cell senescence during viral infection.⁴⁸ Multiple studies have observed an equivalently adverse effect on anti-tumor immunity and further established TIM-3 as a co-inhibitory molecule.^{47,49,50} Moreover, TIM-3 expression is associated with poor prognosis in multiple cancer entities.^{47,51} Notably, our group recently showed that TIM-3 overexpression on CD4-positive bone marrow T cells correlates with increased risk of relapse in B-precursor ALL patients and impairs Blinatumomab-mediated T cell response against leukemic cells.⁵² Co-expression of TIM-3 and PD-1 marks heavily exhausted T-cell subsets and simultaneous blockade of TIM-3 and PD-1 showed synergistic effects in preclinical models, thus improving tumor regression.⁵³ Multiple clinical trials are currently evaluating the efficacy of anti-TIM-3 monoclonal antibodies for treatment of advanced solid tumors as well as myelodysplastic syndrome (MDS) and acute myeloid leukemia (AML) and show encouraging preliminary results.⁵⁴⁻⁵⁶

In recent years, several ligands of TIM-3 have been described. Galectin-9 is a soluble protein that induces apoptosis upon binding to TIM-3, thus compromising anti-tumor immunity in colon cancer and AML.^{57,58} High-mobility group box 1 (HMGB1) is another soluble ligand and is considered a damage-associated molecular pattern molecule that plays a role in innate immune responses and promotes immune-escape in response to chemotherapy or DNA vaccination.⁵⁹ Finally, carcinoembryonic antigen cell adhesion molecule 1 (CEACAM) is known to promote the inhibitory function of TIM-3 via both cis and trans interactions, as TIM-3 and CEACAM are co-expressed on exhausted T-cells.⁶⁰ Co-blockade of CEACAM and TIM-3 could ameliorate tumor regression in a preclinical colorectal cancer model.⁶⁰

Conclusively, there is emerging evidence that immune-targeting of TIM-3 might prove beneficial for CAR T-cell therapy, as was already shown for checkpoint blockade of the PD-1/PD-L1 axis.^{45,46} Yet, successful implementation of TIM-3 based approaches into CAR T-cell therapy requires further knowledge on how CAR T-cell functionality is influenced by TIM-3 expression.

3 Aim of the study

CAR T-cell therapy has demonstrated impressive results in treatment of relapsed or refractory ALL, but durable remissions remain unachievable for many patients. Resistance or absence of response to CAR T cells may develop from their intrinsic dysfunctionality, yet the exact mechanisms that cause impairment of CAR T-cell response, and, therefore, relapse, are not fully understood.

With this in mind, this study aims at further investigating the role of inhibitory checkpoint molecules in CAR T-cell functionality, where adverse effects of PD-1 expression have already been suggested.^{44,46} Herein, we focused on the co-inhibitory molecule TIM-3, which has been described as a marker of T-cell exhaustion and malfunction, yet lacks sufficient characterization in the context of CAR T cells and their functionality.⁴⁷

Moreover, our objective was to overcome TIM-3-mediated inhibition by engineering CAR T cells with a TIM-3/CD28 fusion receptor, which would revert an inhibitory signal provided by TIM-3 into a stimulatory signal through its intracellular CD28 domain and thereby reinforce CAR T-cell response.⁶¹ As signaling strength appeared to depend on precise structure in other fusion receptors, we further aimed at identifying a design that would provide superior activation.

In conclusion, this study aims at providing strategies to maintain CAR T-cell response despite the presence of inhibitory pathways and thus improving CAR T-cell therapy for pediatric ALL.

4 Material

4.1 Equipment and software

Equipment/ Software	Name, Manufacturer
Autoclaves	VX-55, VX-150, DX-65, Systec, Linden, Germany
Cell counting auxiliaries	Cell Counting Chamber Neubauer, Chamber Depth 0.1 mm, Paul Marienfeld, Lauda-Königshofen, Germany
Centrifuges	Multifuge X3R and Mini Centrifuge Fresco 17, Heraeus, Hanau, Germany
Cleaner Box	UVC/T-M-AR, DNA-/RNA UV-cleaner box, Biosan, Riga, Latvia
Cooling units	Cooler (4 °C) Comfort No Frost, Liebherr, Biberach an der Riß, Germany
	Cryogenic Freezer MVE 600 Series, Chart, Luxemburg
	Freezer (-20 °C) Premium No Frost, Liebherr, Biberach an der Riß, Germany
	Freezer (-86 °C) HERAfreeze HFC Series, Heraeus, Hanau, Germany
	Freezer (-86 °C) HERAfreeze HFU T Series, Heraeus, Hanau, Germany
	Thermo Scientific Cryo 200 liquid nitrogen dewar, Thermo Fisher Scientific, Waltham, Massachusetts, USA
Flow cytometer	BD FACSAria III, BD, Franklin Lakes, New Jersey, USA
	MACSQuant Analyzer 10, Miltenyi Biotec, Bergisch Gladbach, Germany
Freezing container	Nalgene Mr. Frosty, Thermo Fisher Scientific, Waltham, Massachusetts, USA
Gel Imager	Gel iX20 Imager, Intas Science Imaging, Göttingen, Germany
Heat block	Eppendorf ThermoMixer comfort, Eppendorf, Hamburg, Germany
Incubator	HERAcell 240, 150i CO ₂ Incubator, Thermo Fisher, Waltham, Massachusetts, USA
Laminar flow hood	HERAsafe, Thermo Fisher, Waltham, Massachusetts, USA
	Uniflow KR130, Uniequip, Planegg, Germany
Magnetic cell separator	MACS MultiStand, Miltenyi Biotec, Bergisch Gladbach, Germany
	MidiMACS Separator, Miltenyi Biotec, Bergisch Gladbach, Germany
	QuadroMACS Separator, Miltenyi Biotec, Bergisch Gladbach, Germany
Microscope	Axiovert 25, Carls Zeiss Microscopy, Jena, Germany
	Leica DM IL, Leica Microsysteme, Wetzlar, Germany
Spectrophotometer	Nanodrop ND-1000 spectrophotometer, Nanodrop Technologies, Wilmington, Delaware, USA
Pipettes (electrical)	Easypet 3, Eppendorf, Hamburg, Germany
Pipettes (manual)	2.5 µl, 20 µl, 200 µl, 1000 µl Eppendorf Research, Eppendorf, Hamburg, Germany
Power Supply	Biorad Power Pac 200, Biorad, Hercules, California, USA

Scale	R 200 D, Sartorius AG, Göttingen, Germany
Software	CorelDRAW Graphics Suite, Corel Corporation, Ottawa, Kanada
	FlowJo 10.0.7r2, Ashland, Oregon, USA
	Gel iX20 Imager Windows Version, Intas Science Imaging, Göttingen, Germany
	GraphPad PRISM 7.0, La Jolla, California, USA
	MACSQuantify, Miltenyi Biotec, Bergisch Gladbach, Germany
	Microsoft Office 2016, Redmond, Washington, USA
Thermocycler	peqSTAR 96 Universal Gradient, Isogen, Utrecht, Netherlands
Vacuum pump	Vakuumsystem BVC 21 NT, Vacuubrand, Wertheim, Germany
Water bath	LAUDA Aqualine AL 18, LAUDA-Brinkmann, Delran, New Jersey, USA

4.2 Solutions, media, and sera for cell culture

Solution/ Medium/ Serum	Order number	Manufacturer
100 bp DNA Ladder Ready to Load	01-11-00050	Solis BioDyne, Tartu, Estonia
Agarose	50004	Seakem Le Agarose, DMA, Rockland, Maine, USA
Albiomin 5 % infusion solution human albumin (HSA)	623 050	Biotest, Dreieich, Germany
Biocoll separating solution	L6115	Biochrom, Berlin, Germany
BLINCYTO® (Blinatumomab)	-	Amgen, Thousand Oaks, California, USA
Brefeldin A	5936	Sigma-Aldrich, Steinheim, Germany
CD3 monoclonal antibody (HIT3a)	16-0039-85	Invitrogen, Thermo Fisher Scientific, Life Technologies Cooperation, Eugene, Oregon, USA
CD28 monoclonal Antibody (CD28.2)	16-0289-85	Invitrogen, Thermo Fisher Scientific, Life Technologies Cooperation, Eugene, Oregon, USA
CellTrace Violet Proliferation Kit	C34557	Invitrogen, Thermo Fisher Scientific, Life Technologies Cooperation, Eugene, Oregon, USA
Compensation beads	552843	BD Biosciences, San Diego, California, USA
	130-097-900, 130-104-693	MACS Comp Bead Kit anti mouse/anti REA, Miltenyi Biotec, Bergisch Gladbach, Germany
Dimethylsulfoxid	D5879	Honeywell, Seelze, Germany
	4720.4	Carl Roth, Karlsruhe, Germany
DMEM	FG1445	Biochrom, Berlin, Germany
DNA Clean & Concentrator -5	D4014	Zymo Research, Irvine, California, USA

DNA Gel Loading Dye (6X)	R0611	Thermo Fisher Scientific, Waltham, Massachusetts, USA
Dulbeccos phosphate buffer saline (PBS)	14190-250	Gibco, Life Technologies, Darmstadt, Germany
Ethidium bromide	2218.1	Roth, Karlsruhe, Germany
FcR Blocking Reagent	130-059-901	Miltenyi Biotec, Bergisch Gladbach, Germany
Fetal Bovine Serum	F0804	Sigma-Aldrich CHEMIE, Steinheim, Germany
Fix & Perm Cell Permeabilization Kit	GAS004	Life Technologies, Frederick, Maryland, USA
Heparin sodium 25,000 I.U./5ml		Ratiopharm, Ulm, Germany
HEPES-Buffer (1M)	L 1613	Biochrom, Berlin, Germany
Human AB serum		Human AB serum was kindly provided by Prof. R. Lotfi, University Hospital Ulm, Institute for Transfusion Medicine and German Red Cross Blood Services Baden-Württemberg—Hessen, Institute for Clinical Transfusion Medicine and Immunogenetics, both from Ulm, Germany
IL-2, IL-7, IL-15 (human, premium grade)	130-097-745 130-95-363, 130-095-764	Miltenyi Biotec, Bergisch Gladbach, Germany
L-Glutamine 200 mM	K 0283	Biochrom, Berlin, Germany
MicroBeads (CD4, CD8, CD56)	130-045-101, 130-045-201, 130-050-401	Miltenyi Biotec, Bergisch Gladbach, Germany
Non-Essential Amino Acids	11140-035	Gibco, Life Technologies, Darmstadt, Germany
Penicillin/Streptomycin	15140-122	Gibco, Life Technologies, Darmstadt, Germany
Protamine sulfate	P3369	Sigma-Aldrich CHEMIE, Steinheim, Germany
Q5 High-Fidelity DNA Polymerase	M0491S	New England BioLabs, Frankfurt am Main, Germany
QIAamp DNA Mini Kit	51306	QIAGEN, Hilden, Germany
RetroNectin Reagent	T100A	Takara, Saint-Germain-en-Laye, France
Sodium pyruvate	11360-039	Gibco, Life Technologies, Darmstadt, Germany
Staphylococcal enterotoxin B	4881	Sigma-Aldrich CHEMIE, Steinheim, Germany
TAE Buffer	A4686	TAE buffer (50x), Applichem, Darmstadt, Germany
TexMACS GMP Medium	170-076-307	Miltenyi Biotec, Bergisch Gladbach, Germany
T cell TransAct, human	130-111-160	Miltenyi Biotec, Bergisch Gladbach, Germany

TransIT-293 Transfection Reagent	Mirumir2704	Mirus Bio LLC, Madison, Wisconsin, USA
Trypan blue	15250-061	Gibco, Life Technologies, Darmstadt, Germany
Tween 20	9127.1	Carl Roth, Karlsruhe, Germany
VLE RPMI 1640 Medium	F1415	Biochrom, Berlin, Germany

4.3 Consumables

Consumable	Order number	Name, Manufacturer
Cannula	851.638.235	Safety-Multifly-Needle, Sarstedt, Nümbrecht, Germany
Cell culture dish	664 160	Cellstar Greiner Labortechnik, Kremsmünster, Austria
Cell culture flasks with ventilation caps	83.3910.002, 83.3911.002, 83.3912.002	T25, T75, T175, Sarstedt, Nümbrecht, Germany
Cell culture multiwell plates, 6 well	657160	Cellstar Greiner Labortechnik, Kremsmünster, Austria
Cell culture multiwell plates, 24 well	3524	Costar Corning Incorporated, Corning, New York, USA
Cell culture multiwell plates, 48 well	3548	Costar Corning Incorporated, Corning, New York, USA
Cell culture multiwell plates, 96 well	163320	Nunclon Delta Surface, Thermo Fisher Scientific, Waltham, Massachusetts, USA
Compresses	18507	Gauze Compresses 10 x 10 cm, Nobamed Paul Danz, Wetter, Germany
Coverslips	C10143263NR1	Menzel-Gläser 20 x 20 mm, Gerhard Menzel, Braunschweig, Germany
FACS buffers and solutions	130-092-747, 130-092-748, 130-092-749	Running Buffer, Storage Solution, Washing Solution, Miltenyi Biotec, Bergisch Gladbach, Germany
	340345, 340346, 342003	FACS clean/rinse/flow, Becton, Dickinson and Company (BD), Franklin Lakes, New Jersey, USA
Freezing tubes	72.379	Cryo Pure Gefäß 1.8 ml, Sarstedt, Nümbrecht, Germany
Magnetic separation columns	130-042-401, 130-042-901	LS Columns, LD Columns, Miltenyi Biotec, Bergisch Gladbach, Germany
Pasteur pipettes	747720	Glass Pasteur Pipettes 230 mm, Brand, Wertheim, Germany
Pipette tips	70.1130.217, 70.760.213,	0.1-2.5 µl, 10 µl, 20 µl, 100 µl, 2-200 µl, 1000 µl, Sarstedt, Nümbrecht, Germany

	70.760.212, 70.762.211	
Reaction vessels	62.554.502	15 ml, Sarstedt, Nümbrecht, Germany
	4440100	50 ml, Orange Scientific, Braine-l'Alleud, Belgium
	72.690.550	1.5 ml, Sarstedt, Nümbrecht, Germany
Round bottom tubes with cell strainer snap cap	352235	5 ml Polystyrene Round Bottom Tube, Falcon, Corning Science, Tamaulipas, Mexico
Safety gloves	9209817	Vaso Nitril Blue, B. Braun Melsungen, Melsungen, Germany
Serological pipettes	86.1685.001, 86.1253.001, 86.1254.001	5 ml, 10 ml, 25ml Serological Pipette, Sarstedt, Nümbrecht, Germany
Skin disinfectant	975512, 306650	Sterilium Classic Pure, Sterilium Virugard, Hartmann, Heidenheim, Germany
Sterile filters	SE2M229104, SE2M230104	0.2µm, 0.45µm, Carl Roth, Karlsruhe, Germany
Surface disinfectant	CLN-1006.5000	Ethanol 80 % MEK/Bitrex, CLN, Niederhummel, Germany
Syringe	309658	3ml, Becton, Dickinson and Company (BD), Franklin Lakes, New Jersey, USA
	4606728V	10ml, B. Braun Melsungen, Melsungen, Germany
	4617509F	50ml, Omnifix, B. Braun Melsungen, Melsungen, Germany

4.4 Antibodies

Fluorochrome	Antigen	Clone	Order number	Manufacturer
7AAD	Viability dye		420404	Biologend, San Diego, California, USA
APC	CD8	SK1	556414	Becton, Dickinson and Company (BD), Franklin Lakes, New Jersey, USA
APC	CD14	TÜK4	130-115-559	Miltenyi Biotec, Bergisch Gladbach, Germany
APC	CD95	DX2	130-092-417	Miltenyi Biotec, Bergisch Gladbach, Germany
APC	CD137	REA765	130-110-764	Miltenyi Biotec, Bergisch Gladbach, Germany
APC	IL-2	5344.111	341116	Becton, Dickinson and Company (BD), Franklin Lakes, New Jersey, USA
APC-Vio770	CD3	REA613	130-113-136	Miltenyi Biotec, Bergisch Gladbach, Germany
APC-Vio770	CD8	REA734	130-110-681	Miltenyi Biotec, Bergisch Gladbach, Germany

BB515	CD19	HIB19	564456	Becton, Dickinson and Company (BD), Franklin Lakes, New Jersey, USA
BB515	TIM-3	7D3	565568	Becton, Dickinson and Company (BD), Franklin Lakes, New Jersey, USA
BV421	CD56	HCD56	318328	Biolegend, San Diego, California, USA
BV421	TIM-3	F38-2E2	345008	Biolegend, San Diego, California, USA
FITC	Anti-c-myc	14D3	130-116-485	Miltenyi Biotec, Bergisch Gladbach, Germany
Pacific Blue	TNF- α	MAb11	502920	Biolegend, San Diego, California, USA
PE	CD19	LT19	130-113-169	Miltenyi Biotec, Bergisch Gladbach, Germany
PE	CD25	REA570	130-113-286	Miltenyi Biotec, Bergisch Gladbach, Germany
PE	CD45RO	UCHL1	304206	Biolegend, San Diego, California, USA
PE	CD56	REA196	130-113-312	Miltenyi Biotec, Bergisch Gladbach, Germany
PE	CEACAM	ASL-32	342304	Biolegend, San Diego, California, USA
PE	IFN- γ	25723.11	340452	Becton, Dickinson and Company (BD), Franklin Lakes, New Jersey, USA
PE-Vio770	CD3	REA613	130-113-140	Miltenyi Biotec, Bergisch Gladbach, Germany
PE-Vio770	CD19	REA675	130-113-647	Miltenyi Biotec, Bergisch Gladbach, Germany
PE-Vio770	CD69	REA824	130-112-615	Miltenyi Biotec, Bergisch Gladbach, Germany
VioBlue	CD62L	145/15	130-098-699	Miltenyi Biotec, Bergisch Gladbach, Germany
VioGreen	CD4	REA623	130-113-230	Miltenyi Biotec, Bergisch Gladbach, Germany

5 Methods

Sections 5.1 to 5.5 were adapted from the MD thesis of Antonia Apfelbeck (“Generation and Characterization of CD19 CAR T cells with PD-1_CD28 fusion receptor”, Ludwig-Maximilian-University, Munich), since identical protocols have been used.

5.1 CAR T-cell generation

5.1.1 PBMC isolation and T-cell activation

Cells were derived from 100 ml of peripheral blood of healthy donors. All donors gave written informed consent before venous puncture for heparin blood collection. Peripheral blood mononuclear cells (PBMCs) were generated via density gradient centrifugation. Heparin blood was diluted 1:2 with PBS and carefully layered on 15 ml Biocoll. After centrifugation at 800 g for 30 minutes without brake PBMCs were aspirated and frozen as described in 5.3. After thawing (see 5.3), T cells were isolated by CD4 MicroBeads and CD8 MicroBeads which was performed according to the manufacturer’s information. T cells were cultured in TexMACS GMP medium supplemented with 2.5% human AB serum and 12.5 ng/ml interleukins 7 and 15. Isolated T cells were activated with T Cell TransAct, human as suggested in the supplier’s information and washed two days after activation.

5.1.2 Virus generation

Producer cells (293Vec-RD114 cells) were previously generated for all constructs according to published literature.^{62,63} Producer cells were kindly provided by Manuel Caruso, BioVec Pharma.

Virus was harvested by aspirating supernatant of 293VEC-RD114 cells. Supernatant was centrifuged at 600 g for 5 minutes, frozen and stored at -80 °C.

5.1.3 Retroviral CAR T-cell transduction

Transduction process was performed two days after T-cell generation. 24-well plates were coated with 2.5 µg RetroNectin Reagent either overnight at 4 °C or for 2 hours at 37 °C. Plates were blocked with 2% Albumin Fraction V in PBS for 30 minutes and afterwards washed with a 1:40 dilution of HEPES 1M in PBS. 1 ml of thawed virus supernatant was centrifuged on coated wells at 3000 g for 90 minutes at 32 °C. For untransduced control, DMEM medium was centrifuged on coated wells instead. Supernatants were discarded and 1×10^6 T cells in 1 ml TexMACS GMP medium/2.5% human AB serum + 12.5 ng/ml interleukins 7 and 15 were added per well. Plates were centrifuged at 450 g for 10 minutes at 32 °C and on day 2 after transduction T cells were washed to remove virus.

T cells were cultured in TexMACS GMP medium/2.5% human AB serum + interleukins 2, 7, and 15 throughout the expansion process. Interleukin 2 was used at 6 Units/ml and interleukins 7 and 15 were used at 12.5 ng/ml. Every two to three days new medium was added and cells were cultured at 1×10^6 per ml. Expansion rate and viability was assessed every two or three days under light microscope after diluting the cells 1:2 with trypan blue. On day 12 after transduction cells were harvested and frozen as described in 5.3.

For characterization of the final product, cellular composition and transduction rate was analyzed by flow cytometry on day 12 after transduction by staining for CD3, CD4, CD8, CD56, c-myc, CD14, CD19 or for CD3, CD4, CD8, CD56, c-myc, TIM-3. The phenotype of the T cells was evaluated on day 12 after transduction by flow cytometric stain for CD3, CD4, CD8, CD62L, CD45RO and CD95. T cells were considered as naive T cells if CD62L⁺/CD95⁻/CD45RO⁻, as stem cell-like memory T cells if CD62L⁺/CD95⁺/CD45RO⁻, as central memory T cells if CD62L⁺/CD95⁺/CD45RO⁺, as effector memory T cells if CD62L⁻/CD95⁺/CD45RO⁺ and as effector T cells if CD62L⁻/CD95⁺/CD45RO⁻.

5.1.4 Functionality assays

T cells were thawed and rested overnight in TexMACS GMP medium supplemented with 2.5% human AB serum and 6 ng/ml of interleukin 2. After thawing, a FITC c-myc or BV421 TIM-3 single stain was performed to reevaluate transduction rate. All conditions were adjusted to the lowest transduction rate within the donor by adding untransduced cells. Effector count was calculated on the number of CAR-positive or fusion receptor-positive T cells. For co-culture experiments, CD19-transduced K562 cells and CD19-/CEACAM-transduced K562 cells were used. Functionality assays were performed in technical duplicates or triplicates. Experiments were measured on a MACSQuant Analyzer 10.

5.1.5 Cytotoxicity assay

Cytotoxicity measurement was performed on day 13 post-transduction. T cells were depleted with CD56 MicroBeads according to the supplier's information in order to remove NKT cells. Transduction rate was reevaluated by a FITC c-myc single stain and all conditions were adjusted to the lowest transduction rate within the donor by adding untransduced cells. Target cells were labeled according to CellTrace Violet Cell Proliferation Kit and co-cultured with CAR T cells at different effector to target ratios. Cells were co-cultured for 48 hours. Absolute cell count of CellTrace Violet-positive cells was measured and killing rate was calculated with following formula: $100 - (100/\text{targets only} * \text{targets left in co-culture})$. "Targets only" describes target cell lines without co-cultured effector cells and were used as reference.

5.1.6 Intracellular cytokine stain (ICS)

T cells were prepared as described in 5.1.4 and were co-cultured with target cells at a 1:1 ratio for 6 or 24 hours as indicated in the figure legends. T cells cultured without target cells were used as negative control. For positive control, T cells were stimulated with 10 µg/ml staphylococcus enterotoxin B (SEB). 2 hours after stimulation, 10 µg/ml Brefeldin A was added. Stimulation was stopped with cold PBS after 4 hours and T cells were washed. Intracellular stain with IFN-γ, TNF-α, and IL-2 was performed with FIX & PERM cell Fixation & Permeabilization Kit according to the supplier's information. T cells were stained for CD3, CD4, CD8, CD56, and c-myc to identify T-cell subsets.

5.1.7 Activation assay

T cells were prepared as described in 5.1.4 and were co-cultured with target cells at a 1:1 ratio for 14 or 48 hours as indicated in the figure legends. T cells cultured without target cells were used as negative control. After co-culture, cells were stained for activation markers CD25, CD69 and CD137, and for CD8, CD4, TIM-3, and c-myc.

5.1.8 Proliferation assay

T cells were prepared as described in 5.1.4. T cells were labeled according to CellTrace Violet Cell Proliferation Kit and co-cultured with target cells at a 1:1 ratio for 72 hours. T cells cultured without target cells were used as negative control. An SEB positive control with 10 µg/ml was performed. Additional to CellTrace Violet the cells were stained for CD3, CD4, CD8, CD19, TIM-3, and c-myc. Absolute numbers of CAR T cells were assessed after 72 hours using a MACSQuant Analyzer 10 and refer to detected events in the gate of CAR-positive T cells in a total volume of 100µl. All conditions were normalized to 1×10^5 CAR T cells/ 200µl at the start of co-culture.

5.1.9 Phenotype assays

T cells were prepared as described in 5.1.4 and were co-cultured with target cells at a 1:1 ratio for 72 hours. T cells cultured without target cells served as control. After co-culture, cells were stained for CD3, CD4, CD8, CD62L, CD45RO, and CD95. Analysis of T-cell subpopulations was conducted as previously described in 5.1.3.

5.1.10 CD3 coating assays

96-well plates were coated with CD3 monoclonal antibody (HIT3a) either overnight at 4 °C or for 2 hours at 37 °C. CD3 monoclonal antibody was used at 2 µg/ml for ICS and at 0.25 µg/ml for proliferation assay. T cells were prepared as described in 5.1.4 and were additionally labeled according to CellTrace Violet Cell Proliferation Kit for proliferation assay. T cells were stimulated by

adding 1×10^5 fusion receptor-positive cells to CD3-coated wells. For unstimulated control, the same amount of T cells was added in un-coated wells (PBS). Intracellular cytokine stain and proliferation measurement were performed after 6 and 72 hours, respectively, as described in 5.1.6 and 5.1.8.

5.2 Transduction of cell lines

CD19_pMP71/ CEACAM_pMP71 and helper plasmids env and gag/pol were transfected into HEK 293T cells using TransIT-293 Transfection Reagent according to the supplier's information. Helper plasmids were kindly provided by Sebastian Kobold, Department of Clinical Pharmacology, Munich. Vector pMP71 was kindly provided by Christopher Baum, Department of Experimental Hematology, Hannover. Vector maps for helper plasmids and pMP71 are shown in the supplements (see 11.3). After 48 hours, viral supernatant was harvested and used for transduction of K562 cells. 24-well plates were coated with 2.5 μ g RetroNectin Reagent overnight at 4 °C. Plates were blocked with 2% Albumin Fraction V in PBS for 30 minutes and washed with a 1:40 dilution of HEPES 1M in PBS. Virus supernatant was centrifuged at 500 g for 5 minutes at 32 °C and filtered with a 0.45 μ m filter. 1 ml of virus supernatant was centrifuged on coated wells at 3000 g for 90 minutes at 32 °C. Supernatant was discarded and 1×10^6 K562 cells in RPMI + 10% fetal bovine serum (FBS) + 1% penicillin/streptomycin + 1% L-glutamine were added per well. 4 μ g of protamine sulfate and 1% HEPES 1M was added. On day 2 after transduction, cells were washed to remove virus. Cells were sorted for CD19⁺ and CD19⁺/CEACAM⁺ K562 cells at a FACSAria III and cultured in RPMI + 10% fetal bovine serum (FBS) + 1% penicillin/streptomycin + 1% L-glutamine. Regular flow-cytometric analysis confirmed identical expression of CD19 in both cell lines based on mean fluorescent intensity.

5.3 General cell culture

Cells were cultured at 37 °C with 5% CO₂.

Cell lines were cultured in RPMI + 10% fetal bovine serum (FBS) + 1% penicillin/streptomycin + 1% L-glutamine and splitted at least every five days in a 1:10 ratio. Identity of cell lines was verified by STR (Short tandem repeat) analysis regularly.

Cell lines were frozen in RPMI + 20% fetal bovine serum (FBS) + 1% penicillin/streptomycin + 1% L-glutamine containing 10% dimethyl sulfoxide (DMSO). Primary T cells were frozen in 5% human serum albumin (HSA) containing 10% DMSO. After cells were frozen in a freezing container at -80 °C they were transferred to liquid nitrogen (-179° C) for preservation.

For thawing cells were rapidly warmed in the water bath, transferred to prewarmed RPMI medium and washed in TexMACS medium.

5.4 Flow cytometry

Antibodies for flow cytometry staining were titrated before use. PBS + 1% fetal bovine serum (FBS) was used as staining buffer. Cells were stained for 10 minutes at 4 °C and washed once with buffer. For stainings involving K562 cells, Fc receptor block was used according to the manufacturer's information. All measurements were performed at a MACSQuant Analyzer 10.

5.5 Statistical analysis

Statistics were performed with GraphPad Prism 7. Statistical differences between experimental conditions were examined using a two-tailed unpaired Student's t test. Multiple comparisons were performed using a one-way ANOVA followed by Tukey's test. A *p* value of <0.05 indicates significant (*) and <0.01 very significant (**) differences. A *p* value of <0.001 and <0.0001 indicates extremely significant (***) and ****) differences.

6 Results

The following results were in part published recently by our group.⁶¹

6.1 Retroviral transduction enables stable overexpression of TIM-3 in CAR T cells

Human primary T cells were transduced with retroviral vectors encoding a first generation CAR construct with an intracellular CD3 ζ stimulatory domain (19_3z) and a second generation CAR construct with an additional 4-1BB costimulatory domain (19_BB_3z, Figure 5a).⁶¹ To generate TIM-3 overexpressing CAR T cells, first and second generation CAR constructs were linked to TIM-3 by an F2A linker (19_3z_TIM-3 and 19_BB_3z_TIM-3). A c-myc tag was inserted between the anti-CD19 scFv and the CD8 transmembrane and extracellular spacer domain, which enabled flow-cytometric detection of CAR transduced T cells. Untransduced T cells as well as T cells transduced with a CAR construct lacking the CD3 ζ stimulatory domain (19t) served as control.

Successful transduction of all CAR constructs was confirmed by flow-cytometric stain for the c-myc tag on day 12 post-transduction (Figure 5b). A mean transduction rate of 67.3% was achieved throughout all constructs (range 44.7-84.0). Both 19_3z_TIM-3 (mean 79.5) and 19_BB_3z_TIM-3 (mean 79.8) consistently showed significantly higher transduction rates than conventional CAR T cells (mean 64.5 in 19_3z and 59.1 in 19_BB_3z, *p* values not shown). A mild donor-dependency of transduction rate could be observed.

TIM-3 expression on CAR T cells was assessed on day 12 post-transduction (Figure 5c). Endogenous TIM-3 expression levels showed inter-individual differences in conventional CAR T cells. 19_3z CAR T cells demonstrated a mean of 44.8% TIM-3 positivity (range 33.4-56.1%) and 19_BB_3z CAR T cells exhibited a mean of 46.0% TIM-3 positivity (range 39.4-52.6%). In contrast, both TIM-3 overexpressing CAR T cells showed almost 100% of TIM-3 expression (mean 97.7% in 19_3z_TIM-3 and 97.4% in 19_BB_3z_TIM-3) with only little variation between donors (range 96.7-98.7% and 96.1-98.6%), suggesting stable co-expression. Lowest TIM-3 expression was observed in 19t control CAR T cells (mean 19.1%, range 11.0-27.1%).

After retroviral transduction, CAR T cells were expanded for 12 days, during which expansion rates and viability of cells was assessed (Figure 6). A mean fold expansion of 43.0 could be achieved throughout all constructs (Figure 6a) and expansion rates were highest for the untransduced control (mean 63.3) and 19t control (mean 73.9). In first generation CAR T cells, TIM-3 overexpressing CAR T cells showed significantly lower expansion rates at day 5, 7, and 9 post-transduction. Yet, overall expansion on day 12 after transduction was not significantly different between 19_3z CAR T cells

(mean 31.7) and 19_3z_TIM-3 CAR T cells (mean 24.1). In second generation CAR T cells, TIM-3 overexpressing and conventional CAR T cells exhibited comparable expansion rates. Overall mean expansion was 23.7-fold for 19_BB_3z_TIM-3 and 41.1-fold for 19_BB_3z CAR T cells.

Compared to conventional first generation CAR T cells, TIM-3 overexpressing CAR T cells exhibited significantly reduced viability on day 5, 7, and 9 post-transduction (Figure 6b). Mean viability over all time points was 88.2% for 19_3z and 82.2% for 19_3z_TIM-3, which equals a very significant difference ($p= 0.0024$, data not shown). Compared to conventional second generation CAR T cells, 19_BB_3z_TIM-3 CAR T cells showed significantly reduced viability on days 5 and 7 after transduction. Mean viability over all time points was significantly decreased in 19_BB_3z_TIM-3 compared to conventional 19_BB_3z CAR T cells (83.0 vs. 89.1, $p= 0.0063$, data not shown).

In order to detect potential alterations in phenotype due to TIM-3 overexpression, phenotypic characterization of CAR T cells was conducted on day 12 post-transduction (Figure 6c). All CAR constructs displayed a central memory- and effector memory-predominant phenotype with a small proportion of naive T cells (under 1%). TIM-3 overexpressing first generation CAR T cells showed no significant differences in mean proportion of effector (9.0% in 19_3z vs. 12.7% in 19_3z_TIM-3), effector memory (45.3% vs. 51.2%) and central memory T cells (34.6% vs. 30.9%). However, the percentage of stem cell-like memory T cells was significantly reduced (10.7% vs. 4.7%, $p= 0.0073$), suggesting a slight tendency towards a more differentiated phenotype in TIM-3 overexpressing first generation CAR T cells. Similarly, the comparison of 19_BB_3z and 19_BB_3z_TIM-3 CAR T cells yielded a significant difference in the percentage of stem cell-like memory T cells (10.8% vs. 3.8%, $p= 0.0057$), but not of effector (11.8% vs. 14.8%), effector memory (47.2% vs. 57.5%) and central memory T cells (29.8% vs. 25.7%). Since no significant differences in phenotype were detected between the 19t and untransduced control, the effect of the transduction process on T cell differentiation is negligible.

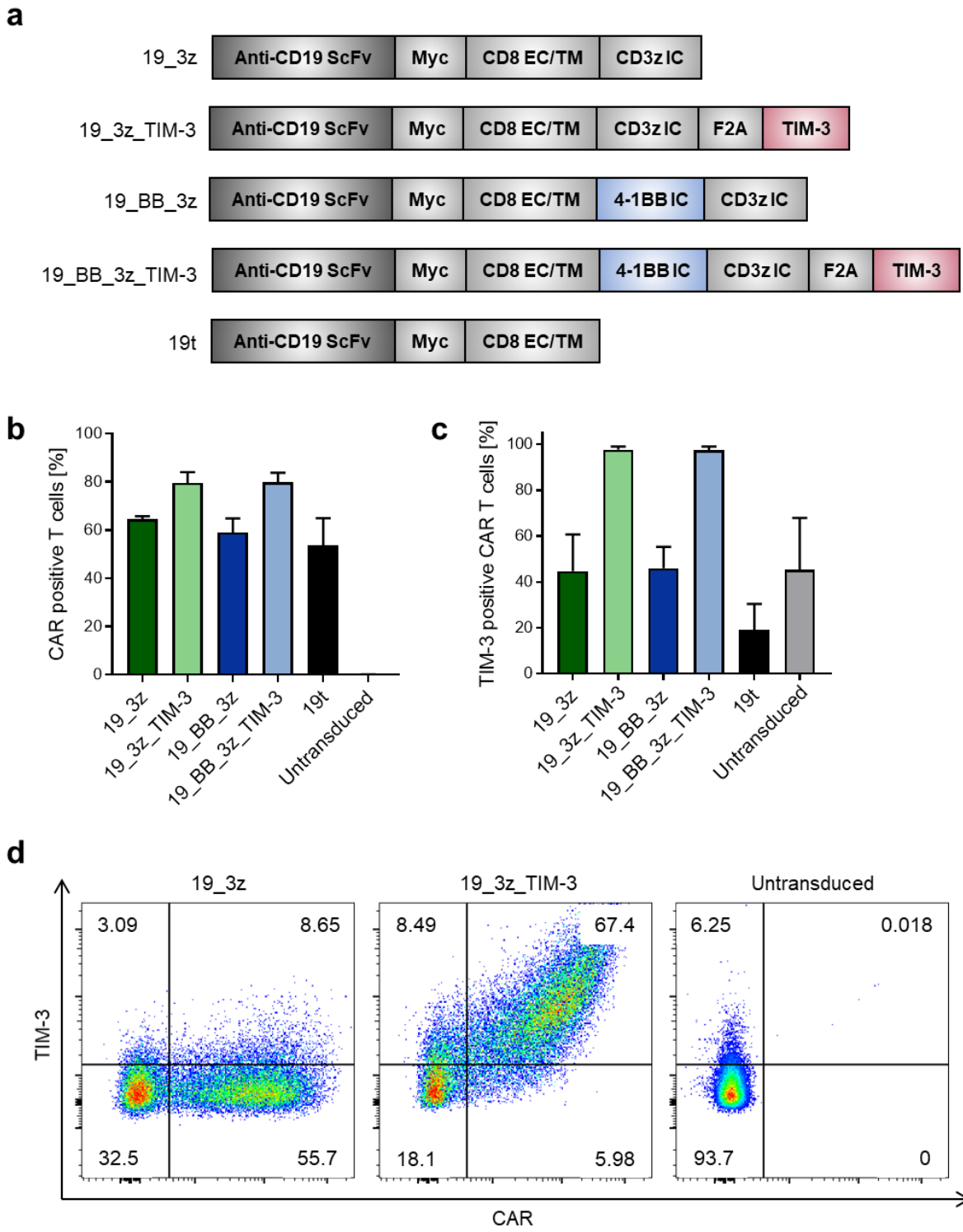


Figure 5: Generation of CD19 CAR T cells with TIM-3 overexpression by retroviral transduction. a, Schematic overview of CAR constructs. **b**, CAR transduction rate at day 12 post-transduction was determined by flow-cytometric stain for c-myc tag. **c**, TIM-3 expression at day 12 post-transduction was measured by flow cytometry. **d**, Representative flow-cytometric analysis of CAR and TIM-3 expression at day 12 post-transduction. Gates were set according to untransduced and unstained control. Data are representative of at least two donors. Data show mean \pm SD. EC= Extracellular; TM= Transmembrane; IC= Intracellular.

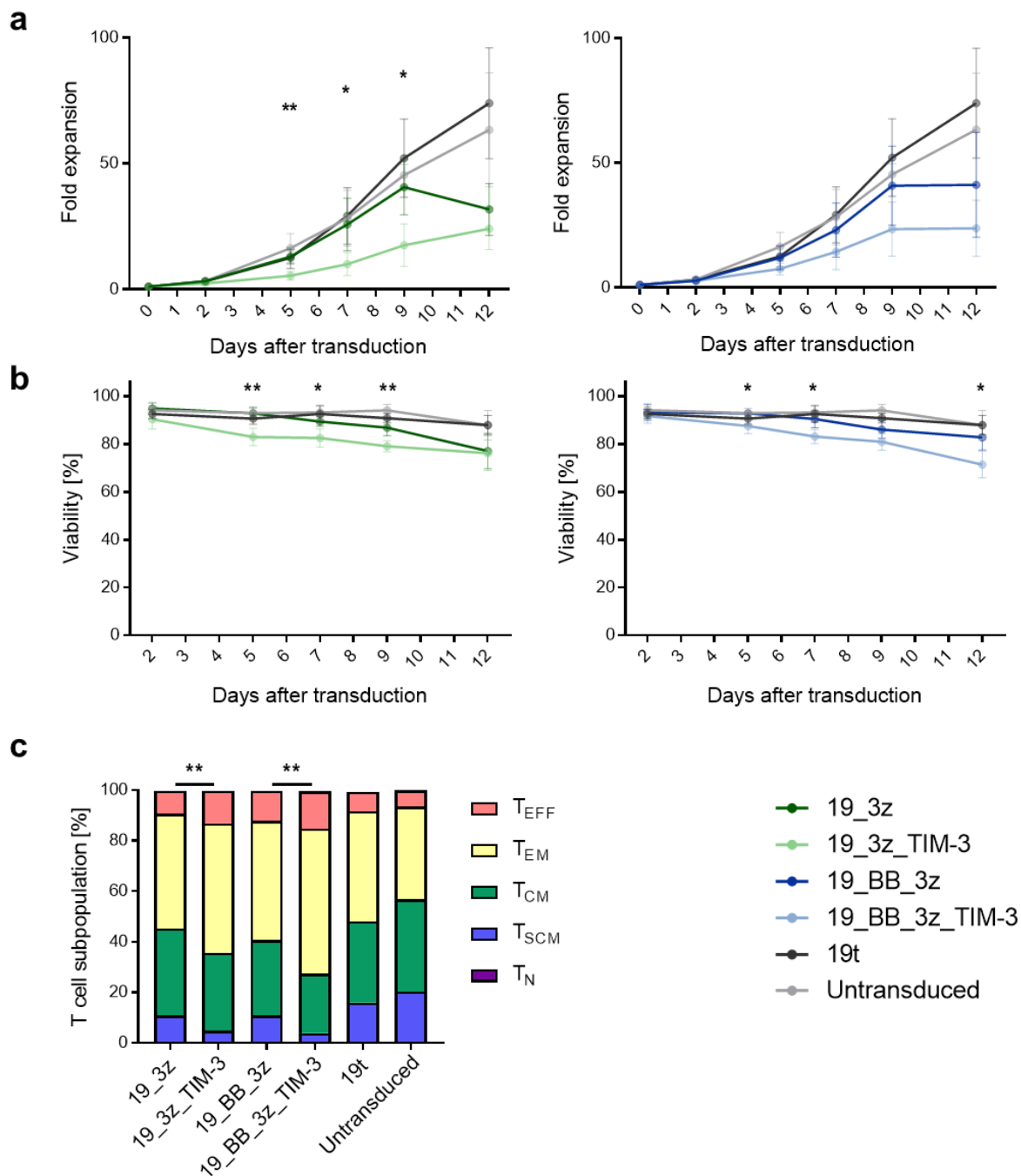


Figure 6: Expansion and phenotypical characterization of TIM-3 overexpressing CAR T cells. **a**, Fold expansion of first generation (left) and second generation (right) CAR T cells relative to initial cell number used for transduction. **b**, Viability of first generation (left) and second generation (right) CAR T cells during the expansion period as determined by count of living cells relative to total cell count. **c**, Phenotypical characterization of CAR T cells at day 12 post-transduction as assessed by flow-cytometric stain for CD62L, CD95, and CD45RO. T cells were considered as naive T cells if CD62L⁺/CD95⁻/CD45RO⁻, as stem cell-like memory T cells if CD62L⁺/CD95⁺/CD45RO⁻, as central memory T cells if CD62L⁺/CD95⁺/CD45RO⁺, as effector memory T cells if CD62L⁻/CD95⁺/CD45RO⁺, and as effector T cells if CD62L⁻/CD95⁻/CD45RO⁻. Significant differences between CAR T cells refer to percentage of T_{SCM} subpopulation. Data are representative of four donors. Data are mean (**c**) and mean ± SD (**a**, **b**). *P* values were determined using a two-tailed unpaired Student's *t* test. For **a** and **b**, significant differences refer to comparison of 19_3z with 19_3z_TIM-3 or 19_BB_3z with 19_BB_3z_TIM-3, respectively. T_{EFF}= Effector T cells; T_{EM}= Effector memory T cells; T_{CM}= Central memory T cells; T_{SCM}= Stem cell-like memory T cells; T_N= Naive T cells.

6.2 CAR T-cell killing capacity is scarcely influenced by TIM-3 expression but is diminished in presence of TIM-3 ligand CEACAM

To investigate the role of TIM-3 expression on CAR T-cell cytotoxicity against CD19-positive leukemic cells, a cytotoxicity measurement was performed as described in the methods section (Figure 7). First generation conventional and TIM-3 overexpressing CAR T cells demonstrated a comparable and effector to target (E: T) ratio-dependent killing of the CD19 transduced K562 target-cell line (Figure 7a). Although a minor, borderline significant difference in cytotoxic killing was detected at the 1:1 E: T ratio (72.1% in 19_3z vs. 68.4% in 19_3z_TIM-3, $p= 0.0403$), a biological relevance remains unlikely. Likewise, second generation CAR T cells with and without TIM-3 overexpression exhibited nearly identical, dose-dependent killing of the CD19-positive target cells (Figure 7b). The 19t control demonstrated 11.6% of unspecific background killing activity at the 1:1 E:T ratio.

In order to evaluate the effect of TIM-3 ligand CEACAM on CAR T cell-mediated killing, the aforementioned experiment was repeated with CD19 and CEACAM double-transduced target cells (Figure 8). Comparison of cytotoxicity against both cell lines revealed significantly reduced killing of CD19⁺/CEACAM⁺ target-cell line in all CAR T cell constructs, regardless of TIM-3 overexpression. In 19_3z CAR T cells, mean killing at the 1:1 E:T ratio decreased from 72.1% (range 68.6%- 75.2%) to 56.7% (range 48.8%- 60.7%, $p < 0.0001$), and at the 0.1:1 E:T ratio from 23.2% (range 18.2%- 27.7%) to 15.7% (range 10.8%- 21.7%, $p= 0.0099$) in presence of CEACAM. Similarly, in 19_3z_TIM-3 CAR T cells, CEACAM provoked a decrease in mean cytotoxicity at the 1:1 E:T ratio from 68.4% (range 64.2%- 71.7%) to 54.8% (range 47.1%- 62.7%, $p= 0.0013$) and at the 0.1:1 E:T ratio from 23.3% (range 16.0%- 28.4%) to 13.0% (range 5.8%- 18.6%, $p= 0.0062$).

In accordance with the results in first generation CAR T cells, the killing capacity of second generation CAR T cells was similarly reduced upon contact with the CEACAM-positive cell line (Figure 8c, d). In presence of CEACAM, mean killing in 19_BB_3z CAR T cells was diminished from 76.8% (range 74.9%- 79.1%) to 63.8% (range 55.9%- 69.7%, $p= 0.0002$) at the 1:1 E:T ratio and from 36.9% (range 34.2%- 42.2%) to 22.5% (range 14.2%- 28.7%, $p= 0.0003$) at the 0.1:1 E:T ratio. In 19_BB_3z_TIM-3 CAR T cells cytotoxicity decreased from 73.1% (range 67.3- 78.7%) to 61.7% (range 47.1-72.4%, $p= 0.0304$) at the 1:1 E:T ratio and from 33.2% (range 27.9-39.6%) to 20.2% (range 8.36- 31.0%, $p= 0.0208$) at the 0.1:1 E:T ratio. At the lowest E:T ratio of 0.01:1, none of the tested CAR T cell constructs showed differences in killing between CD19⁺ and CD19⁺/CEACAM⁺ K562 cells.

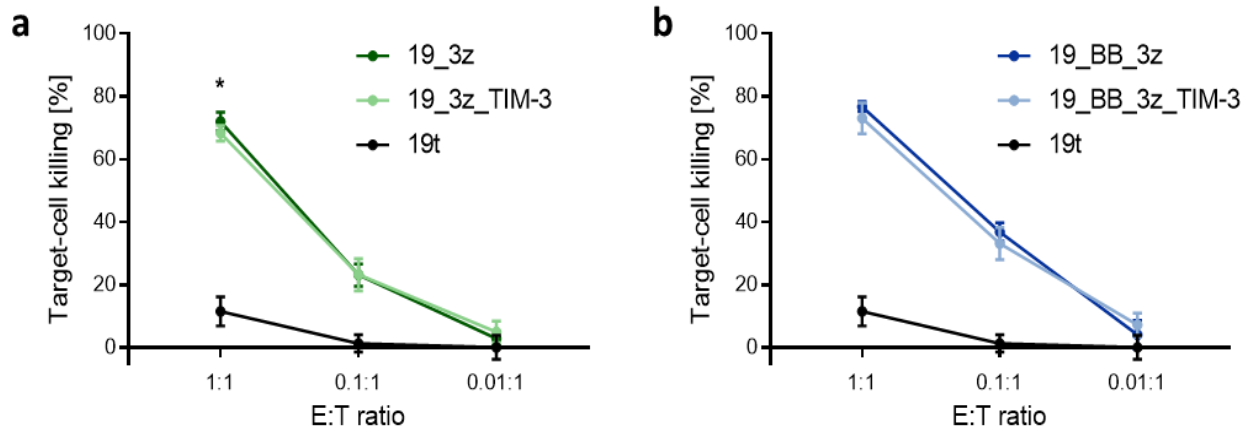


Figure 7: TIM-3 overexpressing CAR T cells demonstrate comparable cytotoxicity against CD19⁺ target-cell line. Cytotoxicity was measured by co-culturing CAR T cells with CD19⁺ K562 target-cell line followed by flow-cytometric analysis. Percentage of target-cell lysis was calculated as described in the methods. **a**, Cytotoxicity of first generation CAR T cells after 48 hours of co-culture with CD19⁺ K562 target-cell line. **b**, Cytotoxicity of second generation CAR T cells after 48 hours of co-culture with CD19⁺ K562 target-cell line. Data are representative of two donors and experiments were performed in technical triplicates. Data are mean \pm SD. *P* values were determined using a two-tailed unpaired Student's *t* test. E:T ratio= Effector to target ratio.

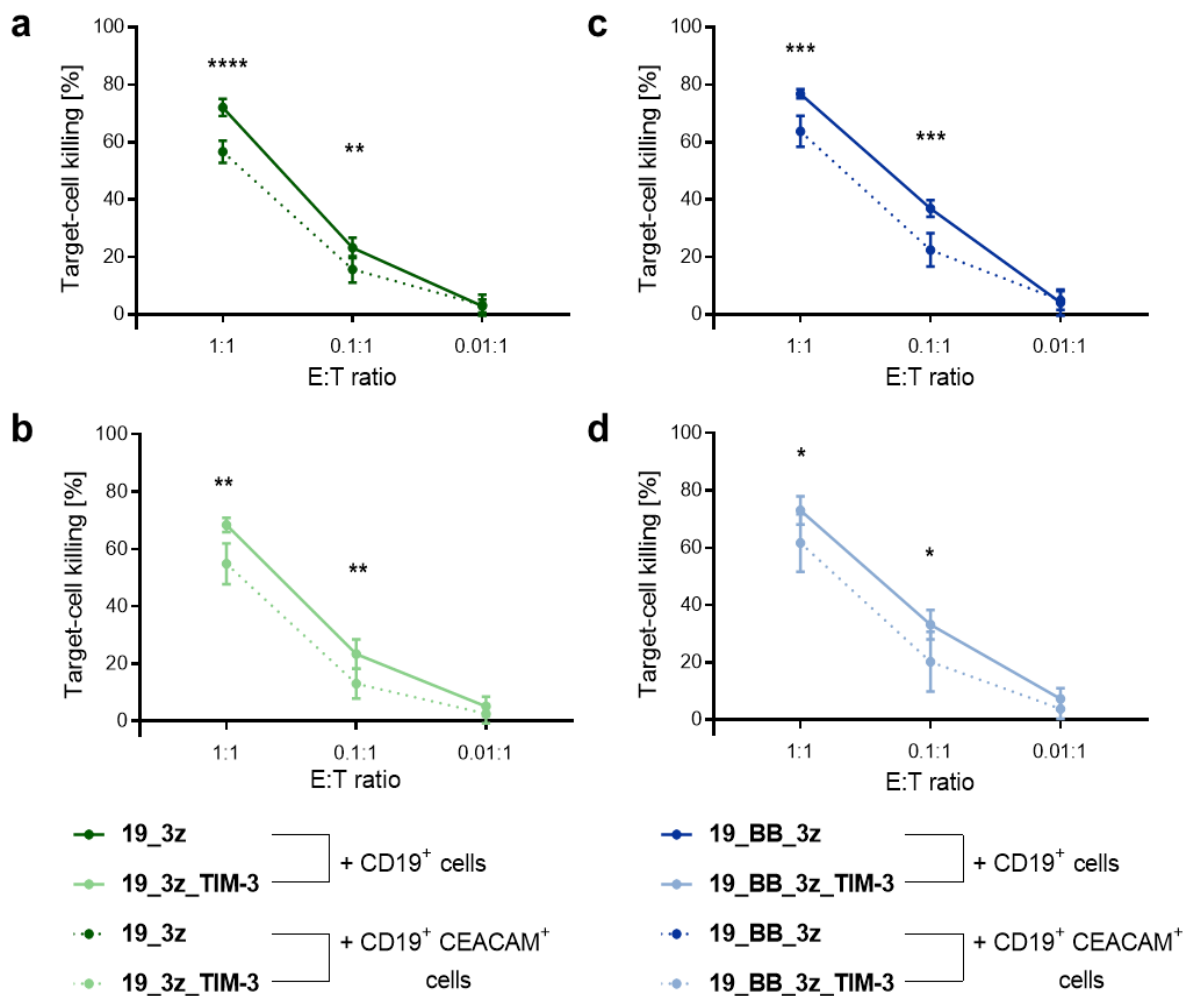


Figure 8: First and second generation CAR T cells show reduced cytotoxic capacity against CEACAM⁺ cell line. **a, b**, Cytotoxicity was measured by co-culturing CAR T cells with CD19⁺ or CD19⁺ CEACAM⁺ K562 target-cell line followed by flow-cytometric analysis. Percentage of target-cell lysis was calculated as described in the methods. **a, b**, Cytotoxicity of 19_3z (**a**) and 19_3z_TIM-3 (**b**) after 48 hours of co-culture with CD19⁺ or CD19⁺ CEACAM⁺ K562 target-cell line. **c, d**, Cytotoxicity of 19_BB_3z (**c**) and 19_BB_3z_TIM-3 (**d**) after 48 hours of co-culture CD19⁺ or CD19⁺ CEACAM⁺ K562 target-cell line. Data are representative of two donors and experiments were performed in technical triplicates. Data are mean \pm SD. *P* values were determined using a two-tailed unpaired Student's *t* test. E:T ratio= Effector to target ratio.

6.3 TIM-3 expression is associated with reduced CAR T-cell functionality in vitro

To further characterize the effect of TIM-3 expression on CAR T-cell functionality, cytokine secretion, activation, and proliferation upon target-cell contact were assessed. As the previous experiments showed significant differences between CD19⁺ and CD19⁺/CEACAM⁺ K562 target cells, both cell lines were used for further functional characterization of CAR T cells.

First, expression of activation markers CD25 and CD137 was measured after 48 hours of co-culture with target cells (Figure 9a, b). Since TIM-3 overexpressing and conventional CAR T cells differed greatly in their intrinsic state of activation marker expression in the unstimulated control (data not shown), fold changes relative to the unstimulated control were calculated. Thus, potential of activation rather than absolute expression of activation markers was determined. In first generation

CAR T cells, fold change of CD25-positive CAR T cells was significantly higher in 19_3z than in 19_3z_TIM-3 CAR T cells, both upon contact with CD19⁺ cells (10.5-fold vs. 5.8-fold, range 7.2-12.5 and 5.1-6.4, $p= 0.0005$) and CD19⁺/CEACAM⁺ cells (11.2-fold vs. 5.2-fold, range 7.4-13.1 and 3.9-6.4, $p= 0.0001$). Fold change of CD137-positive CAR T cells was significantly greater in 19_3z than in 19_3z_TIM-3 CAR T cells after contact with CD19⁺ cells (36.0-fold vs. 12.4-fold, range 33.4-38.2 and 15.6-8.5, $p< 0.0001$) and CD19⁺/CEACAM⁺ cells (26.4-fold vs. 10.5-fold, range 16.7-38.4 and 5.6-15.8, $p= 0.0093$).

Second generation CAR T cells with TIM-3 overexpression showed a similar pattern of reduced activation potential (Figure 10a, b). Mean fold change of CD25-positive CAR T cells was significantly decreased upon contact with CD19⁺ cells (12.3-fold in 19_BB_3z vs. 5.5-fold in 19_BB_3z_TIM-3, range 11.4-13.0 and 4.3-6.4, $p< 0.0001$) and CD19⁺/CEACAM⁺ cells (12.3-fold vs. 5.0-fold, range 11.2-13.2 and 3.4-6.4, $p< 0.0001$). Mean fold change of CD137-positive CAR T cells was marginally lower in 19_BB_3z_TIM-3 upon contact with CD19⁺/CEACAM⁺ target cells (27.7-fold in 19_BB_3z vs. 16.9-fold in 19_BB_3z_TIM-3, range 18.3-36.1 and 10.1-24.0, $p= 0.0418$), but showed no significant difference after contact with CD19⁺ target cells (27.7-fold vs. 20.7-fold, range 18.5-36.5 and 16.9-24.4, $p= 0.1009$). No significant difference in fold increase of CD25 and CD137 expression could be detected between the two target cell lines.

CAR T cells were analyzed for cytokine secretion after 24 hours of co-culture with CD19⁺ and CD19⁺/CEACAM⁺ target cells (Figure 9c, d). Again, fold changes were calculated relative to the unstimulated control in order to equalize inherent differences in cytokine secretion among CAR T cells. In first generation CAR T cells, IFN- γ secretion increased 23.6-fold (range 21.7-24.7) in 19_3z, but only 18.6-fold (range 16.2-18.6, $p< 0.0001$) in 19_3z_TIM-3 CAR T cells upon contact with CD19⁺ cells. Nevertheless, IFN- γ release was not significantly different between first generation CAR T cells after contact with CD19⁺/CEACAM⁺ target cells (20.2-fold in 19_3z vs. 18.4-fold in 19_3z_TIM-3, range 15.7-22.6 and 15.8-20.5, $p= 0.2910$). TNF- α secretion increased 24.7-fold in 19_3z (range 23.1-27.8), yet only 12.7-fold (range 9.9-16.1, $p<0.0001$) in 19_3z_TIM-3 CAR T cells upon contact with CD19⁺ cells. Similar results were observed after co-culture with CD19⁺/CEACAM⁺, where TNF- α secretion increased 19.5-fold (range 18.0-20.5) in 19_3z and 13.5-fold in 19_3z_TIM-3 CAR T cells (range 10.2-17.0, $p= 0.0026$).

In accordance with these results, fold change of IFN- γ and TNF- α secretion was similarly reduced in second generation CAR T cells with TIM-3 overexpression (Figure 10c, d). Upon contact with CD19⁺ cells, 19_BB_3z CAR T cells showed a fold change of IFN- γ -positive CAR T cells of 34.4 (range 27.9-40.4), whereas 19_BB_3z_TIM-3 CAR T cells exhibited a fold-increase of only 20.7 (range 18.4-23.7, $p= 0.0005$). Likewise, TNF- α secretion increased 26.9-fold in 19_3z (range 25.1-29.2), but only 17.4-fold (range 14.9-20.5, $p<0.0001$) in 19_BB_3z_TIM-3 CAR T cells. Comparable results were seen after co-culture with the CD19⁺/CEACAM⁺ leukemic cell line: IFN- γ secretion increased 34.6-

fold (range 28.9-40.9) in 19_BB_3z, but only 21.1-fold (range 18.4-25.1, $p= 0.0004$) in 19_BB_3z_TIM-3 CAR T cells. TNF- α secretion increased 24.5-fold for 19_BB_3z (range 23.1-25.7), but only 16.8-fold (range 15.4-18.3, $p<0.0001$) in 19_BB_3z_TIM-3 CAR T cells after co-culture with CD19⁺/CEACAM⁺ cells. Again, no significant difference in fold increase of cytokine secretion could be detected between the two target cell lines.

Finally, CAR T-cell proliferation was measured using a CellTrace violet based approach as described in the methods (Figure 9e, Figure 10e). In first generation CAR T cells with TIM-3 overexpression, a mean of 27.0% (range 21.9-34.7%) of cells proliferated upon contact with CD19⁺ target cells, whereas 36.6% (range 32.2-39.7%, $p= 0.0036$) of conventional CAR T cells proliferated. Co-culture with CD19⁺/CEACAM⁺ target cells induced 34.5% (range 20.4-47.1%) of proliferation in 19_3z and 28.4% (range 25.6-33.9%) of proliferation in 19_3z_TIM-3 CAR T cells. Conventional 19_BB_3z CAR T cells showed 37.0% (range 26.8-47.2%) of mean proliferation upon contact with CD19⁺ target cells, whereas 19_BB_3z_TIM-3 demonstrated 14.9% of mean proliferation (range 9.0%-21.8%, $p= 0.0008$). Upon contact with CD19⁺/CEACAM⁺ cells, 19_BB_3z CAR T cells showed 36.1% (range 31.1-42.7%) of mean proliferation and a mean of 18.2% (range 7.74-28.9%, $p= 0.003$) of proliferating CAR T cells could be detected in 19_BB_3z_TIM-3 CAR T cells. In both first and second generation CAR T cells, no significant difference was found between co-culture with CD19⁺ and CD19⁺/CECAM⁺ cells.

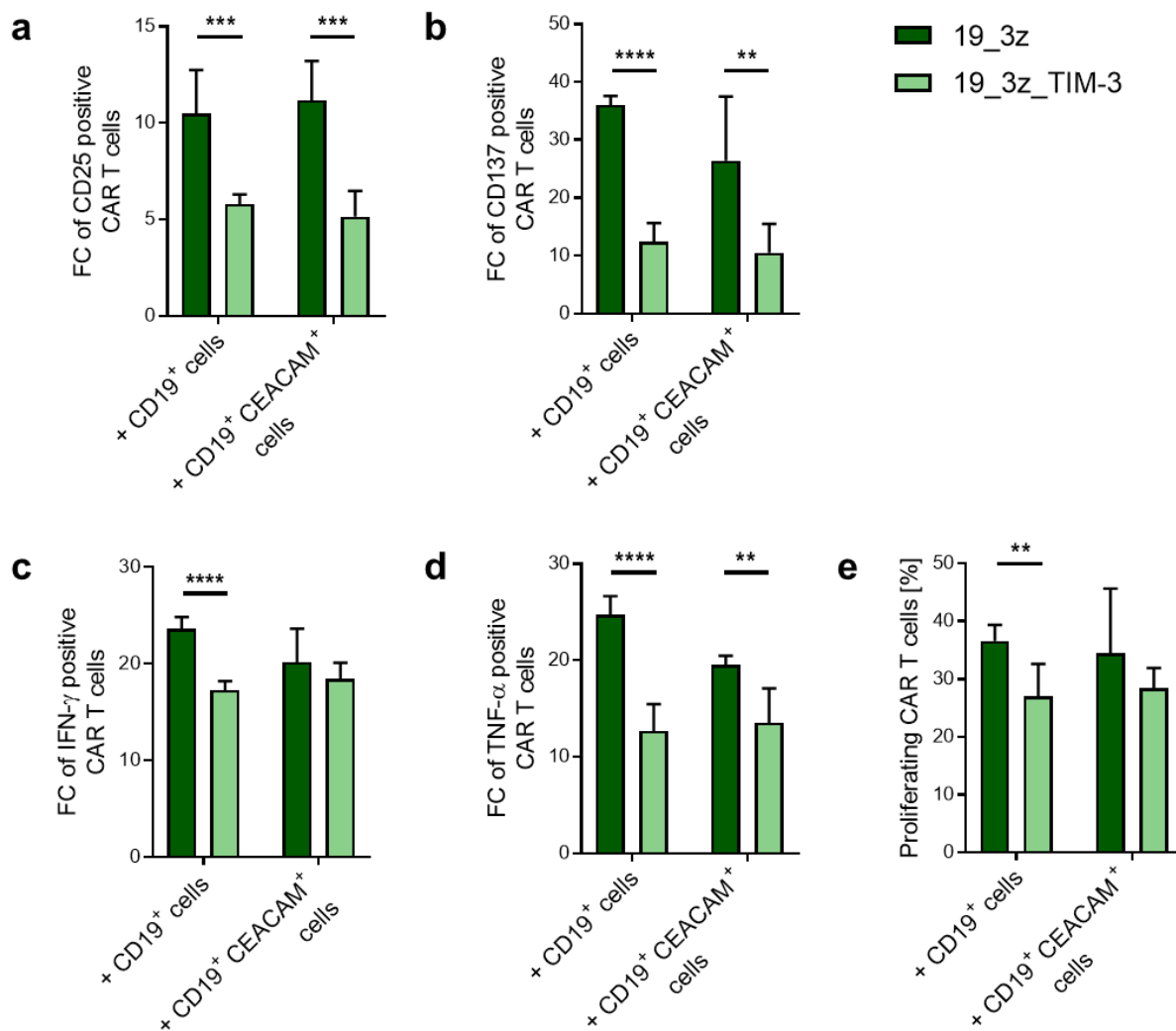


Figure 9: TIM-3 overexpressing first generation CAR T cells demonstrate impaired activation, cytokine secretion, and proliferation potential. Functional characterization was performed by co-culturing CAR T cells with CD19⁺ or CD19⁺ CEACAM⁺ K562 target-cell line followed by flow-cytometric measurement of activation marker expression, cytokine secretion and proliferation. Fold changes were calculated relative to the unstimulated control of each CAR construct. **a, b**, Fold change of CD25- (**a**) and CD137-positive (**b**) CAR T cells after 48 hours of co-culture with K562 target-cell lines. **c, d**, Fold change of IFN- γ - (**c**) and TNF- α -positive (**d**) CAR T cells after 24 hours of co-culture with K562 target-cell lines. Cytokine secretion was assessed by intracellular cytokine staining. **e**, Percentage of proliferating CAR T cells after 72 hours of co-culture with K562 target-cell lines. Proliferation was determined using a CellTrace violet based approach as described in the methods. Data are representative of two donors and experiments were performed in technical triplicates. Data are mean \pm SD. *P* values were determined using a two-tailed unpaired Student's *t* test. FC= Fold change. IFN- γ = Interferon gamma. TNF- α = Tumor necrosis factor alpha

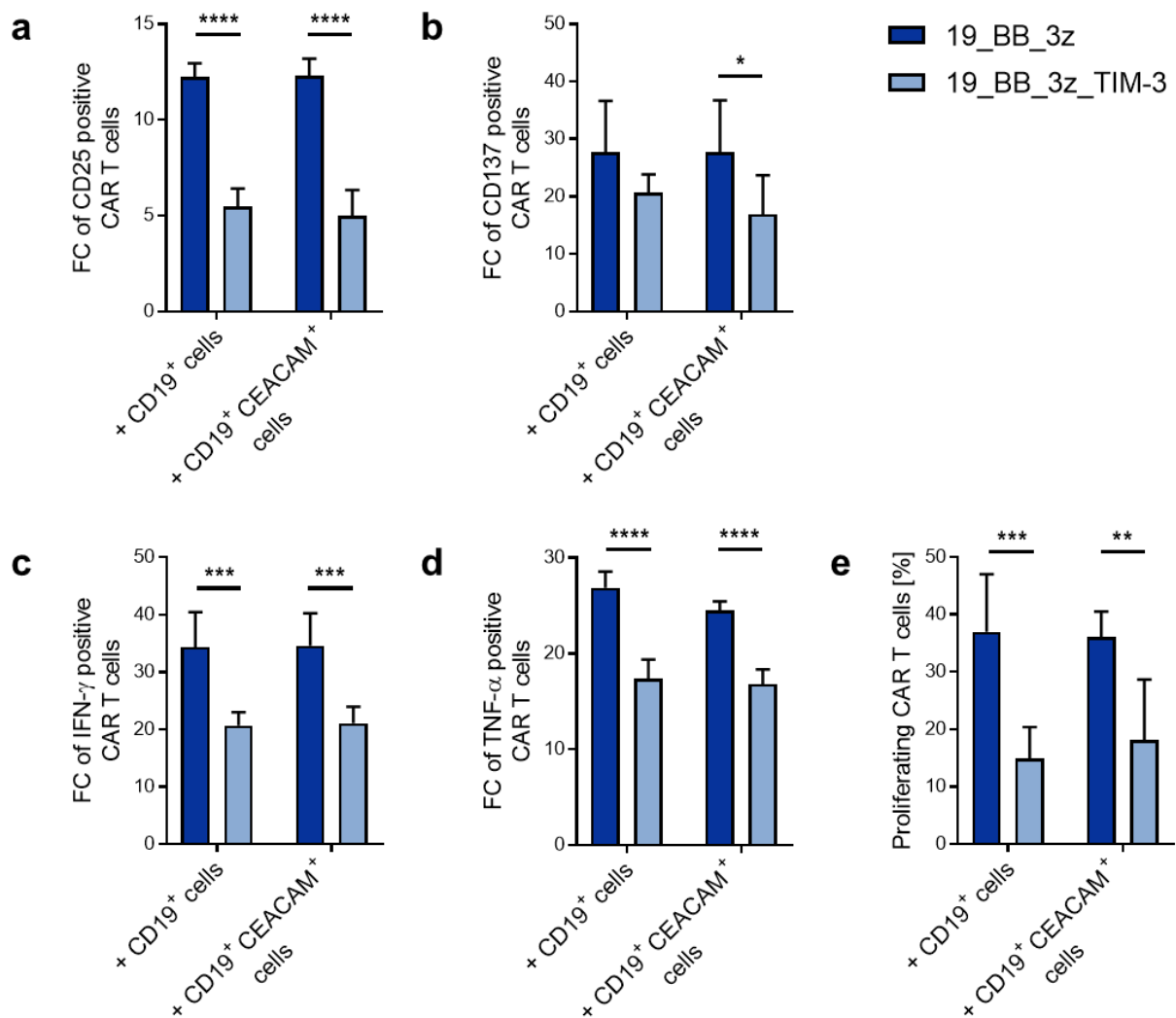


Figure 10: TIM-3 overexpressing second generation CAR T cells demonstrate impaired activation, cytokine secretion, and proliferation potential. Functional characterization was performed by co-culturing CAR T cells with CD19⁺ or CD19⁺ CEACAM⁺ K562 target-cell line followed by flow-cytometric measurement of activation marker expression, cytokine secretion and proliferation. Fold changes were calculated relative to the unstimulated control of each CAR construct. **a, b**, Fold change of CD25- (**a**) and CD137-positive (**b**) CAR T cells after 48 hours of co-culture with K562 target-cell lines. **c, d**, Fold change of IFN- γ - (**c**) and TNF- α -positive (**d**) CAR T cells after 24 hours of co-culture with K562 target-cell lines. Cytokine secretion was assessed by intracellular cytokine staining. **e**, Percentage of proliferating CAR T cells after 72 hours of co-culture with K562 target-cell lines. Proliferation was determined using a CellTrace violet based approach as described in the methods. Data are representative of two donors and experiments were performed in technical triplicates. Data are mean \pm SD. *P* values were determined using a two-tailed unpaired Student's *t* test. FC= Fold change. IFN- γ = Interferon gamma. TNF- α = Tumor necrosis factor alpha.

6.4 Retroviral transduction of T cells with TIM-3/CD28 fusion receptor constructs

To overcome TIM-3-mediated inhibition of CAR T cells, we adopted the concept of a fusion receptor which has been previously described involving the inhibitory molecules PD-1 and CD200R.^{64,65} Incorporating the extracellular domain of TIM-3 and an intracellular domain derived from CD28, the fusion receptor would transform the inhibitory signal mediated by TIM-3 into an activating signal via CD28. In order to identify a design that would provide superior signaling, we generated TIM-3/CD28 fusion receptor constructs with varying intracellular, transmembrane, and extracellular domains and

initially evaluated their functionality in absence of CAR signaling. Hence, human primary T cells were retrovirally transduced with different TIM-3/CD28 fusion receptor constructs, as depicted in Figure 11a. The 8-TM construct incorporated a CD8 transmembrane domain. TIM-3 transmembrane domains were integrated into constructs TIM3-TM1 and TIM3-TM2. Constructs 28-TM1, 28-TM2, and 28-TM3 each contained CD28-derived transmembrane domains. Additional amino acids derived from CD28 were incorporated into the extracellular domains of 28-TM2 (9 amino acids) and 28-TM3 (12 amino acids including cysteine). Thus, 28-TM3 provided a dimerizing motif and displayed the highest CD28 proportion. Untransduced T cells served as control, as well as a truncated TIM-3 construct (TIM3t), which incorporated the extracellular and transmembrane domain of TIM-3 but lacked the intracellular signaling domain. Thus, potential alterations in expansion, phenotype, and cellular composition due to the transduction process could be detected.

On day 12 after transduction, transduction rate was determined by flow-cytometric stain for TIM-3 (Figure 11b, c). Mean transduction rate of all constructs was 69.6% (range 31.3-92.4%). Transduction rate was lowest for 8-TM (mean 41.8%, range 31.3-54.0%) and highest for TIM3-TM2 transduced T cells (mean 83.8%, range 75.3-92.4%). Untransduced T cells showed a mean TIM-3 positivity of 4.6% (range 1.7%-11.9%). Thus, endogenous TIM-3 expression provided a minor, indistinguishable background in transduced T cells. A donor-dependent variation in transduction rate could be observed.

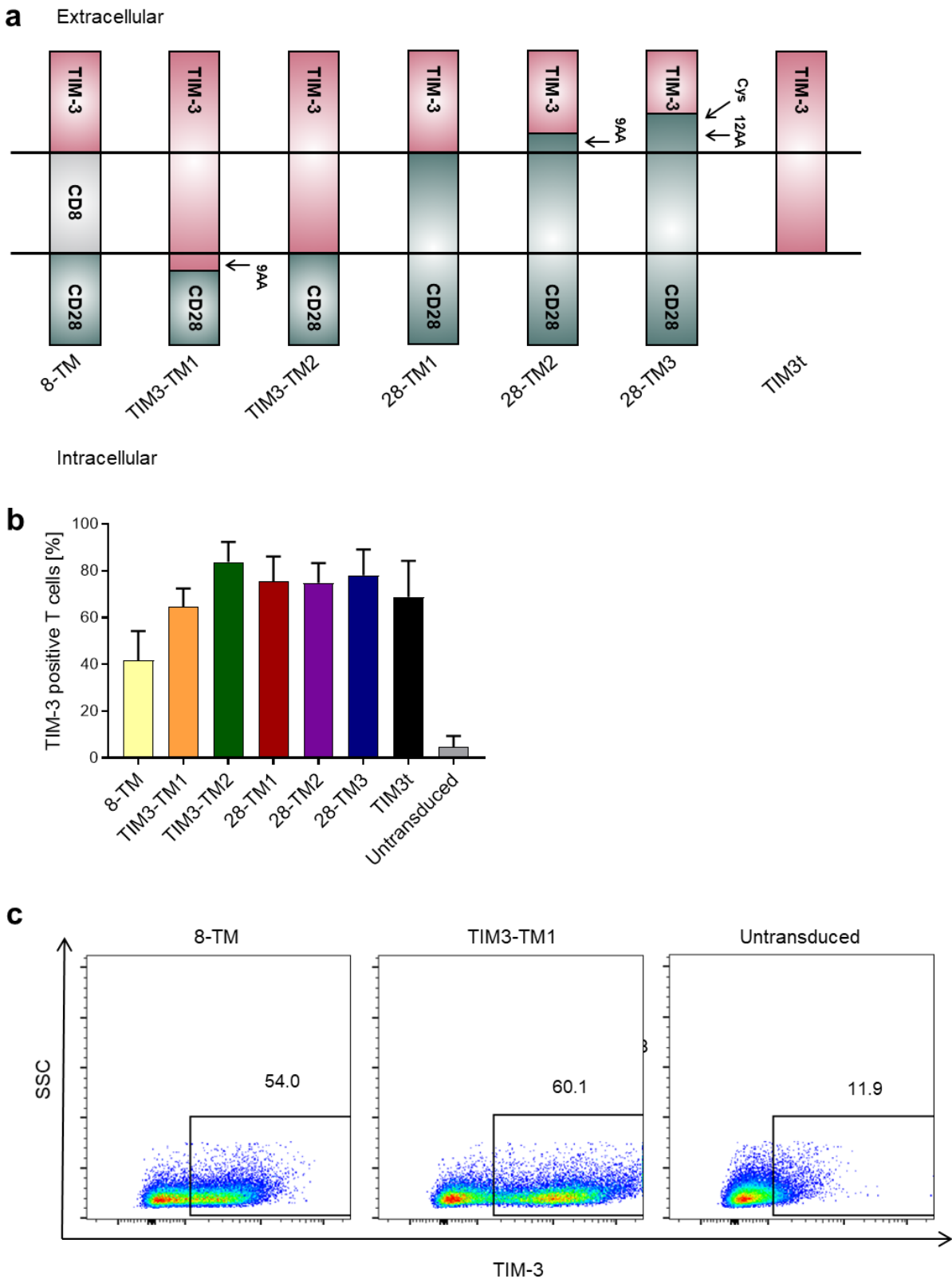


Figure 11: Retroviral transduction of T cells with TIM-3/CD28 fusion receptor constructs incorporating distinct extracellular, transmembrane, and intracellular domains. **a**, Schematic overview of TIM-3/CD28 fusion receptor constructs. **b**, Transduction rate at day 12 post-transduction was determined by flow-cytometric analysis of TIM-3-positive T cells. **c**, Representative flow-cytometric analysis of TIM-3 expression at day 12 post-transduction. Gates were set according to untransduced and unstained control. Data are representative of four donors. Data are mean \pm SD.

6.5 TIM-3/CD28 fusion receptor-transduced T cells exhibit similar expansion rates, viability and phenotype

As described in 6.1, T cells were expanded for 12 days following transduction, during which fold expansion and viability of T cells was determined (Figure 12a). Fusion receptor transduced T cells exhibited mean viability of 83.9% (range 73.1-97.5%) during the expansion process. No significant differences in overall viability were found between constructs. Mean expansion rate was 43.8-fold (range 17.6-79.7) among all fusion receptor transduced T cells. No significant differences in expansion rates were found between fusion receptor transduced T cells.

On day 12 post-transduction, fusion receptor transduced T cells were analyzed for phenotypical differences between constructs (Figure 12b), as described in the methods. All T cells displayed a central memory- and effector memory-predominant phenotype with a small proportion of naive T cells of under 2%. Fusion receptor transduced T cells showed a mean of 3.3% of effector, 61.4% of effector memory, 30.5% of central memory, and 5.1% of stem cell-like memory T cells. Comparison among fusion receptor transduced T cells yielded no significant differences in percentages of T-cell subpopulations.

To verify the purity of the T cell product after the expansion period, analysis of cellular composition was performed on day 12 post-transduction (Figure 12c). In all fusion receptor transduced cells, high purity was confirmed by 97.4% of T cells in the final product. A low CD4/CD8 ratio could be observed, with a mean of 31.3% of CD4-positive and a mean of 62.1% of CD8-positive T cells. Minor percentages of NK cells (mean 0.2%) and NK T cells (mean 2.1%) were detected. No significant differences in cellular composition were found among different T cell constructs.

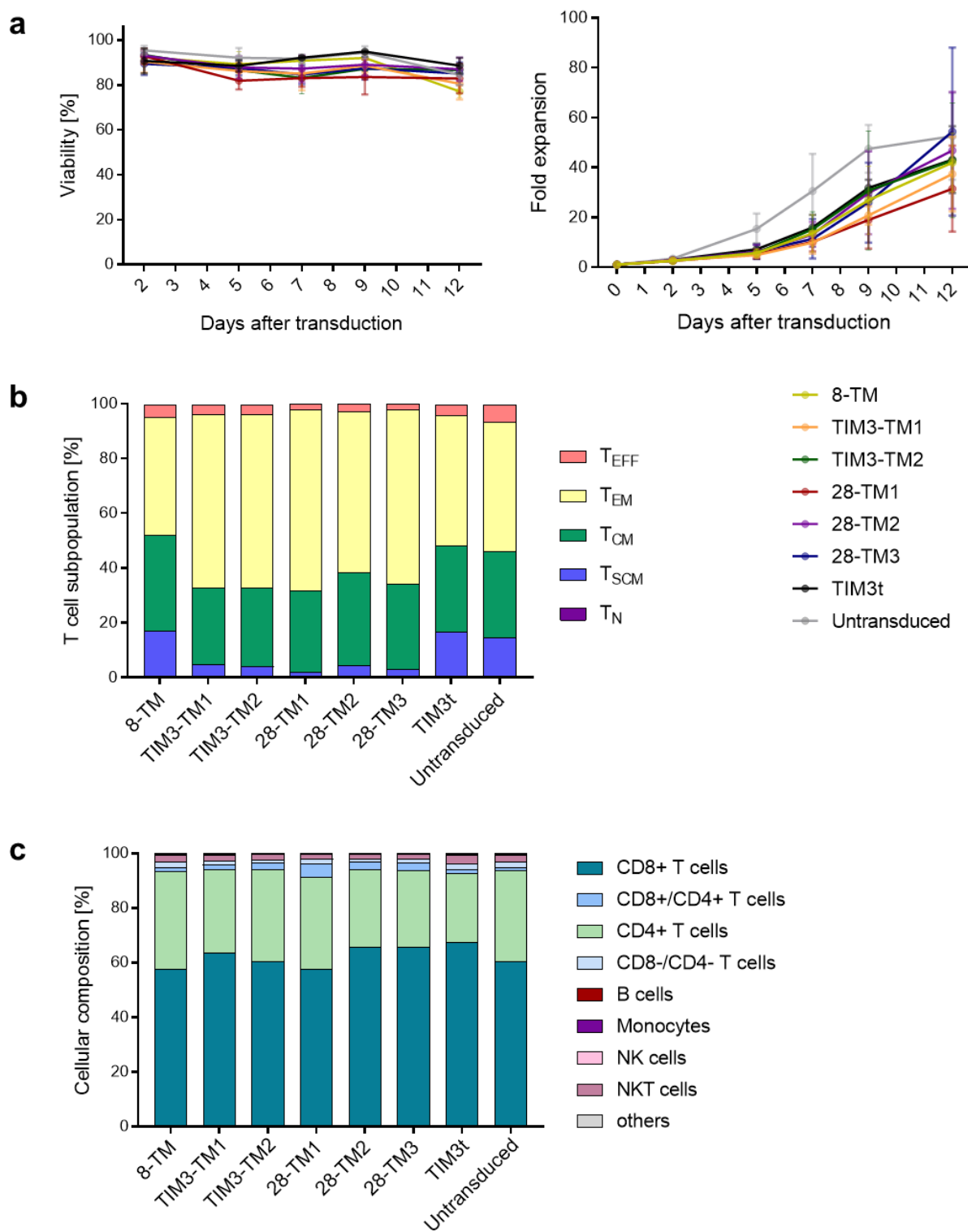


Figure 12: Expansion, phenotype, and cellular composition of TIM-3/CD28 fusion receptor-transduced T cells. **a**, Fold expansion of T cells relative to initial cell number used for transduction. **b**, Viability of T cells during the expansion period as determined by count of living cells relative to total cell count. **c**, Phenotypical characterization of T cells at day 12 post-transduction as assessed by flow-cytometric stain for CD62L, CD95, and CD45RO. T cells were considered as naive T cells if CD62L⁺/CD95⁻/CD45RO⁻, as stem cell-like memory T cells if CD62L⁺/CD95⁺/CD45RO⁻, as central memory T cells if CD62L⁺/CD95⁺/CD45RO⁺, as effector memory T cells if CD62L⁻/CD95⁺/CD45RO⁺, and as effector T cells if CD62L⁻/CD95⁺/CD45RO⁻. **d**, Cellular composition of T-cell product at day 12 post-transduction as determined by flow-cytometric stain for CD3, CD4, CD8, CD14, CD19, and CD56. Analysis of cellular composition was performed as described in the methods. Data are representative of four donors. Data are mean (**c, d**) and mean \pm SD (**a, b**). T_{EFF}= Effector T cells; T_{EM}= Effector memory T cells; T_{CM}= Central memory T cells; T_{SCM}= Stem cell-like memory T cells; T_N= Naive T cells. NK cells= Natural killer cells. NKT cells= Natural killer T cells.

6.6 Functional comparison of TIM-3/CD28 fusion receptor-transduced T cells reveals high activation potential in accordance with CD28 proportion in the construct

In order to identify a TIM-3/CD28 fusion receptor construct with superior activation potential, further functional characterization of fusion receptor transduced T cells was performed (Figure 13). As described in the methods, functional characterization was conducted through CD3 stimulation and subsequent analysis of CD3 activation-induced cytokine secretion and proliferation.

Cytokine secretion was assessed 6 hours after anti-CD3 stimulation (Figure 13a, b). To emphasize fusion receptor-mediated cytokine secretion, fold changes of IFN- γ and TNF- α secretion were calculated relative to the stimulated, untransduced control. Hence, significant differences in fold change of cytokine secretion refer to comparison with the untransduced control. Upon CD3 stimulation, mean fold change of IFN- γ -positive T cells was 2.0 in fusion receptor transduced T cells. IFN- γ secretion increased 1.5-fold (range 1.4-1.6, $p < 0.0001$) in 8-TM, 1.7-fold (range 1.6-1.9, $p < 0.0001$) in TIM3-TM1, and 1.9-fold (range 2.1-1.7, $p < 0.0001$) in TIM3-TM2 transduced T cells. In fusion receptor transduced T cells with CD28 transmembrane domain, IFN- γ secretion increased 2.0-fold (range 1.9-2.2, $p < 0.0001$) in 28-TM1, 2.2-fold (range 2.2-2.3, $p < 0.0001$) in 28-TM2, and 2.4-fold (range 2.3-2.5, $p < 0.0001$) in 28-TM3 transduced T cells.

Fusion receptor transduced T cells showed a mean fold increase in TNF- α secretion of 1.2 upon CD3 stimulation. TNF- α secretion marginally increased in 8-TM (1.0-fold, range 1.0-1.1, $p = 0.0072$) and in TIM3-TM2 transduced T cells (1.1-fold, range 0.9-1.2, $p = 0.6223$). In TIM3-TM1 transduced T cells, TNF- α secretion slightly decreased (0.9-fold, range 0.7-1.3, $p = 0.6163$) relative to the untransduced control. In fusion receptor transduced T cells with CD28 transmembrane domain, TNF- α secretion increased 1.3-fold (range 1.1-1.4, $p = 0.0129$) in 28-TM1, 1.4-fold (range 1.2-1.4, $p = 0.0002$) in 28-TM2, and 1.5-fold (range 1.3-1.5, $p < 0.0001$) in 28-TM3 transduced T cells.

To determine the proliferative capacity of fusion receptor-transduced T cells upon stimulation, proliferation was measured as described in the methods (Figure 13c). Since T cells differed in intrinsic proliferation in their respective unstimulated control (data not shown), fold changes relative to the unstimulated control were calculated, and p values refer to comparison with the untransduced control. After stimulation, untransduced T cells showed an 8.8-fold proliferation (range 6.0-11.7), which was comparable to proliferation of T cells transduced with 8-TM, TIM3-TM1, TIM3-TM2, and 28-TM1. Upon stimulation, 8-TM proliferated 6.6-fold (range 5.0-8.2, $p = 0.2834$), TIM3-TM1 proliferated 9.1-fold (range 6.7-11.7, $p = 0.9093$), TIM3-TM2 proliferated 15.4-fold (range 9.4-21.6, $p = 0.1395$), and 28-TM1 proliferated 12.6-fold (range 7.4-18.0, $p = 0.3155$). In contrast, 28-TM2 and 28-TM3 transduced T cells exhibited a significantly higher fold change of proliferation than

untransduced T cells. Upon stimulation, 28-TM2 proliferated 32.7-fold (range 24.8-40.9, $p= 0.0023$) and 28-TM3 proliferated 34.5-fold (range 29.7-40.4, $p= 0.0002$).

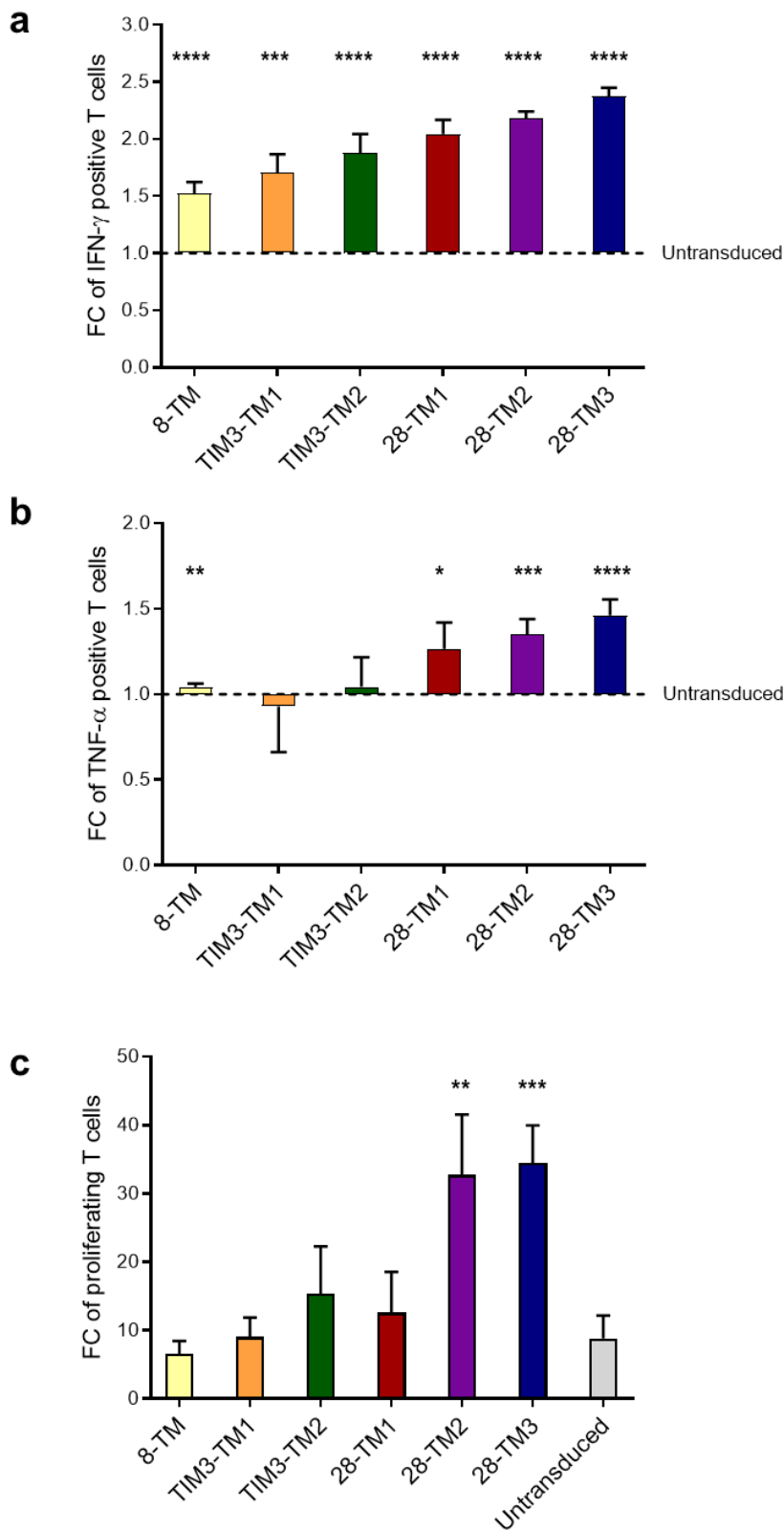


Figure 13: TIM3/CD28 fusion receptor-transduced T cells show superior cytokine secretion and proliferation potential upon CD3 stimulation. Functional characterization was performed by stimulation of T cells with an anti-CD3 antibody and subsequent flow-cytometric analysis of cytokine secretion and proliferation. Fold changes were calculated relative to the untransduced control (a, b) or relative to the unstimulated control of each construct (c). a, b, Fold change of IFN- γ - (a) and TNF- α -positive (b) T cells after 6 hours of CD3 stimulation. Cytokine secretion was assessed by intracellular cytokine staining. c, Fold change of proliferating T cells after 72 hours of CD3 stimulation. Data are representative of two donors and experiments were performed in technical duplicates. Data are mean \pm SD. P values were determined using a two-tailed unpaired Student's *t* test. Significant differences refer to comparison with untransduced T cells. FC= Fold change. IFN- γ = Interferon gamma. TNF- α = Tumor necrosis factor alpha.

6.7 Generation of CD19 CAR T cells incorporating TIM-3/CD28 fusion receptor constructs with superior activation potential

First and second generation CAR T cells with and without TIM-3/CD28 fusion receptor were generated by retroviral transduction of primary human T cells (Figure 14a). Hence, either the 28-TM2 or the 28-TM3 fusion-receptor constructs were combined with the first and second generation CAR constructs defined in 6.1. CAR T cells with fusion receptor incorporated a c-myc tag, which was inserted between the anti-CD19 scFv and the CD8 transmembrane and extracellular spacer domain, thus enabling flow-cytometric detection of CAR transduced T cells. The fusion receptor was linked to the CAR constructs by an F2A linker, thus providing co-expression of CAR and fusion receptor. As in 6.1, 19t CAR T cells and untransduced T cells were used as control.

Transduction rate was measured by flow-cytometric stain for the c-myc tag on day 12 post-transduction (Figure 14b, c). In first generation CAR T cells, both 19_3z_28-TM2 and 19_3z_28-TM3 showed comparable transduction rates (mean=63.9% and 77.9%, range= 56.1-71.8% and 76.5-79.4%), that were not significantly different from conventional 19_3z CAR T cells (mean=75.6%, range 67.4-83.3%, $p= 0.4149$ and $p= 0.7782$).

Second generation CAR T cells with fusion receptor demonstrated mean transduction rates of 62.6% (range 54.8-70.3%) in 19_BB_3z_28-TM2 and 56.4% in 19_BB_3z_28-TM3. Conventional second generation CAR T cells showed a comparable mean transduction rate of 64.2% (range 60.0-68.4%, $p= 0.8688$ and $p= 0.3680$). Flow-cytometric staining for TIM-3 and the c-myc tag showed correlation of both, suggesting co-expression of CAR and fusion receptor in CAR T cells with TIM-3/CD28 fusion receptor (Figure 14c, data not shown for other constructs).

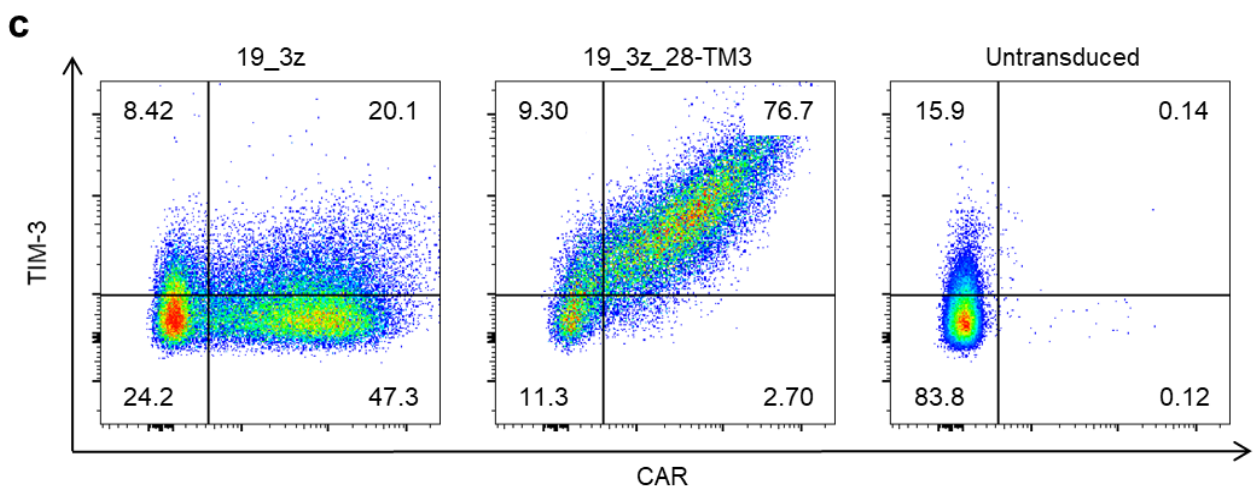
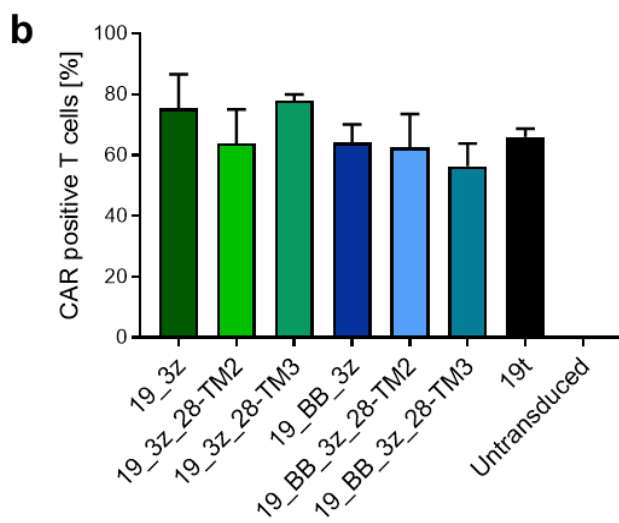
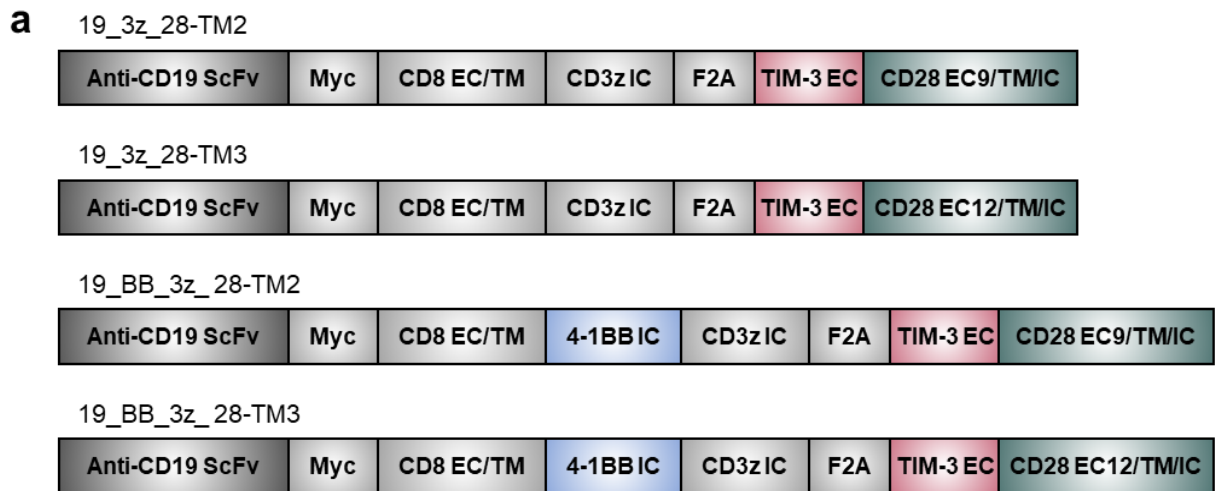


Figure 14: Generation of CD19 CAR T cells incorporating TIM-3/CD28 fusion receptors. a, Schematic overview of CAR constructs. **b**, CAR transduction rate at day 12 post-transduction was determined by flow-cytometric stain for c-myc tag. **c**, Representative flow-cytometric analysis of CAR and TIM-3 expression at day 12 post-transduction. Gates were set according to untransduced and unstained control. Data are representative of two donors. Data are mean \pm SD. EC= Extracellular; TM= Transmembrane; IC= Intracellular.

6.8 CAR T cells with a TIM-3/CD28 fusion receptor show comparable expansion rates and viability

As previously described, CAR T-cell viability and expansion rates were assessed regularly after transduction. First generation CAR T cells with and without fusion receptor showed comparable expansion rates on day 12 post-transduction (Figure 15a). 19_3z CAR T cells showed 44.3-fold expansion on day 12 post-transduction. 19_3z_28-TM2 CAR T cells exhibited 98.9-fold expansion, and 19_3z_28-TM3 CAR T cells showed 130.0-fold expansion on day 12 post-transduction. Similarly, expansion rates were comparable between second generation CAR T cells with and without fusion receptor. Mean expansion rates were 70.2-fold in 19_BB_3z, 93.4-fold in 19_BB_3z_28-TM2, and 96.2-fold in 19_BB_3z_28-TM3 CAR T cells. No significant difference in expansion rate could be observed among CAR T cells (p values and range not shown).

CAR T cells displayed mean viability of 92.9% throughout the expansion process (Figure 15b). In first generation CAR T cells, viability among constructs was comparable (p values and range not shown). Mean viability was 92.1% in 19_3z, 94.1% in 19_3z_28-TM2, and 92.0% in 19_3z_28-TM3 CAR T cells. Second generation CAR T cells equally showed comparable viability throughout all time points (p values and range not shown). Mean viability was 92.0% in 19_BB_3z, 93.8% in 19_BB_3z_28-TM2, and 92.2% in 19_BB_3z_28-TM3 CAR T cells.

CAR T cells were analyzed for their cellular composition on day 12 post-transduction to detect potential alterations in CAR T cells with fusion receptor (Figure 15c). High purity was confirmed by 97.0% of T cells in the final product. A high CD4/CD8 ratio could be observed, with a mean of 64.0% of CD4-positive and a mean of 29.9% of CD8-positive T cells. Minor percentages of NK cells (mean 0.3%) and NK T cells (mean 1.2%) were detected. No significant differences in cellular composition were found among CAR T cells.

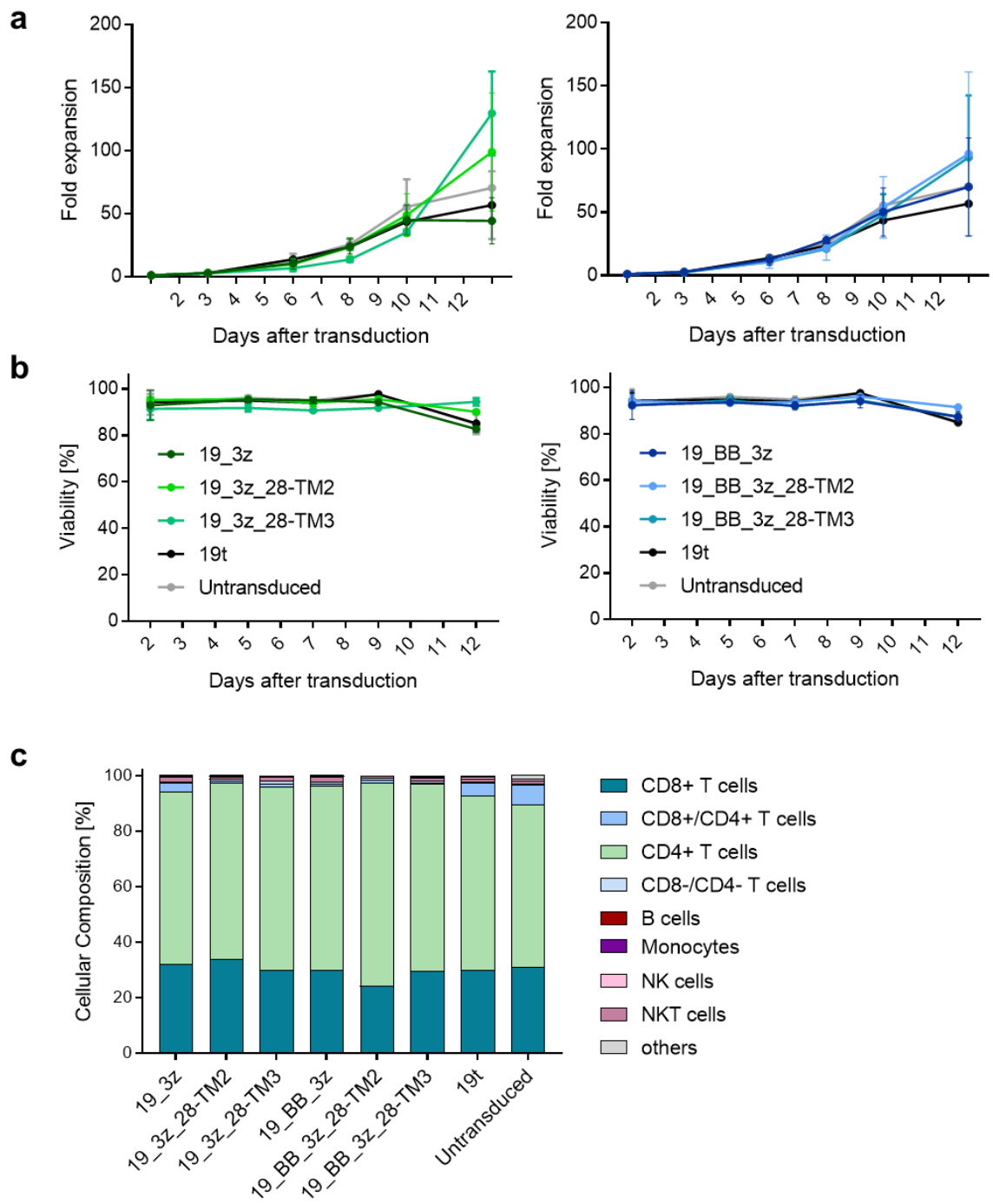


Figure 15: Expansion, viability, and cellular composition of CAR T cells with TIM-3/CD28 fusion receptors. **a**, Fold expansion of 19_3z (left) and 19_BB_3z (right) CAR T cells relative to initial cell number used for transduction. **b**, Viability of 19_3z (left) and 19_BB_3z (right) CAR T cells during the expansion period as determined by count of living cells relative to total cell count. **c**, Cellular composition of T cell product at day 12 post-transduction as determined by flow-cytometric stain for CD3, CD4, CD8, CD14, CD19, and CD56. Analysis of cellular composition was performed as described in the methods. Data are representative of two donors (**a**, **b**) and one donor (**c**). Data are mean (**c**) and mean \pm SD (**a**, **b**). NK cells= Natural killer cells. NKT cells= Natural killer T cells.

6.9 TIM-3/CD28 fusion receptor CAR T cells undergo comparable differentiation of phenotype upon contact with CD19-positive target cells

In order to detect potential differences in phenotype between CAR T cells, characterization of T-cell subpopulations was conducted (Figure 16). Phenotype of CAR T cells was then reevaluated after co-culture with CD19⁺ K562 cells, to determine phenotypical differentiation upon contact with target cells.

Inherent phenotype was found to be significantly altered between conventional CAR T cells and CAR T cells with TIM-3/CD28 fusion receptors (Figure 16, left). In first generation CAR T cells, significant differences were found in mean proportion of effector, effector memory, central memory, and stem cell-like memory T cells (Figure 16a, left). 19_3z showed a mean of 34.9% of effector, 33.1% of effector memory, 7.9% of central memory, and 23.1% of stem cell-like memory T cells. In contrast, 19_3z_28-TM2 CAR T cells showed a mean 15.7% of effector ($p= 0.0008$), 47.7% of effector memory ($p= 0.0142$), 25.7% of central memory ($p= 0.0004$), and 11.1% of stem cell-like memory T cells ($p= 0.0219$). 19_3z_28-TM3 CAR T cells exhibited 14.8% of effector ($p= 0.0082$), 42.1% of effector memory ($p= 0.0651$), 35.8% of central memory ($p= 0.0003$), and 7.47% of stem cell-like memory T cells ($p= 0.0137$).

Likewise, comparison of second generation CAR T cells with and without fusion receptor yielded a significant difference in percentages of effector and stem cell-like memory T cells (Figure 16b, left). 19_BB_3z showed a mean of 24.6% of effector, 47.0% of effector memory, 9.8% of central memory, and 18.4% of stem cell-like memory T cells. 19_BB_3z_28-TM2 CAR T cells displayed a mean of 16.6% of effector ($p= 0.0361$), 51.0% of effector memory ($p= 0.1993$), 18.4% of central memory ($p= 0.0082$), and 14.0% of stem cell-like memory T cells ($p= 0.1771$). 19_BB_3z_28-TM3 CAR T cells exhibited 17.8% of effector ($p= 0.0086$), 46.8% of effector memory ($p= 0.3095$), 18.4% of central memory ($p= 0.0082$), and 16.7% of stem cell-like memory T cells ($p= 0.1998$).

After co-culture with CD19⁺ target cells, T-cell phenotype equally transformed to a central memory- and effector memory-predominant phenotype in all CAR T cells (Figure 16, right). A negligible proportion of naive (mean 0.10%) and stem cell-like memory T cells (mean 1.82%) was observed. First generation CAR T cells showed a mean of 14.5% of effector, 55.4% in effector memory, and 39.3% in central memory T cells (Figure 16a, right). Second generation CAR T cells exhibited a mean of 1.71% of effector, 64.5% of effector memory, and 34.0% of central memory T cells (Figure 16b, right). Upon contact with target cells, no significant difference was found between conventional CAR T cells and CAR T cells with fusion receptor.

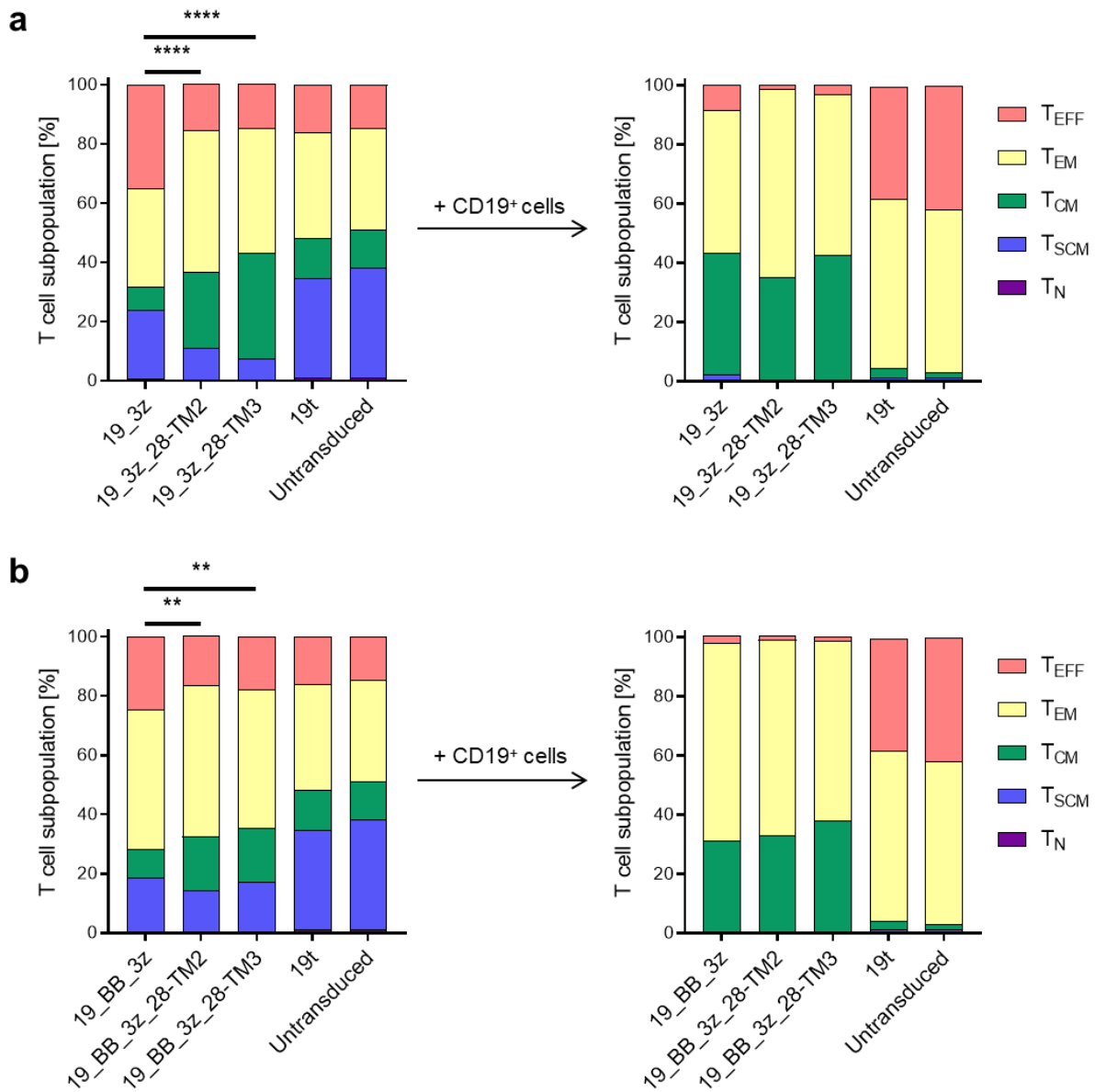


Figure 16: Phenotypical characterization of CAR T cells with TIM-3/CD28 fusion receptors upon target-cell contact. Phenotype of CAR T cells was assessed by co-culturing CAR T cells with CD19⁺ K562 target-cell line. Flow-cytometric stain for CD62L, CD95, and CD45RO was performed 72 hours after start of co-culture. T cells were considered as naive T cells if CD62L⁺/CD95⁻/CD45RO⁻; as stem cell-like memory T cells if CD62L⁺/CD95⁺/CD45RO⁻; as central memory T cells if CD62L⁺/CD95⁺/CD45RO⁺; as effector memory T cells if CD62L⁻/CD95⁺/CD45RO⁺; and as effector T cells if CD62L⁻/CD95⁺/CD45RO⁻. **a**, Phenotypical characterization of 19_3z CAR T cells prior to (left) and after (right) co-culture with CD19⁺ K562 target-cell line. Significant differences between CAR T cells refer to percentage of T_{SCM} ($p < 0.05$), T_{CM} ($p < 0.0001$), T_{EM} ($p < 0.05$) and T_{EFF} ($p < 0.01$). **b**, Phenotypical characterization of 19_BB_3z CAR T cells prior to (left) and after (right) co-culture with CD19⁺ K562 target-cell line. Significant differences between CAR T cells refer to percentage of T_{CM} ($p < 0.01$) and T_{EFF} ($p < 0.01$). Data are representative of one donor and experiments were performed in technical duplicates. Data are mean. P values were determined using a one-way ANOVA followed by Tukey's multiple comparison test. T_{EFF}= Effector T cells; T_{EM}= Effector memory T cells; T_{CM}= Central memory T cells; T_{SCM}= Stem cell-like memory T cells; T_N= Naive T cells.

6.10 Combination of first generation CAR T cells with a TIM-3/CD28 fusion receptor leads to augmented functionality against CEACAM-positive cell line

Further characterization of first generation CAR T cells with fusion receptors was conducted through functional analysis in co-culture experiments with CD19⁺/CEACAM⁺ target cells. Cytotoxicity, activation marker expression, cytokine secretion, and proliferative capacity upon target cell contact were assessed and compared to results for conventional CAR T cells.

Cytotoxic capacity of CAR T cells was analyzed 48 hours after start of co-culture (Figure 17a). First generation CAR T cells with and without fusion receptor showed an E:T ratio-dependent killing of CD19⁺/CEACAM⁺ cells. Compared to conventional CAR T cells, CAR T cells with TIM-3/CD28 fusion receptor constructs demonstrated significantly higher cytotoxicity at all E:T ratios. At the 1:1 E:T ratio, 19_3z CAR T cells killed 70.7% (range 69.3-73.7%) of target cells. In contrast, 19_3z_28-TM2 showed 82.8% (range 79.7-86.2%, $p=0.0010$) and 19_3z_28-TM3 CAR T cells demonstrated 82.3% (range 82.3-83.3%, $p=0.0030$) of mean target-cell lysis. At the 0.1:1 E:T ratio, cytotoxicity was significantly greater in 19_3z_28-TM2 (mean 45.1%, range 35.1-54.1%, $p=0.0151$) and in 19_3z_28-TM3 (mean 50.1%, range 47.3-52.6%, $p< 0.0001$) than in 19_3z CAR T cells (mean 26.7%, range 22.8-29.9%). At the lowest E:T of 0.01:1, higher target-cell killing was observed in 19_3z_28-TM2 (mean 11.5%, range 9.7-13.7%, $p=0.0177$) and in 19_3z_28-TM3 (mean 13.5%, range 11.1-16.5%, $p= 0.0208$) compared to 19_3z CAR T cells (mean 3.0%, range -3.6-7.8%). No significant difference in cytotoxicity was observed among the two different fusion receptors.

Activation of CAR T cells was determined by expression of activation markers CD25 and CD137 (4-1BB) 14 hours after start of co-culture (Figure 17b). Mean fluorescence intensity (MFI) of activation markers was utilized as indicator for surface expression of CD25 and CD137. First generation CAR T cells with TIM-3/CD28 fusion receptor demonstrated elevated surface expression of CD25 compared with conventional CAR T cells. MFI of CD25 was 7196 ($p= 0.0003$) in 19_3z_28-TM2 and 6151 ($p= 0.0001$) in 19_3z_28-TM3 CAR T cells. 19_3z CAR T cells showed an MFI of 3292 for CD25. MFI of CD137 was not significantly different between CAR T cells with and without fusion receptor. MFI of CD137 was observed to be 2537 ($p= 0.5876$) in 19_3z_28-TM2, 3112 ($p= 0.1238$) in 19_3z_28-TM3, and 2367 in 19_3z CAR T cells. Comparison among CAR T cells with fusion receptor showed a higher MFI of CD25 in 19_3z_28-TM2 CAR T cells ($p= 0.0219$) but no significant difference in the MFI of CD137 ($p= 0.1041$).

After 6 hours of co-culture with CD19⁺/CEACAM⁺ target cells, cytokine secretion was measured by intracellular cytokine stain (Figure 17c). A tendency towards increased IFN- γ secretion in CAR T cells with fusion receptor was observed. Yet, comparison with conventional CAR T cells yielded no significant difference between 19_3z_28-TM2 (mean 27.7%, range 23.8-31.9%, $p= 0.0758$), 19_3z_28-TM3 (mean 32.6%, range 28.8-36.0%, $p= 0.0503$), and 19_3z (mean 23.2%, range 20.9-

25.1%). IL-2 secretion was found to be significantly higher in CAR T cells with fusion receptor than in conventional CAR T cells. A mean of 29.8% (range 22.3-37.4%, $p= 0.0199$) of 19_3z_28-TM2 CAR T cells showed IL-2 secretion and 40.6% (range 39.1-41.7%, $p< 0.0001$) were IL-2-positive in 19_3z_28-TM3 CAR T cells. 19_3z CAR T cells showed 16.8% (range 13.9-20.1%) of IL-2 positivity. CAR T cells with fusion receptor demonstrated significantly higher levels of TNF- α secretion than conventional CAR T cells. 19_3z_28-TM2 CAR T cells showed a mean 26.6% (range 26.3-27.5%, $p= 0.0001$) of TNF- α secretion and 19_3z_28-TM3 CAR T cells exhibited a mean 37.1% (range 29.0-45.2%, $p= 0.0048$) of TNF- α -positive CAR T cells. 19_3z CAR T cells showed a mean 16.9% (range 15.0-19.3%) of TNF- α positivity. Comparison among the two different fusion receptors yielded a significantly higher percentage of IL-2-positive T cells in 19_3z_28-TM3 CAR T cells ($p= 0.0296$), but no difference was found in IFN- γ and TNF- α secretion ($p= 0.2858$ and $p= 0.0600$)

CAR T-cell proliferation upon target-cell contact was measured as previously described. First generation CAR T cells demonstrated high levels of proliferation after co-culture with CD19⁺/CEACAM⁺ target cells (Figure 17d). A significantly greater percentage of proliferating CAR T cells was found in 19_3z_28-TM2 (mean 94.0%, range 91.2-96.7%, $p= 0.0007$) CAR T cells than in conventional 19_3z CAR T cells (mean 81.5%, range 77.6-83.7%). Comparison with conventional CAR T cells showed no significant difference in 19_3z_28-TM3 CAR T cells (mean= 85.8%, range 78.2-93.5%, $p= 0.3818$). CAR T cells differed greatly in inherent proliferation without stimulation through CD19⁺/CEACAM⁺ target cells. In the unstimulated control, 55.4% of 19_3z_28-TM2 (range 45.3-66.3%, $p< 0.0001$) and 75.7% of 19_3z_28-TM3 CAR T cells (range 72.6-78.4%, $p< 0.0001$) proliferated, whereas 19_3z showed a mean proliferation of 2.06% (range 1.6-2.6%). Among CAR T cells with fusion receptors, 19_3z_28-TM3 transduced T cells showed significantly higher proliferation in the unstimulated control ($p= 0.0121$).

Analysis of absolute CAR T-cell numbers confirmed and extended these results (Figure 17e). Although the experimental setup included identical CAR T cell numbers for all constructs, significant differences in absolute number of CAR T cells were found after 72 hours of culture. Co-culture with target cells revealed a mean of 1.6×10^4 ($p< 0.0001$) of 19_3z_28-TM2 and 1.7×10^4 ($p= 0.0225$) of 19_3z_28-TM3 CAR T cells, but a mean of 2.6×10^2 of 19_3z CAR T cells. Similar results were seen in the condition of unstimulated CAR T cells (CAR T cells only). In the unstimulated control, mean CAR T cell count was 3.0×10^4 ($p= 0.0007$) in 19_3z_28-TM2 and 5.4×10^4 ($p< 0.0001$) in 19_3z_28-TM3 CAR T cells, but 2.2×10^3 in 19_3z CAR T cells. Among CAR T cells with fusion receptors, 19_3z_28-TM3 transduced T cells showed significantly higher cell numbers in the unstimulated control ($p= 0.0064$).

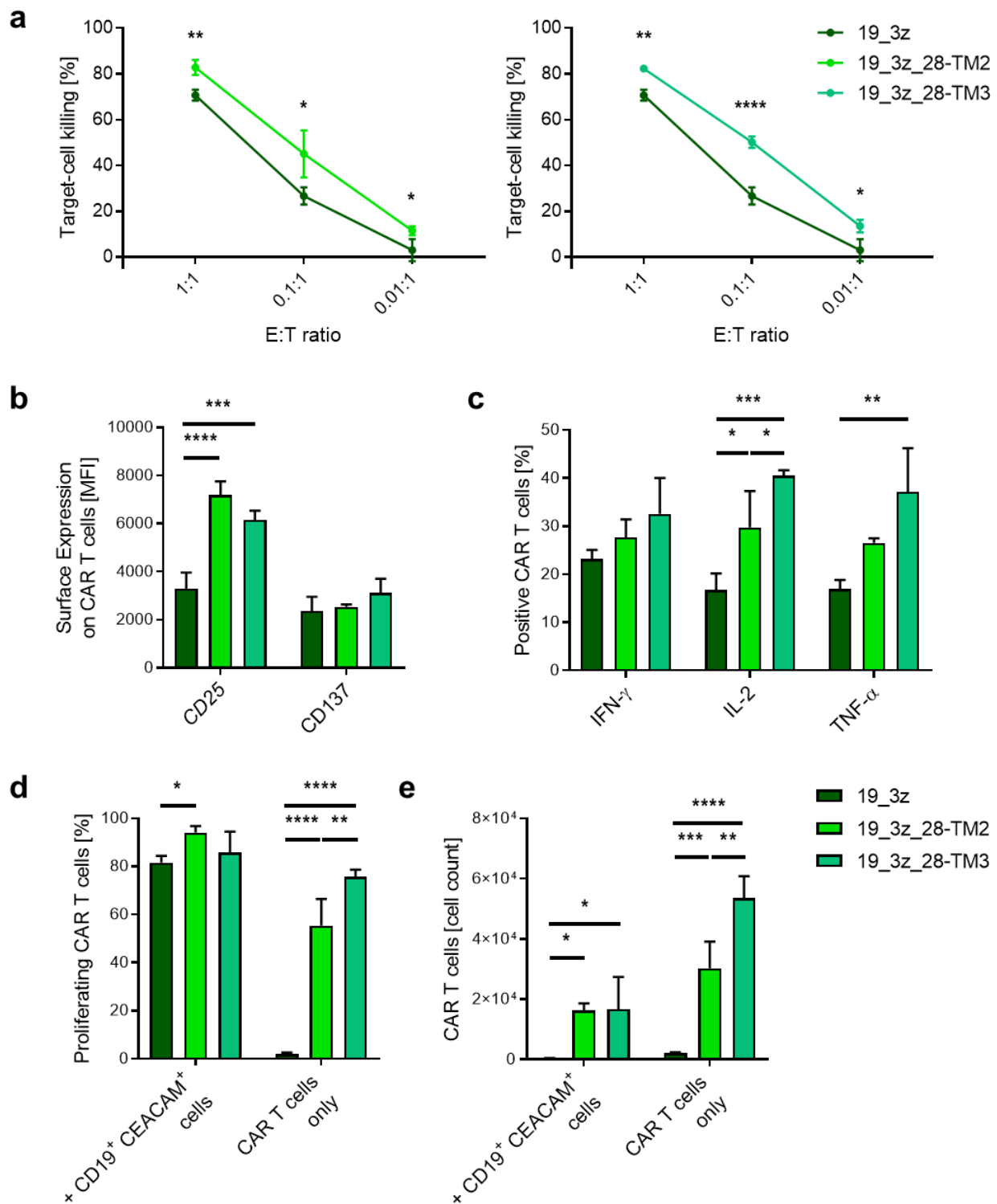


Figure 17: First generation CAR T cells with TIM-3/CD28 fusion receptors exhibit superior cytotoxicity, activation, cytokine secretion, and proliferation upon target-cell contact. Functional characterization was performed by co-culturing CAR T cells with CD19⁺ CEACAM⁺ K562 target-cell line followed by flow-cytometric measurement of cytotoxicity, activation-marker expression, cytokine secretion, and proliferation. **a**, Cytotoxicity of 19_3z_28-TM2 (left) and 19_3z_28-TM3 (right) after 48-hours of co-culture with CD19⁺ CEACAM⁺ K562 target-cell line. Cytotoxicity was measured using a CellTrace violet based approach and percentage of target-cell lysis was calculated as described in the methods. **b**, Surface expression of activation markers as determined by mean fluorescence intensity of CD25 and CD137 after 14 hours of co-culture with CD19⁺ CEACAM⁺ K562 target-cell line. **c**, Percentage of IFN- γ , IL-2-, and TNF- α -positive CAR T cells after 6 hours of co-culture with CD19⁺ CEACAM⁺ K562 target-cell line. **d**, Percentage of proliferating CAR T cells after 72 hours of co-culture with CD19⁺ CEACAM⁺ K562 target-cell line. Proliferation was determined using a CellTrace violet based approach as described in the methods. **e**, Absolute count of CAR T cells after 72 hours of co-culture with CD19⁺ CEACAM⁺

K562 target-cell line. All conditions were normalized to 5×10^4 CAR⁺ T cells per well prior to start of co-culture. Data are representative of two donors and experiments were performed in technical duplicates. Data are mean \pm SD. *P* values were determined using a one-way ANOVA followed by Tukey's multiple comparison test. E:T ratio= Effector to target ratio. MFI= Mean fluorescence intensity. IFN- γ = interferon gamma. IL-2= Interleukin-2. TNF- α = tumor necrosis factor alpha.

6.11 Second generation CAR T cells with a TIM-3/CD28 fusion receptor show marginal functional advantages over conventional CAR T cells

Second generation CAR T cells with TIM-3/CD28 fusion receptor were equally characterized in their functionality against CD19⁺/CEACAM⁺ target cells.

Cytotoxic capacity of second generation CAR T cells was assessed as previously described in 6.10. Second generation CAR T cells with and without fusion receptor demonstrated comparable cytotoxic killing of the CD19⁺/CEACAM⁺ K562 target cell line (Figure 18a). Cytotoxicity appeared to be slightly higher for 19_BB_3z_28-TM2 than in 19_BB_3z CAR T cells, and a significant difference was found at the 1:1 E:T ratio (mean 81.3% vs. 75.7%, range 79.6-82.8% vs. 74.5-76.7%, *p*= 0.0006), but not at the E:T ratio of 0.1:1 (mean 42.3% vs. 35.5%, range 37.9-44.9% vs. 32.7-38.8%, *p*= 0.0867) and 0.01:1 (mean 10.1% vs. 7.8%, range 7.7-12.1% vs. 3.3-11.3%, *p*= 0.0870). Compared to conventional CAR T cells, 19_BB_3z_28-TM3 CAR T cells showed no significant difference in killing at E:T ratios 1:1 (mean 73.8%, range 67.3-80.3%, *p*= 0.5650), 0.1:1 (mean 32.3%, range 24.3-40.0%, *p*= 0.3610) and 0.01:1 (mean 5.3%, range -0.6-8.8%, *p*= 0.4957).

Expression of activation markers CD25 and CD137 differed significantly between second generation CAR T cells (Figure 18b). MFI of CD25 was significantly higher in both 19_BB_3z_28-TM2 (mean 7495, *p*= 0.0076) and 19_BB_3z_28-TM3 (mean 7791, *p*= 0.0004) than in conventional 19_BB_3z CAR T cells (mean 4462). Contrarily, MFI of CD137 was significantly reduced in 19_BB_3z_28-TM3 (mean 1611, *p*= 0.0026) compared to conventional 19_BB_3z CAR T cells (mean 2162). 19_BB_3z_28-TM2 showed a mean of 2025 of MFI for CD137, which was comparable to 19_3z (*p*= 0.3089) and significantly higher than 19_BB_3z_28-TM3 (*p*= 0.0085).

Cytokine secretion of second generation CAR T cells was measured as previously described in 6.10. Compared to conventional CAR T cells, a tendency towards reduced cytokine secretion was observed in second generation CAR T cells with fusion receptor (Figure 18c). IFN- γ secretion was significantly higher in 19_BB_3z (mean 35.2%, range 28.2-43.1%) than in 19_BB_3z_28-TM3 CAR T cells (mean 23.8%, range 20.1-27.7%, *p*= 0.0401), but comparable to 19_BB_3z_28-TM2 CAR T cells (mean 27.5%, range 21.9-33.2%, *p*= 0.1748). Similarly, IL-2 secretion was significantly higher in 19_BB_3z (mean 43.6%, range 36.4-50.4%) than in 19_BB_3z_28-TM2 CAR T cells (mean 34.9%, range 34.6-35.3%, *p*= 0.0369) and 19_BB_3z_28-TM3 CAR T cells (mean 26.8%, range 23.9-30.1%, *p*= 0.0035). No significant differences in TNF- α secretion were found between CAR T cells. 19_BB_3z CAR T cells showed 29.3% (range 22.4-36.4%) of TNF- α secretion, 19_BB_3z_28-TM2 CAR T cells

demonstrated 28.8% (range 22.0-34.3%, $p= 0.9358$) of TNF- α secretion and 22.43% (range 20.1-24.6%, $p= 0.1486$) of TNF- α -positive CAR T cells were detected in 19_BB_3z_28-TM3 CAR T cells.

Analysis of proliferation in second generation CAR T cells were consistent with the results observed in first generation CAR T cells (Figure 18d). Upon target-cell contact, 19_BB_3z_28-TM2 CAR T cells showed 89.7% (range 87.0-91.9%) of mean proliferation, which was significantly greater than proliferation in both 19_BB_3z (mean 82.1%, range 80.4-83.9%, $p= 0.0011$) and 19_BB_3z_28-TM3 CAR T cells (mean 82.1%, range 81.3-83.6%, $p= 0.0007$). Comparison of 19_BB_3z and 19_BB_3z_28-TM3 CAR T cells found nearly equal percentages of proliferating CAR T cells ($p> 0.9999$) upon target-cell contact. In the unstimulated control, proliferation was significantly elevated in both 19_BB_3z_28-TM2 (mean 46.7%, range 43.9-50.2%, $p< 0.0001$) and 19_BB_3z_28-TM3 (mean 41.3%, range 39.6-45.4%, $p< 0.0001$), compared to 19_BB_3z CAR T cells (mean 7.7%, range 4.4-11.0%). Proliferation of 19_BB_3z_28-TM2 and 19_BB_3z_28-TM3 CAR T cells were comparable in the unstimulated control ($p= 0.0609$).

Analysis of absolute CAR T cells numbers confirmed the previous results (Figure 18e). Significant differences in absolute number of CAR T cells were found after 72 hours of co-culture and in the unstimulated control. Co-culture with target cells showed a mean of 1.3×10^4 ($p< 0.0001$) of 19_BB_3z_28-TM2 and 1.3×10^4 ($p< 0.0001$) of 19_BB_3z_28-TM3 CAR T cells, but a mean of 1.9×10^3 of 19_BB_3z CAR T cells. In the unstimulated control, mean CAR T-cell count was 2.6×10^4 ($p= 0.0064$) in 19_BB_3z_28-TM2 and 2.6×10^4 ($p= 0.0008$) in 19_BB_3z_28-TM3 CAR T cells, but 5.6×10^3 in 19_BB_3z CAR T cells. Absolute cell numbers of 19_BB_3z_28-TM2 and 19_BB_3z_28-TM3 CAR T cells were comparable both after co-culture ($p= 0.0973$) and in the unstimulated control ($p= 0.9172$).

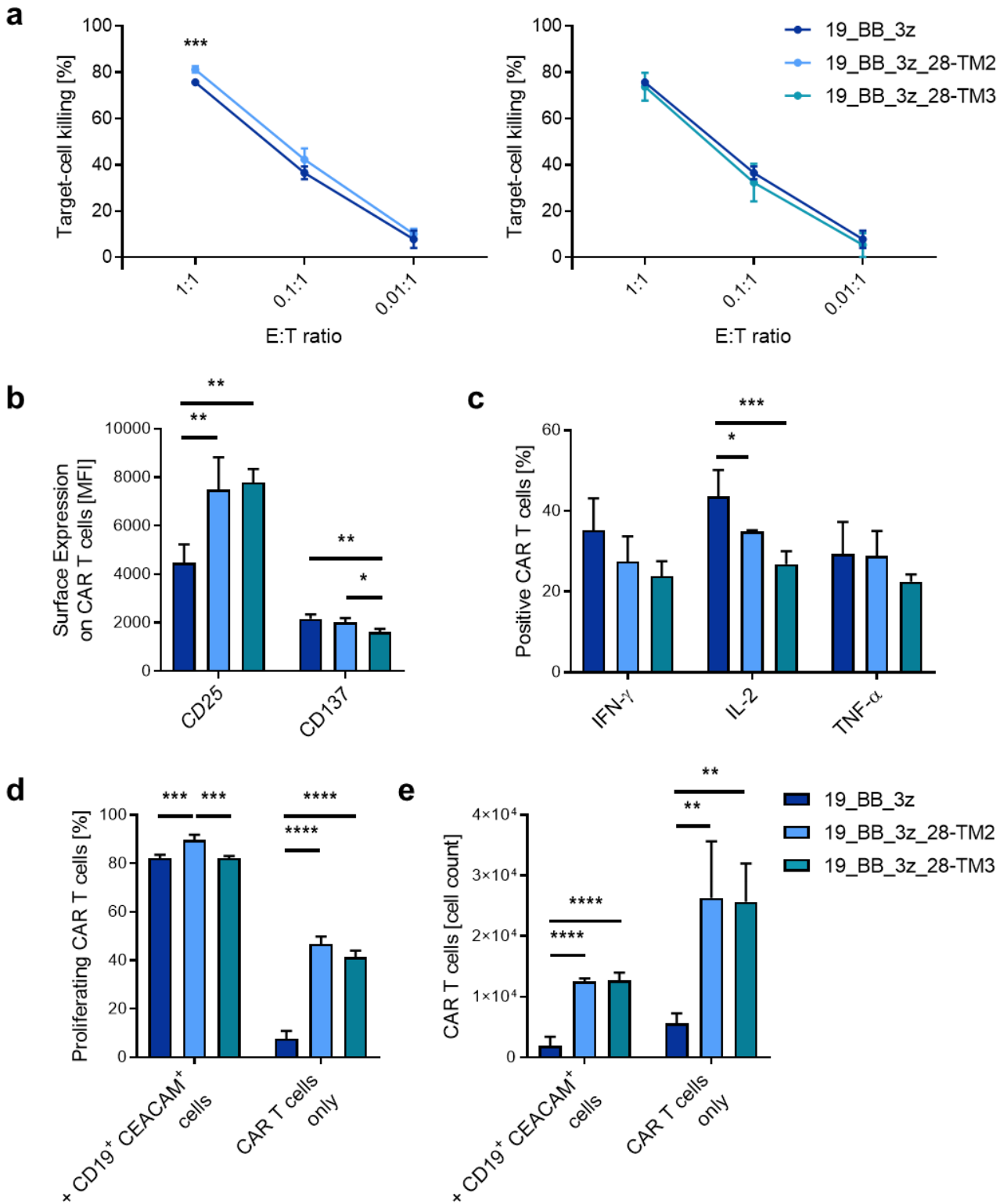


Figure 18: Second generation CAR T cells with TIM-3/CD28 fusion receptors show increased proliferation but comparable cytotoxicity and reduced cytokine secretion upon target-cell contact. Functional characterization was performed by co-culturing CAR T cells with CD19⁺ CEACAM⁺ K562 target-cell line followed by flow-cytometric measurement of cytotoxicity, activation marker expression, cytokine secretion, and proliferation. **a**, Cytotoxicity of 19_BB_3z_28-TM2 (left) and 19_BB_3z_28-TM3 (right) after 48-hours of co-culture with CD19⁺ CEACAM⁺ K562 target-cell line. Cytotoxicity was measured using a CellTrace violet based approach and percentage of target-cell lysis was calculated as described in the methods. **b**, Surface expression of activation markers as determined by mean fluorescence intensity of CD25 and CD137 after 14 hours of co-culture with CD19⁺ CEACAM⁺ K562 target-cell line. **c**, Percentage of IFN- γ -, IL-2-, and TNF- α -positive CAR T cells after 6 hours of co-culture with CD19⁺ CEACAM⁺ K562 target-cell line. **d**, Percentage of proliferating CAR T

cells after 72 hours of co-culture with CD19⁺ CEACAM⁺ K562 target-cell line. Proliferation was determined using a CellTrace violet based approach as described in the methods. **e**, Absolute count of CAR T cells after 72 hours of co-culture with CD19⁺ CEACAM⁺ K562 target-cell line. All conditions were normalized to 5x10⁴ CAR⁺ T cells per well prior to start of co-culture. Data are representative of two donors and experiments were performed in technical duplicates. Data are mean ± SD. *P* values were determined using a one-way ANOVA followed by Tukey's multiple comparison test. E:T ratio= Effector to target ratio

7 Discussion

CAR T-cell therapy has revolutionized treatment of children with refractory or relapsed ALL. Clinical trials observed response rates up to 93% upon treatment with anti-CD19 CAR T cells, but 50% of patients relapse within 12 months after therapy. Since relapse or non-response may arise from intrinsic T-cell dysfunction, identifying and targeting the pathways involved in inhibition and exhaustion of T cells might provide more durable responses in CAR T-cell therapy.

In consequence, immune checkpoint molecules are increasingly investigated in the context of ameliorating CAR functionality, and promising results were particularly established concerning the co-inhibitory molecule PD-1. Blockage of the PD-1/PD-L1 axis could be safely combined with anti-CD19 CAR T cells and the combination was associated with enhanced persistence in preclinical models and, more recently, in a small patient cohort.^{45,46,66} Despite the encouraging result for PD-1 blockade, there is insufficient data on the role of the co-inhibitory checkpoint TIM-3. Since PD-1 and TIM-3 are co-expressed in activated, as well as in highly exhausted T-cell subsets, this indicates that targeting TIM-3 might prove equally beneficial and underlines the need for further data on the role of TIM-3 in the context of CAR T cells.^{53,67}

7.1 TIM-3 expression coincides with CAR T-cell exhaustion

In order to determine the effect of the co-inhibitory molecule TIM-3 on CAR T-cell functionality, TIM-3 overexpressing first and second generation CAR T-cells were generated.⁶¹ An F2A linker was incorporated into CAR design to achieve equimolar expression of two separate proteins. CAR and TIM-3 expression strongly correlated on TIM-3 overexpressing CAR T cells, which indicates stable co-expression of both proteins. TIM-3 overexpressing CAR T cells showed slightly higher transduction rates than conventional CAR T cells. However, both differed greatly in TIM-3 expression, suggesting that any observed alterations in functionality could be ascribed to differences in TIM-3 expression.

TIM-3 overexpressing CAR T cells exhibited slightly diminished viability and expansion rates in the expansion period following transduction. It is plausible that TIM-3 would mediate such effects on CAR T cells, as TIM-3 has been associated with apoptosis in primary T cells, in particular upon interaction with its ligand Galectin-9.^{68,69} Another possible explanation could be the differentiation of phenotype associated with TIM-3 expression, which has been previously established for T cells and could be confirmed in this study in the context of CAR T cells.^{47,60} The percentage of stem cell-like memory T cells was significantly decreased in TIM-3 overexpressing CAR T cells and an overall tendency

towards a more differentiated phenotype was observed. This indicates that TIM-3 may actively promote terminal differentiation of CAR T-cells rather than being only upregulated upon maturation of phenotype. However, a mere correlation between differentiation of phenotype and a larger size of construct in TIM-3 overexpressing CAR T cells remains equally possible.

7.2 TIM-3 is associated with impaired CAR T-cell functionality

Further functional analysis revealed impaired functionality against CD19-positive leukemic cells in TIM-3-overexpressing CAR T cells, which was indicated through reduced potential of activation, cytokine secretion, and proliferation.⁶¹ Yet, TIM-3-overexpressing CAR T cells showed comparable cytotoxicity against the CD19-positive cell line. As TIM-3 is associated with both activation and terminal differentiation in T cells, it is plausible that TIM-3 overexpression would not affect killing but rather persistence and activation potential of CAR T cells.^{47,60} In line with this hypothesis, TIM-3-overexpressing CAR T cells exhibited higher cytokine secretion and activation in the unstimulated control but ultimately failed to adequately elevate stimulation upon contact with leukemic cells. Conclusively, it remains unclear, whether the reduced functionality is directly caused by TIM-3 expression or results from the unfavorable phenotype observed in TIM-3-overexpressing CAR T cells.

Unexpectedly, expression of TIM-3 ligand CEACAM on target cells did not affect activation, proliferation, and cytokine secretion, yet significantly diminished cytotoxicity of both conventional and TIM-3-overexpressing CAR T cells. As previous studies provided evidence for endogenous expression of CEACAM in T cells, the inhibitory effect of TIM-3 might be fully exploited through the interaction with endogenous CEACAM, thereby denying an additional effect through CEACAM-positive target cells.⁶⁰ Interestingly and in contradiction to the results of Huang et al., a recent study suggests that CEACAM might not interact with TIM-3, which provides a possible explanation for our observations.^{60,70} On the other hand, the absence of an effect in presence of CEACAM raises the question, whether the reduced functionality of TIM-3-overexpressing CAR T cells resulted from the interaction of TIM-3 with an unknown ligand present on target cells.

Nevertheless, presence of CEACAM significantly reduced target-cell killing in both TIM-3-overexpressing CAR T cells and conventional CAR T cells. These results are consistent with the observations of Rupp et al., who reported reduced CAR T-cell cytotoxicity against target cells that express PD-L1, a ligand for the inhibitory molecule PD-1, which ultimately resulted in impaired clearance of PD-L1-positive tumor xenografts.⁴⁴ Although reduction of CAR T cell-mediated killing through CEACAM appears contradictory to the observed comparable cytokine secretion and activation, this could indicate a potential role of CEACAM in other cytotoxic pathways that were not

investigated in this study. An inhibitory effect of CEACAM on granzyme B and perforin mediated killing or on death receptor pathways appears possible and should be addressed in further studies.

7.3 Overcoming TIM-3-mediated CAR T-cell suppression

Although the precise role of ligand interaction remains unclear, these data provide strong evidence for TIM-3-mediated inhibition of CAR T cells. In line with these results, other groups established equally adverse effects for the co-inhibitory molecule PD-1 but could restore CAR T-cell response by PD-1 disruption, or through implementation of a PD-1/CD28 fusion receptor.^{44,64,71} Notably, CAR T cells with a PD-1/CD28 fusion receptor even showed enhanced antitumor efficacy compared to CAR T cells alone and in combination with an anti-PD-1 antibody. In view of these results, the concept of a fusion receptor appears transferable to TIM-3 and might prove an effective approach in order to overcome TIM-3-mediated CAR T-cell inhibition.

The group of Kobold et al. reported that the strength of T-cell response upon activation of the fusion receptor might depend on details in its design. Interestingly, they observed higher functionality of a PD-1/CD28 fusion receptor incorporating a PD-1-derived transmembrane domain, which possibly resulted from enhanced binding of the ligand PD-L1.⁷²

In order to identify a design that would provide superior activation of a TIM-3/CD28 fusion receptor, we engineered fusion receptor constructs with varying intracellular, transmembrane, and extracellular domains.⁶¹ In response to the observations of Kobold et al., the TIM-3 transmembrane domain was incorporated into the constructs TIM3-TM1 and TIM3-TM2.⁷² In contrast, the constructs 28-TM1, 28-TM2, and 28-TM3 contained CD28 transmembrane domains, following the hypothesis that a greater CD28 proportion might augment CD28 signaling.⁶⁵ Additionally, the CD28 ectodomain of 28-TM3 included a cysteine, which could promote homodimerization of the receptor through disulfide bond formation and thus enhance CD28 signaling.^{65,73} The construct 8-TM incorporated a CD8-derived transmembrane domain, which is commonly used in CAR design and has been associated with reduced activation-induced cell death.^{32,74,75}

7.4 Identification of a superior TIM-3/CD28 fusion receptor

Ultimately aiming at identifying the most functional TIM-3/CD28 fusion receptor, we initially transduced human primary T cells with the aforementioned constructs.⁶¹ Unlike the CAR constructs, the fusion receptor constructs did not contain a tag for flow-cytometric detection, but successful transduction of T cells was implied by highly positive staining for TIM-3 compared to the untransduced control. Initial characterization of T cells in terms of expansion, viability, phenotype,

and cellular composition yielded equal results in fusion receptor transduced T cells, although 8-TM displayed a slight, non-significant tendency towards more stem cell-like memory T cells.

We further analyzed functionality of TIM-3/CD28 fusion receptor constructs using a CD3 stimulation approach. This allowed for a more precise measurement of fusion receptor-mediated activation, as the CD28 signaling would only depend on CD3 stimulation, thus avoiding potential disruptive factors in co-culture approaches.

Upon CD3 stimulation, TIM-3/CD28 fusion receptor transduced T cells outperformed untransduced T cells in terms of cytokine release, and the effect was more pronounced in IFN- γ secretion than in TNF- α secretion. However, only the constructs 28-TM2 and 28-TM3 were able to outcompete untransduced T cells in proliferation potential. Interestingly, functionality of the fusion receptor constructs appeared to correlate with the respective amount of CD28, as the constructs 28-TM2 and 28-TM3 consistently showed the highest cytokine secretion and proliferation upon CD3 stimulation. Although opposing the results for PD-1/CD28 fusion receptors, our results are in line with observations in CD200R/CD28 fusion receptors, where constructs incorporating a CD28 transmembrane domain and a dimerizing motif, as present in 28-TM3, were associated with superior functionality.^{65,72}

7.5 TIM-3/CD28 fusion receptors restore CAR T-cell functionality

Based on the results in T cells, both 28-TM2 and 28-TM3 appeared as the most suitable candidates for transfer into a CAR T-cell approach.⁶¹ Hence, we engineered first and second generation anti-CD19 CAR T cells with either the 28-TM2 or the 28-TM3 fusion receptor in order to determine their functionality compared to conventional CAR T cells. In a recent study by Zhao et al., second generation CAR T cells equipped with a TIM-3/CD28 fusion receptor similar to the 28-TM1 construct showed augmented functionality and antileukemic efficacy *in vitro* and *in vivo*.⁷⁶

The fusion receptor constructs were linked to the CAR by an F2A linker, but the design was otherwise identical to that of conventional CAR T cells. Generation of CAR T cells with fusion receptor was feasible, as transduction rate, expansion, and viability were comparable to conventional CAR T cells. Expression of TIM-3 and CAR strongly correlated and thus indicated co-expression of both molecules on the surface.

CAR T cells with fusion receptors were further characterized in their efficacy against CEACAM-positive leukemic cells. Notably, first generation CAR T cells with fusion receptor showed markedly improved cytotoxicity compared to conventional CAR T cells, which had previously demonstrated hampered cytotoxicity in presence of CEACAM, thus suggesting that the fusion receptor could overcome CEACAM-mediated inhibition of CAR T-cell cytotoxicity. In accordance with

these results, CAR T cells with fusion receptor exhibited enhanced cytokine release and could outperform conventional CAR T cells in IL-2 and TNF- α secretion. Moreover, expression of CD25, but not of CD137, was markedly increased in CAR T cells with fusion receptor, which may indicate different kinetics in upregulation of activation markers. Interestingly, CAR T cells with fusion receptor exhibited significantly increased proliferation not only upon contact with target cells but also without additional external stimulation. Although possibly indicating tonic signaling through the CD28 co-stimulatory domain in the fusion receptor, this notion remains unlikely, as neither cytokine secretion nor activation marker expression was elevated in the unstimulated controls after short-term culture. It appears more plausible that the fusion receptor would augment stimulation through repeated interactions with endogenously expressed CEACAM and thus enhance proliferation of CAR T cells without external target-cell contact.⁶⁰ Evaluation of absolute CAR T-cell numbers supports this notion, since the significantly elevated cell count both in the unstimulated control and upon co-culture suggest less activation-induced cell death, thereby providing an additional survival benefit in CAR T cells with fusion receptor. This notion is supported by the observations of Zhao et al., who reported upregulation of the anti-apoptotic molecules Bcl-2 and Bcl-xL and reduced expression of caspase-3 in CAR T cells with a TIM-3/CD28 fusion receptor, ultimately resulting in their superior persistence and proliferation in vivo.⁷⁶

In recent years, multiple studies have emphasized the importance of CAR T-cell phenotype and associated potent effector function with T-cell exhaustion and, therefore, lack of persistence.^{23,41,77} Importantly, the enhanced functionality of first generation CAR T cells with fusion receptor did not coincide with alterations in T-cell senescence, as we observed an equally differentiated phenotype in CAR T cells with and without fusion receptor upon target-cell contact. However, the differences in inherent phenotype without prior stimulation may raise the question, if the superior functionality of CAR T cells with a TIM-3/CD28 fusion receptor results from a more favorable phenotype rather than presence of the fusion receptor.

In conclusion, first generation CAR T cells with a TIM-3/CD28 fusion receptor were superior to conventional CAR T cells in every aspect of functionality investigated in this study. These results are contrary to the observations in second generation CAR T cells, where a TIM-3/CD28 fusion receptor provided only marginal advantages in CAR T-cell functionality. Although the outcomes in proliferation and activation were consistent with the results in first generation CAR T cells, cytotoxicity was merely comparable, and cytokine release even diminished in CAR T cells with fusion receptor. As the combination of a second generation CAR construct with a fusion receptor endows T cells with two co-stimulatory signals, this resembles the setting in third generation CAR T cells, which incorporate two co-stimulatory domains in the CAR and, similarly, have shown no functional advantages over second generation CAR T cells.⁷⁸

Consistent with the observations in TIM-3 overexpression, presence of CEACAM on target cells did not affect functionality of CAR T cells with a TIM-3/CD28 fusion receptor, and neither did addition of TIM-3 ligands HMGB1 and Galectin-9 into co-culture with CD19-positive cells. As with the previous results, this suggests either that the fusion receptor is exhausted in its activation potential through interaction with endogenous CEACAM, or that it is engaged by presence of an unknown ligand on target cells. Hence, future studies might have to further investigate on the identification of novel ligands to TIM-3 in order to prove specificity of the fusion receptor.

7.6 Clinical application of CAR T cells with a TIM-3/CD28 fusion receptor

The clinical significance of CAR T cells with TIM-3/CD28 fusion receptor is implied not only by the promising results observed in their in vitro characterization but also by our previous results concerning TIM-3 overexpression.⁶¹ Consequently, further in vivo experiments are required to evaluate their functionality in a more physiological setting and may provide insights into ligand-specific activation of the fusion receptor, which will pave the way for clinical implementation.⁷⁶

However, safety of the fusion receptor may prove a vital issue for its successful transfer into CAR T-cell therapy. Although we could not detect unspecific activation of the fusion receptor in absence of prior anti-CD19 stimulation, CAR T cells with TIM-3/CD28 fusion receptor could be engineered with an inducible safety switch in order to eliminate them upon inadequate activation.^{79,80} As recently demonstrated, the tyrosine kinase inhibitor Dasatinib acts as a pharmacological suppressor for CAR T-cell function and should be considered as a reversible safety switch for CAR T cells with TIM-3/CD28 fusion receptor.⁸¹

Furthermore, high potency of CAR T cells with a fusion receptor could coincide with an increased risk for CRS and other toxicities. As recent studies have successfully introduced the concept of compromising CAR affinity and immunogenicity in order to reduce toxic side effects, the combination of a TIM-3/CD28 fusion receptor with low-affinity CAR T cells might prove effective in order to maintain CAR T-cell efficacy in an immunosuppressive environment while minimizing unwanted toxicity.^{38,40,77}

In summary, this study demonstrates that CAR T-cell functionality is hampered in presence of the inhibitory molecule TIM-3 but may be reestablished through implementation of a highly efficacious TIM-3/CD28 fusion receptor.⁶¹ Thus, our work forms the basis for further in vivo evaluation of CAR T cells with a TIM-3/CD28 fusion receptor and, ultimately, a transfer into CAR T-cell therapy.

8 Summary

CAR T-cell therapy is a promising new option for treatment of relapsed or refractory pediatric ALL, yet durable remissions remain unachievable for many patients. Relapse after CAR T-cell therapy has been associated with intrinsic dysfunctionality and exhaustion of CAR T cells. Although the cause of CAR T-cell malfunction remain poorly understood, an involvement of co-inhibitory checkpoints appears likely. With this in mind, this study aims at characterizing the role of co-inhibitory molecule TIM-3 in CAR T cells and provides strategies to overcome CAR T-cell dysfunctionality.⁶¹

First, we determined the effect of TIM-3 on CAR T cells using an overexpression model. CAR T cells with TIM-3 overexpression showed diminished viability and expansion rates after retroviral transduction and displayed a tendency towards a more differentiated phenotype compared to conventional CAR T cells. Notably, both first and second generation CAR T cells with TIM-3 overexpression demonstrated impaired functionality against CD19-positive target cells, yet this effect was not further amplified through addition of the TIM-3 ligand CEACAM. Interestingly, cytotoxicity was not influenced by TIM-3 overexpression, but presence of CEACAM markedly decreased killing in CAR T cells, regardless of TIM-3 overexpression. To circumvent TIM-3-mediated inhibition of CAR T cells, we generated TIM-3/CD28 fusion receptors incorporating differentially designed intracellular, transmembrane, and extracellular domains and first evaluated their functionality in primary T cells. The synthetic fusion protein would transform TIM-3-mediated inhibition into CD28-mediated T-cell activation. Fusion receptor-transduced T cells outperformed untransduced T cells in terms of cytokine secretion and proliferation. Interestingly, activation potential of fusion receptor transduced T cells correlated with CD28 proportion in the construct and was highest for constructs 28-TM2 and 28-TM3. Based on these results, we chose these constructs for further characterization in a first and second generation CAR T-cell setting. First generation CAR T cells were able to outperform conventional CAR T cells in terms of activation, cytotoxicity, cytokine secretion, and proliferation after co-culture with CEACAM-positive target cells. Yet, second generation CAR T cells with a fusion receptor were only superior in proliferation and activation but showed no advantages over conventional CAR T cells in cytokine secretion and cytotoxicity. Despite the high functionality of CAR T cells with fusion receptor upon target-cell contact, their phenotype was comparable to that of conventional CAR T cells.

Collectively, this study shows that TIM-3 expression is associated with impaired CAR T-cell response in vitro, but implementation of a TIM-3/CD28 fusion receptor can restore functionality. Thus, our results provide a framework for further in vivo characterization of TIM-3/CD28 fusion receptors and their successful transfer into CAR T-cell therapy.

9 Zusammenfassung

Die CAR-T-Zell-Therapie ist ein vielversprechender Ansatz zur Behandlung der fortgeschrittenen pädiatrischen ALL. Trotz anfangs gutem Therapieansprechen erleidet ein Großteil der Patienten nach wenigen Monaten ein Rezidiv, welches durch einen Funktionsverlust der CAR-T-Zellen entstehen kann. Obwohl die genauen Ursachen eines Funktionsverlusts weitestgehend unbekannt sind, ist eine Involvierung von ko-inhibitorischen Immuncheckpoints denkbar. Unsere Arbeit greift dieses Thema auf und beschäftigt sich mit der Frage, welche Rolle der ko-inhibitorische Checkpoint TIM-3 auf CAR-T-Zellen ausübt und bietet Strategien für eine Verbesserung der CAR-T-Zell-Antwort.⁶¹

Die Rolle von TIM-3 auf CAR-T-Zellen wurde mithilfe eines Überexpressions-Modells untersucht. CAR-T-Zellen mit TIM-3 Überexpression zeigten eine reduzierte Expansion und Viabilität, sowie einen tendenziell ausdifferenzierteren Phänotyp als konventionelle CAR-T-Zellen. Sowohl Erst- als auch Zweitgenerations-CAR-T-Zellen mit TIM-3 Überexpression waren weniger funktionell gegen Leukämiezelllinien hinsichtlich Zytokinsekretion, Proliferation und Aktivierung, zeigten aber keinen signifikanten Unterschied in der Zytotoxizität. Die Hinzunahme des TIM-3 Liganden CEACAM hatte keine Auswirkungen auf die Funktionalität mit Ausnahme der Zytotoxizität, da alle CAR-T-Zellen unabhängig von TIM-3 Überexpression verminderte Zytotoxizität gegen CEACAM-positive Leukämiezellen zeigten. Angesichts der starken Inhibition durch TIM-3 entwarfen wir TIM-3/CD28 Fusionsrezeptoren mit unterschiedlich aufgebauten intra-, trans-, und extrazellulären Membrandomänen, um sie hinsichtlich ihrer Funktionalität zunächst in T Zellen zu untersuchen. Das Prinzip der Fusionsrezeptoren basiert auf der Umwandlung des TIM-3-vermittelten, inhibitorischen Signals in ein aktivierendes Signal über die intrazelluläre CD28-Domäne. Es zeigte sich, dass die Funktionalität der Fusionsrezeptoren mit dem CD28-Anteil im Konstrukt korrelierte und die Konstrukte 28-TM2 und 28-TM3 dementsprechend die höchste Aktivierbarkeit aufwiesen. Daher charakterisierten wir diese Fusionsrezeptoren anschließend in Erst- und Zweitgenerations-CAR-T-Zellen hinsichtlich ihrer Funktionalität gegen CEACAM-positive Leukämiezellen. CAR-T-Zellen mit Fusionsrezeptor waren konventionellen Erstgenerations-CAR-T-Zellen funktionell überlegen, wiesen jedoch keinen Vorteil gegenüber konventionellen Zweitgenerations-CAR-T-Zellen auf. Trotz ihrer hohen Funktionalität zeigten die CAR-T-Zellen mit Fusionsrezeptor keine stärkere Ausdifferenzierung des Phänotyps nach Kontakt mit Leukämiezellen.

Zusammenfassend konnten wir zeigen, dass TIM-3 einen inhibitorischen Effekt auf die Funktionalität von CAR-T-Zellen ausübt, diese jedoch durch den Einbau eines TIM-3/CD28 Fusionsrezeptors wiederhergestellt und sogar verbessert werden kann. Damit bildet diese Arbeit die Grundlage für eine

weitere in vivo Charakterisierung des TIM-3/CD28 Fusionsrezeptors und somit dessen erfolgreiche Integration in die CAR-T-Zell-Therapie.

10 Literature

1. Cunningham, R. M., Walton, M. A. & Carter, P. M. The Major Causes of Death in Children and Adolescents in the United States. *N. Engl. J. Med.* **379**, 2468–2475 (2018).
2. Childhood Cancer by the ICCO, CSR 1975-2013.
3. Hunger, S. P. & Mullighan, C. G. Acute Lymphoblastic Leukemia in Children. *N. Engl. J. Med.* **373**, 1541–1552 (2015).
4. Ding, L.-W. *et al.* Mutational Landscape of Pediatric Acute Lymphoblastic Leukemia. *Cancer Res.* **77**, 390–400 (2017).
5. Smith, M. *et al.* Uniform approach to risk classification and treatment assignment for children with acute lymphoblastic leukemia. *J. Clin. Oncol.* **14**, 18–24 (1996).
6. Vrooman, L. M. *et al.* Refining risk classification in childhood B acute lymphoblastic leukemia: results of DFCI ALL Consortium Protocol 05-001. *Blood Adv.* **2**, 1449–1458 (2018).
7. Borowitz, M. J.; Devidas, M.; Hunger, S. P.; Bowman, W. P.; Carroll, A. J.; Carroll, W. L.; Linda, S. *et al.* Clinical significance of minimal residual disease in childhood acute lymphoblastic leukemia and its relationship to other prognostic factors: A Children ' s Oncology Group study. *Blood* **111**, 5477–5485 (2008).
8. Van Dongen, J. J. M., Van Der Velden, V. H. J., Brüggemann, M. & Orfao, A. Minimal residual disease diagnostics in acute lymphoblastic leukemia: Need for sensitive, fast, and standardized technologies. *Blood* **125**, 3996–4009 (2015).
9. George, P. *et al.* A study of 'total therapy' of acute lymphocytic leukemia in children. *J. Pediatr.* **72**, 399–408 (1968).
10. Schrappe, M. *et al.* Outcomes after Induction Failure in Childhood Acute Lymphoblastic Leukemia. *N. Engl. J. Med.* **366**, 1371–1381 (2012).
11. Vora, A. *et al.* Influence of Cranial Radiotherapy on Outcome in Children With Acute Lymphoblastic Leukemia Treated With Contemporary Therapy. *J. Clin. Oncol.* **34**, 919–926 (2016).
12. von Stackelberg, A. *et al.* Phase I/Phase II Study of Blinatumomab in Pediatric Patients With Relapsed/Refractory Acute Lymphoblastic Leukemia. *J. Clin. Oncol.* **34**, 4381–4389 (2016).
13. Bhojwani, D. & Pui, C. H. Relapsed childhood acute lymphoblastic leukaemia. *Lancet Oncol.* **14**, e205–e217 (2013).
14. Sun, W. *et al.* Outcome of children with multiply relapsed B-cell acute lymphoblastic leukemia: a therapeutic advances in childhood leukemia & lymphoma study. *Leukemia* **32**, 2316–2325 (2018).
15. Maude, S. L. *et al.* Tisagenlecleucel in children and young adults with B-cell lymphoblastic leukemia. *N. Engl. J. Med.* **378**, 439–448 (2018).
16. Maude, S. L. *et al.* Sustained remissions with CD19-specific chimeric antigen receptor (CAR)-modified T cells in children with relapsed/refractory ALL. *J. Clin. Oncol.* **34**, 3011–3011 (2016).
17. U.S. Food and Drug Administration: FDA approves tisagenlecleucel for B-cell ALL and tocilizumab for cytokine release syndrome.

18. Eshhar, Z., Waks, T., Bendavid, A. & Schindler, D. G. Functional expression of chimeric receptor genes in human T cells. *J. Immunol. Methods* **248**, 67–76 (2001).
19. van der Stegen, S. J. C., Hamieh, M. & Sadelain, M. The pharmacology of second-generation chimeric antigen receptors. *Nat. Rev. Drug Discov.* **14**, 499–509 (2015).
20. Maus, M. V, Grupp, S. a, Porter, D. L. & June, C. H. Antibody-modified T cells: CARs take the front seat for hematologic malignancies. *Blood* **123**, 2625–2635 (2014).
21. Hucks, G. & Rheingold, S. R. The journey to CAR T cell therapy: the pediatric and young adult experience with relapsed or refractory B-ALL. *Blood Cancer J.* **9**, (2019).
22. Benjamin, R. *et al.* Genome-edited, donor-derived allogeneic anti-CD19 chimeric antigen receptor T cells in paediatric and adult B-cell acute lymphoblastic leukaemia: results of two phase 1 studies. *Lancet* **396**, 1885–1894 (2020).
23. Fraietta, J. A. *et al.* Disruption of TET2 promotes the therapeutic efficacy of CD19-targeted T cells. *Nature* **558**, 307–312 (2018).
24. Ruella, M. *et al.* Induction of resistance to chimeric antigen receptor T cell therapy by transduction of a single leukemic B cell. *Nat. Med.* **24**, 1499–1503 (2018).
25. Norelli, M. *et al.* Monocyte-derived IL-1 and IL-6 are differentially required for cytokine-release syndrome and neurotoxicity due to CAR T cells. *Nat. Med.* **24**, 739–748 (2018).
26. Giavridis, T. *et al.* CAR T cell-induced cytokine release syndrome is mediated by macrophages and abated by IL-1 blockade. *Nat. Med.* **24**, 731–738 (2018).
27. Sotillo, E. *et al.* Convergence of Acquired Mutations and Alternative Splicing of CD19 Enables Resistance to CART-19 Immunotherapy. **5**, 1282–1295 (2016).
28. Gardner, R. *et al.* Acquisition of a CD19-negative myeloid phenotype allows immune escape of MLL-rearranged B-ALL from CD19 CAR-T-cell therapy. *Blood* **127**, 2406–2410 (2016).
29. Fry, T. J. *et al.* CD22-targeted CAR T cells induce remission in B-ALL that is naive or resistant to CD19-targeted CAR immunotherapy. *Nat. Med.* **24**, 20–28 (2018).
30. Shah, N. N. *et al.* Bispecific anti-CD20, anti-CD19 CAR T cells for relapsed B cell malignancies: a phase 1 dose escalation and expansion trial. *Nat. Med.* **26**, 1569–1575 (2020).
31. Frank, M. J. *et al.* CD22-CAR T-Cell Therapy Mediates High Durable Remission Rates in Adults with Large B-Cell Lymphoma Who Have Relapsed after CD19-CAR T-Cell Therapy. *Blood* **138**, 741–741 (2021).
32. Maude, S. L. *et al.* Chimeric Antigen Receptor T Cells for Sustained Remissions in Leukemia. *N. Engl. J. Med.* **371**, 1507–1517 (2014).
33. Lee, D. W. *et al.* T cells expressing CD19 chimeric antigen receptors for acute lymphoblastic leukaemia in children and young adults: a phase 1 dose-escalation trial. *Lancet (London, England)* **385**, 517–528 (2015).
34. Turtle, C. J. *et al.* CD19 CAR–T cells of defined CD4+:CD8+ composition in adult B cell ALL patients. *J. Clin. Invest.* **126**, 2123–2138 (2016).
35. Lee, D. W. *et al.* Long-Term Outcomes Following CD19 CAR T Cell Therapy for B-ALL Are Superior in Patients Receiving a Fludarabine/Cyclophosphamide Preparative Regimen and Post-CAR Hematopoietic Stem Cell Transplantation. *Blood* **128**, 218–218 (2016).
36. Park, J. H. *et al.* Long-Term Follow-up of CD19 CAR Therapy in Acute Lymphoblastic

Leukemia. *N. Engl. J. Med.* **378**, 449–459 (2018).

37. Majzner, R. G. & Mackall, C. L. Tumor Antigen Escape from CAR T-cell Therapy. *Cancer Discov.* **8**, 1219–26 (2018).
38. Ghorashian, S. *et al.* Enhanced CAR T cell expansion and prolonged persistence in pediatric patients with ALL treated with a low-affinity CD19 CAR. *Nat. Med.* (2019) doi:10.1038/s41591-019-0549-5.
39. Ramakrishna, S. *et al.* Modulation of Target Antigen Density Improves CAR T-cell Functionality and Persistence. *Clin. Cancer Res.* 1–14 (2019) doi:10.1158/1078-0432.ccr-18-3784.
40. Brudno, J. N. *et al.* Safety and feasibility of anti-CD19 CAR T cells with fully human binding domains in patients with B-cell lymphoma. *Nat. Med.* **26**, 270–280 (2020).
41. Fraietta, J. A. *et al.* Determinants of response and resistance to CD19 chimeric antigen receptor (CAR) T cell therapy of chronic lymphocytic leukemia. *Nat. Med.* **24**, 563–571 (2018).
42. Finney, O. C. *et al.* CD19 CAR T cell product and disease attributes predict leukemia remission durability. *J. Clin. Invest.* **129**, 2123–2132 (2019).
43. Feucht, J. *et al.* T-cell responses against CD19+ pediatric acute lymphoblastic leukemia mediated by bispecific T-cell engager (BiTE) are regulated contrarily by PD-L1 and CD80/CD86 on leukemic blasts. *Oncotarget* **7**, 8–11 (2016).
44. Rupp, L. J. *et al.* CRISPR/Cas9-mediated PD-1 disruption enhances anti-Tumor efficacy of human chimeric antigen receptor T cells. *Sci. Rep.* **7**, 1–10 (2017).
45. Li, A. M. *et al.* Checkpoint Inhibitors Augment CD19-Directed Chimeric Antigen Receptor (CAR) T Cell Therapy in Relapsed B-Cell Acute Lymphoblastic Leukemia. *Blood* **132**, 556 (2018).
46. Li, F. *et al.* PD-1 abrogates the prolonged persistence of CD8+ CAR-T cells with 4-1BB co-stimulation. *Signal Transduct. Target. Ther.* **5**, 164 (2020).
47. Das, M., Zhu, C. & Kuchroo, V. K. Tim-3 and its role in regulating anti-tumor immunity. *Immunol. Rev.* **276**, 97–111 (2017).
48. Golden-mason, L. *et al.* Negative Immune Regulator Tim-3 Is Overexpressed on T Cells in Hepatitis C Virus Infection and Its Blockade Rescues Dysfunctional CD4+ and CD8+ T Cells. **83**, 9122–9130 (2009).
49. Banerjee, H. *et al.* Expression of Tim-3 drives phenotypic and functional changes in Treg cells in secondary lymphoid organs and the tumor microenvironment. *Cell Rep.* **36**, 109699 (2021).
50. Dixon, K. O. *et al.* TIM-3 restrains anti-tumour immunity by regulating inflammasome activation. *Nature* **595**, 101–106 (2021).
51. Tu, L. *et al.* Assessment of the expression of the immune checkpoint molecules PD-1, CTLA4, TIM-3 and LAG-3 across different cancers in relation to treatment response, tumor-infiltrating immune cells and survival. *Int. J. Cancer* **147**, 423–439 (2020).
52. Blaeschke, F. *et al.* Leukemia-induced dysfunctional TIM-3+CD4+ bone marrow T cells increase risk of relapse in pediatric B-precursor ALL patients. *Leukemia* **34**, 2607–2620 (2020).
53. Sakuishi, K. *et al.* Targeting Tim-3 and PD-1 pathways to reverse T cell exhaustion and restore anti-tumor immunity. *J. Exp. Med.* **207**, 2187–2194 (2010).

54. Harding, J. J. *et al.* Blocking TIM-3 in Treatment-refractory Advanced Solid Tumors: A Phase Ia/b Study of LY3321367 with or without an Anti-PD-L1 Antibody. *Clin. Cancer Res.* **27**, 2168–2178 (2021).
55. Borate, U. *et al.* Phase Ib Study of the Anti-TIM-3 Antibody MBG453 in Combination with Decitabine in Patients with High-Risk Myelodysplastic Syndrome (MDS) and Acute Myeloid Leukemia (AML). *Blood* **134**, 570–570 (2019).
56. Zeidan, A. *et al.* AML-187: The STIMULUS Clinical Trial Program: Evaluating Combination Therapy with MBG453 in Patients with Higher-Risk Myelodysplastic Syndrome (HR-MDS) or Acute Myeloid Leukemia. *Clin. Lymphoma Myeloma Leuk.* **20**, S188 (2020).
57. Kang, C.-W. *et al.* Apoptosis of tumor infiltrating effector TIM-3+CD8+ T cells in colon cancer. *Sci. Rep.* **5**, 15659 (2015).
58. Gonçalves Silva, I. *et al.* The Tim-3-galectin-9 Secretory Pathway is Involved in the Immune Escape of Human Acute Myeloid Leukemia Cells. *EBioMedicine* **22**, 44–57 (2017).
59. Chiba, S. *et al.* Tumor-infiltrating DCs suppress nucleic acid-mediated innate immune responses through interactions between the receptor TIM-3 and the alarmin HMGB1. *Nat. Immunol.* **13**, 832–842 (2012).
60. Huang, Y. *et al.* CEACAM1 regulates TIM-3-mediated tolerance and exhaustion. *Nature* **517**, 386–390 (2015).
61. Blaeschke, F. *et al.* Design and Evaluation of TIM-3-CD28 Checkpoint Fusion Proteins to Improve Anti-CD19 CAR T-Cell Function. *Front. Immunol.* **13**, (2022).
62. Ghani, K., Cottin, S., Kamen, A. & Caruso, M. Generation of a high-titer packaging cell line for the production of retroviral vectors in suspension and serum-free media. *Gene Ther.* **14**, 1705–1711 (2007).
63. Ghani, K., Wang, X., Campos-lima, P. O. De & Olszewska, M. Efficient Human Hematopoietic Cell Transduction Using RD114- and GALV-Pseudotyped Retroviral Vectors Produced in Suspension and Serum-Free Media. *Hum. Gene Ther.* **20**, 966–974 (2009).
64. Liu, X. *et al.* A chimeric switch-receptor targeting PD1 augments the efficacy of second generation CAR T-Cells in advanced solid tumors. *Cancer Res.* **10**, 4173–4183 (2016).
65. Oda, S. K. *et al.* A CD200R-CD28 fusion protein appropriates an inhibitory signal to enhance T-cell function and therapy of murine leukemia. *Blood* **130**, 2410–2419 (2017).
66. Rafiq, S. *et al.* Enhancing CAR T Cell Anti-Tumor Efficacy through Secreted Single Chain Variable Fragment (scFv) Immune Checkpoint Blockade. *Blood* **130**, 842 LP – 842 (2017).
67. Jin, H.-T. *et al.* Cooperation of Tim-3 and PD-1 in CD8 T-cell exhaustion during chronic viral infection. *Proc. Natl. Acad. Sci.* **107**, 14733–14738 (2010).
68. Zhu, C. *et al.* The Tim-3 ligand galectin-9 negatively regulates T helper type 1 immunity. *Nat. Immunol.* **6**, 1245–1252 (2005).
69. Yang, R. *et al.* Galectin-9 interacts with PD-1 and TIM-3 to regulate T cell death and is a target for cancer immunotherapy. *Nat. Commun.* **12**, 832 (2021).
70. De Sousa Linhares, A. *et al.* TIM-3 and CEACAM1 do not interact in cis and in trans. *Eur. J. Immunol.* **50**, 1126–1141 (2020).
71. Blaeschke, F. *et al.* Augmenting anti-CD19 and anti-CD22 CAR T-cell function using PD-1-CD28 checkpoint fusion proteins. *Blood Cancer J.* **11**, 108 (2021).

72. Kobold, S. *et al.* Impact of a New Fusion Receptor on PD-1-Mediated Immunosuppression in Adoptive T Cell Therapy. *J. Natl. Cancer Inst.* **107**, 1–10 (2015).
73. Lazar-Molnar, E., Almo, S. C. & Nathenson, S. G. The interchain disulfide linkage is not a prerequisite but enhances CD28 costimulatory function. *Cell. Immunol.* **244**, 125–129 (2006).
74. Grupp, S. A. *et al.* Chimeric Antigen Receptor–Modified T Cells for Acute Lymphoid Leukemia. *N. Engl. J. Med.* **368**, 1509–1518 (2013).
75. Alabanza, L. *et al.* Function of Novel Anti-CD19 Chimeric Antigen Receptors with Human Variable Regions Is Affected by Hinge and Transmembrane Domains. *Mol. Ther.* **25**, 2452–2465 (2017).
76. Zhao, S. *et al.* Switch receptor T3/28 improves long-term persistence and antitumor efficacy of CAR-T cells. *J. Immunother. Cancer* **9**, e003176 (2021).
77. Feucht, J. *et al.* Calibration of CAR activation potential directs alternative T cell fates and therapeutic potency. *Nat. Med.* **25**, 82–88 (2019).
78. Till, B. G. *et al.* CD20-specific adoptive immunotherapy for lymphoma using a chimeric antigen receptor with both CD28 and 4-1BB domains: pilot clinical trial results. *Blood* **119**, 3940–3950 (2012).
79. Gargett, T. & Brown, M. P. The inducible caspase-9 suicide gene system as a safety switch to limit on-target, off-tumor toxicities of chimeric antigen receptor T cells. *Front. Pharmacol.* **5**, (2014).
80. Diaconu, I. *et al.* Inducible Caspase-9 Selectively Modulates the Toxicities of CD19-Specific Chimeric Antigen Receptor-Modified T Cells. *Mol. Ther.* **25**, 580–592 (2017).
81. Weber, E. W. *et al.* Pharmacologic control of CAR-T cell function using dasatinib. *Blood Adv.* **3**, 711–717 (2019).

11 Supplements

11.1 Primer sequences

CAR_ident_forw	GCCAAACATTATTACTACGGTGGTA
CAR_ident_rev	TATGGGAATAAATGGCGGTAAGATG

11.2 T-cell sequences

11.2.1 Sequence of 19_3z CAR

ATGCTTCTCCTGGTGACAAGCCTTCTGCTCTGTGAGTTACCACACCCAGCATTCTCCTGATCCC
AGACATCCAGATGACACAGACTACATCCTCCCTGTCTGCCTCTCTGGGAGACAGAGTCACCATC
AGTTGCAGGGCAAGTCAGGACATTAGTAAATATTTAAATTGGTATCAGCAGAAACCAGATGGAAC
TGTTAAACTCCTGATCTACCATACATCAAGATTACACTCAGGAGTCCCATCAAGGTTTCAGTGGCA
GTGGGTCTGGAACAGATTATTCTCTCACCATTAGCAACCTGGAGCAAGAAGATATTGCCACTTAC
TTTTGCCAACAGGGTAATACGCTTCCGTACACGTTCCGGAGGGGGGACTAAGTTGGAATAACAG
GCTCCACCTCTGGATCCGGCAAGCCCGGATCTGGCGAGGGATCCACCAAGGGCGAGGTGAAA
CTGCAGGAGTCAGGACCTGGCCTGGTGGCGCCCTCACAGAGCCTGTCCGTCACATGCACTGTC
TCAGGGGTCTCATTACCCGACTATGGTGTAAGCTGGATTCGCCAGCCTCCACGAAAGGGTCTG
GAGTGGCTGGGAGTAATATGGGGTAGTGAAACCACATACTATAATTCAGCTCTCAAATCCAGAC
TGACCATCATCAAGGACAACCTCAAGAGCCAAGTTTTCTTAAAAATGAACAGTCTGCAAACCTGAT
GACACAGCCATTTACTACTGTGCCAAACATTATTACTACGGTGGTAGCTATGCTATGGACTACTG
GGGTCAAGGAACCTCAGTCACCGTCTCCTCAGAGCAAAAGCTCATTTCTGAAGAGGACTTGTTT
GTGCCGGTCTTCTGCCAGCGAAGCCCACCACGACGCCAGCGCCGCGACCACCAACACCCGGC
GCCACCATCGCGTCGCAGCCCCTGTCCCTGCGCCCAGAGGCGTGCCGGCCAGCGGGCGGGG
GGCGCAGTGACACGAGGGGGCTGGACTTCGCCTGTGATATCTACATCTGGGCGCCCTTGGCC
GTCGCTAAAGAAGGAAGAACCCTCAGGAAGGCCTGTACAATGAACTGCAGAAAGATAAGATGG
CGGAGGCCTACAGTGAGATTGGGATGAAAGGCGAGCGCCGGAGGGGCAAGGGGACACGATGG
CCTTTACCAGGGTCTCAGTACAGCCACCAAGGACACCTACGACGCCCTTCACATGCAGGCCCT
GCCCCCTCGCTAA

11.2.2 Sequence of 19_3z_28-TM2 CAR

ATGCTTCTCCTGGTGACAAGCCTTCTGCTCTGTGAGTTACCACACCCAGCATTCTCCTGATCCC
AGACATCCAGATGACACAGACTACATCCTCCCTGTCTGCCTCTCTGGGAGACAGAGTCACCATC
AGTTGCAGGGCAAGTCAGGACATTAGTAAATATTTAAATTGGTATCAGCAGAAACCAGATGGAAC
TGTTAAACTCCTGATCTACCATAACATCAAGATTAACTCAGGAGTCCCATCAAGGTTTCAAGTGGCA
GTGGGTCTGGAACAGATTATTCTCTCACCATTAGCAACCTGGAGCAAGAAGATATTGCCACTTAC
TTTTGCCAACAGGGTAATACGCTTCCGTACACGTTTCGGAGGGGGGACTAAGTTGGAATAACAG
GCTCCACCTCTGGATCCGGCAAGCCCGGATCTGGCGAGGGATCCACCAAGGGCGAGGTGAAA
CTGCAGGAGTCAGGACCTGGCCTGGTGGCGCCCTCACAGAGCCTGTCCGTCACATGCACTGTC
TCAGGGGTCTCATTACCCGACTATGGTGTAAGCTGGATTCCGACGCTCCACGAAAGGGTCTG
GAGTGGCTGGGAGTAATATGGGGTAGTGAAACCACATACTATAATTCAGCTCTCAAATCCAGAC
TGACCATCATCAAGGACAACCTCCAAGAGCCAAGTTTTCTTAAAAATGAACAGTCTGCAAACCTGAT
GACACAGCCATTTACTACTGTGCCAAACATTATTACTACGGTGGTAGCTATGCTATGGACTACTG
GGGTCAAGGAACCTCAGTCACCGTCTCCTCAGAGCAAAAGCTCATTTCTGAAGAGGACTTGTTT
GTGCCGGTCTTCTGCCAGCGAAGCCCACCACGACGCCAGCGCCGCGACCACCAACACCGGC
GCCACCATCGCGTCGCAGCCCCTGTCCCTGCGCCAGAGGGCGTGCCGGCCAGCGGCGGGG
GGCGCAGTGACACGAGGGGGCTGGACTTCGCCTGTGATATCTACATCTGGGCGCCCTTGGCC
GGGACTTGTTGGGGTCTTCTCCTGTCACTGGTTATCACCCCTTTACTGCAACCACAGGAACAGAG
TGAAGTTCAGCAGGAGCGCAGACGCCCCGCGTACCAGCAGGGCCAGAACCAGCTCTATAACG
AGCTCAATCTAGGACGAAGAGAGGAGTACGATGTTTTGGACAAGAGACGTGGCCGGGACCCTG
AGATGGGGGGAAAGCCGAGAAGGAAGAACCCTCAGGAAGGCCTGTACAATGAACTGCAGAAAG
ATAAGATGGCGGAGGCCTACAGTGAGATTGGGATGAAAGGCGAGCGCCGGAGGGGGCAAGGGG
CACGATGGCCTTTACCAGGGTCTCAGTACAGCCACCAAGGACACCTACGACGCCCTTCACATGC
AGGCCCTGCCCCCTCGCGTGAAACAGACTTTGAATTTTGACCTTCTCAAGTTGGCGGGAGACGT
GGAGTCCAACCCAGGCCCGATGTTTTACATCTTCCCTTTGACTGTGTCTGCTGCTGCTGCTG
CTACTACTTACAAGGTCTCAGAAGTGGAATACAGAGCGGAGGTTCGGTCAGAATGCCTATCTGC
CCTGCTTCTACACCCCAGCCGCCCCAGGGAACCTCGTGCCCGTCTGCTGGGGCAAAGGAGCCT
GTCCTGTGTTTGAATGTGGCAACGTGGTGTCTCAGGACTGATGAAAGGGATGTGAATTATTGGAC
ATCCAGATACTGGCTAAATGGGGATTTCCGCAAAGGAGATGTGTCCCTGACCATAGAGAATGTG
ACTCTAGCAGACAGTGGGATCTACTGCTGCCGGATCCAAATCCCAGGCATAATGAATGATGAAA
AATTTAACCTGAAGTTGGTCATCAAACCAGCCAAGGTCACCCCTGCACCGACTCTGCAGAGAGA
CTTCACTGCAGCCTTTCCAAGGATGCTTACCACCAGGGGACATGGCCCAGCAGAGACACAGAC
ACTGGGGAGCCTCCCTGATATAAATCTAACACAAATATCCACATTGGCCAATGAGTTACGGGACT
CTAGATTGGCCAATGACTTACGGCCCCTATTTCCCGGACCTTCTAAGCCCTTTTGGGTGCTGGT
GGTGGTTGGTGGAGTCCTGGCTTGCTATAGCTTGCTAGTAACAGTGGCCTTTATTATTTTCTGGG
TGAGGAGTAAGAGGAGCAGGCTCCTGCACAGTGACTACATGAACATGACTCCCCGCCGCCCG

GGCCACCCGCAAGCATTACCAGCCCTATGCCCCACCACGCGACTTCGCAGCCTATCGCTCCT
GA

11.2.3 Sequence of 19_3z_28-TM3 CAR

ATGCTTCTCCTGGTGACAAGCCTTCTGCTCTGTGAGTTACCACACCCAGCATTCTCCTGATCCC
AGACATCCAGATGACACAGACTACATCCTCCCTGTCTGCCTCTCTGGGAGACAGAGTCACCATC
AGTTGCAGGGCAAGTCAGGACATTAGTAAATATTTAAATTGGTATCAGCAGAAACCAGATGGAAC
TGTTAAACTCCTGATCTACCATACATCAAGATTACACTCAGGAGTCCCATCAAGGTTTCAAGTGGCA
GTGGGTCTGGAACAGATTATTCTCTCACCATTAGCAACCTGGAGCAAGAAGATATTGCCACTTAC
TTTTGCCAACAGGGTAATACGCTTCCGTACACGTTCCGGAGGGGGGACTAAGTTGGAATAACAG
GCTCCACCTCTGGATCCGGCAAGCCCGGATCTGGCGAGGGATCCACCAAGGGCGAGGTGAAA
CTGCAGGAGTCAGGACCTGGCCTGGTGGCGCCCTCACAGAGCCTGTCCGTCACATGCACTGTC
TCAGGGGTCTCATTACCCGACTATGGTGTAAGCTGGATTTCGCCAGCCTCCACGAAAGGGTCTG
GAGTGGCTGGGAGTAATATGGGGTAGTGAAACCACATACTATAATTCAGCTCTCAAATCCAGAC
TGACCATCATCAAGGACAACCTCAAGAGCCAAGTTTTCTTAAAAATGAACAGTCTGCAAATGAT
GACACAGCCATTTACTACTGTGCCAAACATTATTACTACGGTGGTAGCTATGCTATGGACTACTG
GGGTCAAGGAACCTCAGTCACCGTCTCCTCAGAGCAAAAGCTCATTTCTGAAGAGGACTTGTTT
GTGCCGGTCTTCTGCCAGCGAAGCCCACCACGACGCCAGCGCCGCGACCACCAACACCGGC
GCCACCATCGCGTCGCAGCCCCTGTCCCTGCGCCCAGAGGGCGTGCCGGCCAGCGGGCGGGG
GGCGCAGTGACACGAGGGGGCTGGACTTCGCCTGTGATATCTACATCTGGGCGCCCTTGGCC
GGGACTTGTGGGGTCTTCTCCTGTCACTGGTTATCACCCCTTTACTGCAACCACAGGAACAGAG
TGAAGTTCAGCAGGAGCGCAGACGCCCCCGCGTACCAGCAGGGCCAGAACCAGCTCTATAACG
AGCTCAATCTAGGACGAAGAGAGGAGTACGATGTTTTGGACAAGAGACGTGGCCGGGACCCTG
AGATGGGGGGAAAGCCGAGAAGGAAGAACCCTCAGGAAGGCCTGTACAATGAACTGCAGAAAG
ATAAGATGGCGGAGGCCTACAGTGAGATTGGGATGAAAGGCGAGCGCCGGAGGGGGCAAGGGG
CACGATGGCCTTTACCAGGGTCTCAGTACAGCCACCAAGGACACCTACGACGCCCTTCACATGC
AGGCCCTGCCCCCTCGCGTGAAACAGACTTTGAATTTTACCTTCTCAAGTTGGCGGGAGACGT
GGAGTCCAACCCAGGCCCGATGTTTTACATCTTCCCTTTGACTGTGTCTGCTGCTGCTGCTG
CTACTACTTACAAGGTCTCAGAAGTGAATACAGAGCGGAGGTTCGGTTCAGAATGCCTATCTGC
CCTGCTTCTACACCCCAGCCGCCCCAGGGAACCTCGTGCCCGTCTGCTGGGGCAAAGGAGCCT
GTCCTGTGTTTGAATGTGGCAACGTGGTGTCTCAGGACTGATGAAAGGGATGTGAATTATTGGAC
ATCCAGATACTGGCTAAATGGGGATTTCCGCAAAGGAGATGTGTCCCTGACCATAGAGAATGTG
ACTCTAGCAGACAGTGGGATCTACTGCTGCCGGATCCAAATCCCAGGCATAATGAATGATGAAA
AATTTAACCTGAAGTTGGTCATCAAACCAGCCAAGGTCACCCCTGCACCGACTCTGCAGAGAGA
CTTCACTGCAGCCTTTCCAAGGATGCTTACCACCAGGGGACATGGCCCAGCAGAGACACAGAC
ACTGGGGAGCCTCCCTGATATAAATCTAACACAAATATCCACATTGGCCAATGAGTTACGGGACT
CTAGATTGGCCAATTGTCCAAGTCCCCTATTTCCCGGACCTTCTAAGCCCTTTTGGGTGCTGGT

GGTGGTTGGTGGAGTCCTGGCTTGCTATAGCTTGCTAGTAACAGTGGCCTTTATTATTTTCTGGG
TGAGGAGTAAGAGGAGCAGGCTCCTGCACAGTGACTIONATGAACATGACTCCCCGCCGCCCG
GGCCCACCCGCAAGCATTACCAGCCCTATGCCCCACCACGCGACTTCGCAGCCTATCGCTCCT
GA

11.2.4 Sequence of 19_3z_TIM-3 CAR

CAGCATCGTTCTGTGTTGTCTGTCTGACTGTGTTTCTGTATTTGTCTGAAAATTAGCTCGACAA
AGTTAAGTAATAGTCCCTCTCTCCAAGCTCACTTACAGGCGGCCGCGCCGCCACCATGCTTCTC
CTGGTGACAAGCCTTCTGCTCTGTGAGTTACCACACCCAGCATTCTCCTGATCCCAGACATCC
AGATGACACAGACTACATCCTCCCTGTCTGCCTCTCTGGGAGACAGAGTCACCATCAGTTGCAG
GGCAAGTCAGGACATTAGTAAATATTTAAATTGGTATCAGCAGAAACCAGATGGAAGTGTAAAC
TCCTGATCTACCATACATCAAGATTACACTCAGGAGTCCCATCAAGGTTCAAGTGGCAGTGGGTC
TGGAACAGATTATTCTCTCACCATTAGCAACCTGGAGCAAGAAGATATTGCCACTTACTTTTGCC
AACAGGGTAATACGCTTCCGTACACGTTCCGAGGGGGGACTAAGTTGGAAATAACAGGCTCCA
CCTCTGGATCCGGCAAGCCCGGATCTGGCGAGGGATCCACCAAGGGCGAGGTGAAACTGCAG
GAGTCAGGACCTGGCCTGGTGGCGCCCTCACAGAGCCTGTCCGTACATGCACTGTCTCAGGG
GTCTCATTACCCGACTATGGTGTAAAGCTGGATTCCGACGCTCCACGAAAGGGTCTGGAGTGG
CTGGGAGTAATATGGGGTAGTGAAACCACATACTATAATTCAGCTCTCAAATCCAGACTGACCAT
CATCAAGGACAACCTCCAAGAGCCAAGTTTTCTTAAAAATGAACAGTCTGCAAACCTGATGACACAG
CCATTTACTACTGTGCCAAACATTATTACTACGGTGGTAGCTATGCTATGGACTACTGGGGTCAA
GGAACCTCAGTCACCGTCTCCTCAGAGCAAAAGCTCATTCTGAAGAGGACTTGTTTCGTGCCGG
TCTTCCTGCCAGCGAAGCCCACCACGACGCCAGCGCCGCGACCACCAACACCCGGCGCCCACC
ATCGCGTCGCAGCCCCTGTCCCTGCGCCCAGAGGCGTGCCGGCCAGCGGGCGGGGGCGCAG
TGCACACGAGGGGGCTGGACTTCGCCTGTGATATCTACATCTGGGCGCCCTTGCCGGGACTT
GTGGGGTCCTTCTCCTGTCACTGGTTATCACCTTTACTGCAACCACAGGAACAGAGTGAAGTT
CAGCAGGAGCGCAGACGCCCCCGGTACCAGCAGGGCCAGAACCAGCTCTATAACGAGCTCA
ATCTAGGACGAAGAGAGGAGTACGATGTTTTGGACAAGAGACGTGGCCGGGACCCTGAGATGG
GGGGAAAGCCGAGAAGGAAGAACCCTCAGGAAGGCCTGTACAATGAACTGCAGAAAGATAAGA
TGCGCGAGGCCTACAGTGAGATTGGGATGAAAGGCGAGCGCCGGAGGGGCAAGGGGCACGAT
GGCCTTTACCAGGGTCTCAGTACAGCCACCAAGGACACCTACGACGCCCTTCACATGCAGGCC
CTGCCCCCTCGCGTGAAACAGACTTTGAATTTTGACCTTCTCAAGTTGGCGGGAGACGTGGAGT
CCAACCCAGGCCCGTTTTTCACATCTTCCCTTTGACTGTGTCCTGCTGCTGCTGCTGCTACTACTT
ACAAGGTCCTCAGAAGTGGAAATACAGAGCGGAGGTCGGTCAGAATGCCTATCTGCCCTGCTTCT
ACACCCAGCCGCCCCAGGGAACCTCGTGCCCGTCTGCTGGGGCAAAGGAGCCTGTCTCTGTG
TTTGAATGTGGCAACGTGGTGCTCAGGACTGATGAAAGGGATGTGAATTATTGGACATCCAGAT
ACTGGCTAAATGGGGATTTCCGCAAAGGAGATGTGTCCCTGACCATAGAGAATGTGACTCTAGC
AGACAGTGGGATCTACTGCTGCCGGATCCAAATCCCAGGCATAATGAATGATGAAAAATTTAAC

CTGAAGTTGGTCATCAAACCAGCCAAGGTCACCCCTGCACCGACTCGGCAGAGAGACTTCACT
GCAGCCTTTCCAAGGATGCTTACCACCAGGGGACATGGCCCAGCAGAGACACAGACTGGGG
AGCCTCCCTGATATAAATCTAACACAAATATCCACATTGGCCAATGAGTTACGGGACTCTAGATT
GGCCAATGACTTACGGGACTCTGGAGCAACCATCAGAATAGGCATCTACATCGGAGCAGGGAT
CTGTGCTGGGCTGGCTCTGGCTCTTATCTTCGGCGCTTTAATTTTCAAATGGTATTCTCATAGCA
AAGAGAAGATACAGAATTTAAGCCTCATCTCTTTGGCCAACCTCCCTCCCTCAGGATTGGCAAAT
GCAGTAGCAGAGGGAATTCGCTCAGAAGAAAACATCTATAACCATTGAAGAGAACGTATATGAAG
TGGAGGAGCCCAATGAGTATTATTGCTATGTCAGCAGCAGGCAGCAACCCTCACAACCTTTGGG
TTGTCGCTTTGCAATGCCATAGCAATTCGAGCATCTTACCGCCATTTATTCCCATATTTGTTCTGT
TTTTCTTGATTTGGGTATACATTTAAATG

11.2.5 Sequence of 19_BB_3z CAR

ATGCTTCTCCTGGTGACAAGCCTTCTGCTCTGTGAGTTACCACACCCAGCATTCTCCTGATCCC
AGACATCCAGATGACACAGACTACATCCTCCCTGTCTGCCTCTCTGGGAGACAGAGTCACCATC
AGTTGCAGGGCAAGTCAGGACATTAGTAAATATTTAAATTGGTATCAGCAGAAACCAGATGGAAC
TGTTAAACTCCTGATCTACCATACATCAAGATTACACTCAGGAGTCCCATCAAGGTTTCAAGTGGCA
GTGGGTCTGGAACAGATTATTCTCTCACCATTAGCAACCTGGAGCAAGAAGATATTGCCACTTAC
TTTTGCCAACAGGGTAATACGCTTCCGTACACGTTCCGGAGGGGGGACTAAGTTGGAATAACAG
GCTCCACCTCTGGATCCGGCAAGCCCGGATCTGGCGAGGGATCCACCAAGGGCGAGGTGAAA
CTGCAGGAGTCAGGACCTGGCCTGGTGGCGCCCTCACAGAGCCTGTCCGTCACATGCACTGTC
TCAGGGGTCTCATTACCCGACTATGGTGTAAGCTGGATTCCGCCAGCCTCCACGAAAGGGTCTG
GAGTGGCTGGGAGTAATATGGGGTAGTGAAACCACATACTATAATTCAGCTCTCAAATCCAGAC
TGACCATCATCAAGGACAACCTCCAAGAGCCAAGTTTTCTTAAAAATGAACAGTCTGCAAACCTGAT
GACACAGCCATTTACTACTGTGCCAAACATTATTACTACGGTGGTAGCTATGCTATGGACTACTG
GGGTCAAGGAACCTCAGTCACCGTCTCCTCAGAGCAAAAGCTCATTTCTGAAGAGGACTTGTTT
GTGCCGGTCTTCTGCCAGCGAAGCCACCACGACGCCAGCGCCGCGACCACCAACACCGGC
GCCACCATCGCGTCGCAGCCCTGTCCCTGCGCCAGAGGCGTGCCGGCCAGCGGGCGGGG
GGCGCAGTGACACGAGGGGGCTGGACTTCGCCTGTGATATCTACATCTGGGCGCCCTTGGCC
GGGACTTGTGGGGTCTTCTCCTGTCACTGGTTATCACCCCTTTACTGCAACCACAGGAACAAAC
GGGGCAGAAAGAACTCCTGTATATATTCAAACAACCATTTATGAGACCAGTACAACTACTCAA
GAGGAAGATGGCTGTAGCTGCCGATTTCCAGAAGAAGAAGAAGGAGGATGTGAACTGAGAGTG
AAGTTCAGCAGGAGCGCAGACGCCCGCGTACCAGCAGGGCCAGAACCAGCTCTATAACGA
GCTCAATCTAGGACGAAGAGAGGAGTACGATGTTTTGGACAAGAGACGTGGCCGGGACCCTGA
GATGGGGGGAAAGCCGAGAAGGAAGAACCCTCAGGAAGGCCTGTACAATGAACTGCAGAAAGA
TAAGATGGCGGAGGCCTACAGTGAGATTGGGATGAAAGGCGAGCGCCGGAGGGGCAAGGGGC

ACGATGGCCTTTACCAGGGTCTCAGTACAGCCACCAAGGACACCTACGACGCCCTTCACATGCA
GGCCCTGCCCCCTCGCTAA

11.2.6 Sequence of 19_BB_3z_28-TM2 CAR

ATGCTTCTCCTGGTGACAAGCCTTCTGCTCTGTGAGTTACCACACCCAGCATTCTCCTGATCCC
AGACATCCAGATGACACAGACTACATCCTCCCTGTCTGCCTCTCTGGGAGACAGAGTCACCATC
AGTTGCAGGGCAAGTCAGGACATTAGTAAATATTTAAATTGGTATCAGCAGAAACCAGATGGAAC
TGTTAAACTCCTGATCTACCATACATCAAGATTACACTCAGGAGTCCCATCAAGGTTGAGTGGCA
GTGGGTCTGGAACAGATTATTCTCTCACCATTAGCAACCTGGAGCAAGAAGATATTGCCACTTAC
TTTTGCCAACAGGGTAATACGCTTCCGTACACGTTTCGGAGGGGGGACTAAGTTGGAAATAACAG
GCTCCACCTCTGGATCCGGCAAGCCCGGATCTGGCGAGGGATCCACCAAGGGCGAGGTGAAA
CTGCAGGAGTCAGGACCTGGCCTGGTGGCGCCCTCACAGAGCCTGTCCGTACATGCACTGTC
TCAGGGGTCTCATTACCCGACTATGGTGTAAAGCTGGATTCGCCAGCCTCCACGAAAGGGTCTG
GAGTGGCTGGGAGTAATATGGGGTAGTGAAACCACATACTATAATTCAGCTCTCAAATCCAGAC
TGACCATCATCAAGGACAACCTCCAAGAGCCAAGTTTTCTTAAAAATGAACAGTCTGCAAACCTGAT
GACACAGCCATTTACTACTGTGCCAAACATTATTACTACGGTGGTAGCTATGCTATGGACTACTG
GGGTCAAGGAACCTCAGTCACCGTCTCCTCAGAGCAAAAAGCTCATTCTGAAGAGGACTTGTTTC
GTGCCGGTCTTCTCCTGCCAGCGAAGCCACCACGACGCCAGCGCCGCGACCACCAACACCGGC
GCCACCATCGCGTCGCAGCCCCTGTCCCTGCGCCCAGAGGCGTGCCGGCCAGCGGCGGGG
GGCGCAGTGACACGAGGGGGCTGGACTTCGCCTGTGATATCTACATCTGGGCGCCCTTGGCC
GGGACTTGTGGGGTCTTCTCCTGTCACTGGTTATCACCCCTTTACTGCAACCACAGGAACAAAC
GGGGCAGAAAGAACTCCTGTATATATTCAAACAACCATTTATGAGACCAGTACAACTACTCAA
GAGGAAGATGGCTGTAGCTGCCGATTTCCAGAAGAAGAAGAAGGAGGATGTGAACTGAGAGTG
AAGTTCAGCAGGAGCGCAGACGCCCCGCGTACCAGCAGGGCCAGAACCAGCTCTATAACGA
GCTCAATCTAGGACGAAGAGAGGAGTACGATGTTTTGGACAAGAGACGTGGCCGGGACCCTGA
GATGGGGGGAAAGCCGAGAAGGAAGAACCCTCAGGAAGGCCTGTACAATGAACTGCAGAAAGA
TAAGATGGCGGAGGCCTACAGTGAGATTGGGATGAAAGGCGAGCGCCGGAGGGGCAAGGGGC
ACGATGGCCTTTACCAGGGTCTCAGTACAGCCACCAAGGACACCTACGACGCCCTTCACATGCA
GGCCCTGCCCCCTCGCGTGAAACAGACTTTGAATTTTGACCTTCTCAAGTTGGCGGGAGACGTG
GAGTCCAACCCAGGCCCGATGTTTTACATCTTCCCTTTGACTGTGTCCTGCTGCTGCTGCTGC
TACTACTTACAAGGTCCTCAGAAGTGAATACAGAGCGGAGGTCGGTCAGAATGCCTATCTGCC
CTGCTTCTACACCCAGCCGCCCCAGGGAACCTCGTGCCCGTCTGCTGGGGCAAAGGAGCCTG
TCCTGTGTTTGAATGTGGCAACGTGGTGTCTCAGGACTGATGAAAGGGATGTGAATTATTGGACA
TCCAGATACTGGCTAAATGGGGATTTCCGCAAAGGAGATGTGTCCCTGACCATAGAGAATGTGA
CTCTAGCAGACAGTGGGATCTACTGCTGCCGGATCCAAATCCCAGGCATAATGAATGATGAAAA
ATTTAACCTGAAGTTGGTCATCAAACCAGCCAAGGTCACCCCTGCACCGACTCTGCAGAGAGAC

TTCAGTGCAGCCTTTCCAAGGATGCTTACCACCAGGGGACATGGCCCAGCAGAGACACAGACA
CTGGGGAGCCTCCCTGATATAAATCTAACACAAATATCCACATTGGCCAATGAGTTACGGGACT
CTAGATTGGCCAATGACTTACGGCCCCTATTTCCCGGACCTTCTAAGCCCTTTTGGGTGCTGGT
GGTGGTTGGTGGAGTCCTGGCTTGCTATAGCTTGCTAGTAACAGTGGCCTTTATTATTTTCTGGG
TGAGGAGTAAGAGGAGCAGGCTCCTGCACAGTGACTACATGAACATGACTCCCCGCCGCCCG
GGCCACCCGCAAGCATTACCAGCCCTATGCCCCACCACGCGACTTCGCAGCCTATCGCTCCT
GA

11.2.7 Sequence of 19_BB_3z_28-TM3 CAR

ATGCTTCTCCTGGTGACAAGCCTTCTGCTCTGTGAGTTACCACACCCAGCATTCTCCTGATCCC
AGACATCCAGATGACACAGACTACATCCTCCCTGTCTGCCTCTCTGGGAGACAGAGTCACCATC
AGTTGCAGGGCAAGTCAGGACATTAGTAAATATTTAAATTGGTATCAGCAGAAACCAGATGGAAC
TGTTAAACTCCTGATCTACCATACATCAAGATTACACTCAGGAGTCCCATCAAGGTTTCAAGTGGCA
GTGGGTCTGGAACAGATTATTCTCTCACCATTAGCAACCTGGAGCAAGAAGATATTGCCACTTAC
TTTTGCCAACAGGGTAATACGCTTCCGTACACGTTTCGGAGGGGGGACTAAGTTGGAATAACAG
GCTCCACCTCTGGATCCGGCAAGCCCGGATCTGGCGAGGGATCCACCAAGGGCGAGGTGAAA
CTGCAGGAGTCAGGACCTGGCCTGGTGGCGCCCTCACAGAGCCTGTCCGTACATGCACTGTC
TCAGGGGTCTCATTACCCGACTATGGTGTAAAGCTGGATTCCGACGCTCCACGAAAGGGTCTG
GAGTGGCTGGGAGTAATATGGGGTAGTGAAACCACATACTATAATTCAGCTCTCAAATCCAGAC
TGACCATCATCAAGGACAACCTCCAAGAGCCAAGTTTTCTTAAAAATGAACAGTCTGCAAACCTGAT
GACACAGCCATTTACTACTGTGCCAAACATTATTACTACGGTGGTAGCTATGCTATGGACTACTG
GGGTCAAGGAACCTCAGTCACCGTCTCCTCAGAGCAAAGCTCATTCTGAAGAGGACTTGTTT
GTGCCGGTCTTCTGCCAGCGAAGCCACCACGACGCCAGCGCCGCGACCACCAACACCGGC
GCCACCATCGCGTCGCAGCCCCTGTCCCTGCGCCAGAGGCGTGCCGGCCAGCGGCGGGG
GGCGCAGTGACACGAGGGGGCTGGACTTCGCCTGTGATATCTACATCTGGGCGCCCTTGGCC
GGGACTTGTGGGGTCTTCTCCTGTCACTGGTTATCACCCCTTTACTGCAACCACAGGAACAAC
GGGGCAGAAAGAACTCCTGTATATATTCAAACAACCATTTATGAGACCAGTACAACTACTCAA
GAGGAAGATGGCTGTAGCTGCCGATTTCCAGAAGAAGAAGAAGGAGGATGTGAACTGAGAGTG
AAGTTCAGCAGGAGCGCAGACGCCCCCGGTACCAGCAGGGCCAGAACCAGCTCTATAACGA
GCTCAATCTAGGACGAAGAGAGGAGTACGATGTTTTGGACAAGAGACGTGGCCGGGACCCTGA
GATGGGGGGAAAGCCGAGAAGGAAGAACCCTCAGGAAGGCCTGTACAATGAACTGCAGAAAGA
TAAGATGGCGGAGGCCTACAGTGAGATTGGGATGAAAGGCGAGCGCCGGAGGGGCAAGGGGC
ACGATGGCCTTTACCAGGGTCTCAGTACAGCCACCAAGGACACCTACGACGCCCTTACATGCA
GGCCCTGCCCCCTCGCGTGAAACAGACTTTGAATTTTACCTTCTCAAGTTGGCGGGAGACGTG
GAGTCCAACCCAGGCCCGATGTTTTCACATCTTCCCTTTGACTGTGTCCTGCTGCTGCTGCTGC
TACTACTTACAAGGTCCTCAGAAGTGAATACAGAGCGGAGGTCGGTCAGAATGCCTATCTGCC
CTGCTTCTACACCCAGCCGCCCCAGGGAACCTCGTGCCCGTCTGCTGGGGCAAAGGAGCCTG

TCCTGTGTTTGAATGTGGCAACGTGGTGCTCAGGACTGATGAAAGGGATGTGAATTATTGGACA
TCCAGATACTGGCTAAATGGGGATTTCCGCAAAGGAGATGTGTCCCTGACCATAGAGAATGTGA
CTCTAGCAGACAGTGGGATCTACTGCTGCCGGATCCAAATCCCAGGCATAATGAATGATGAAAA
ATTTAACCTGAAGTTGGTCATCAAACCAGCCAAGGTCACCCCTGCACCGACTCTGCAGAGAGAC
TTCAGTGCAGCCTTTCCAAGGATGCTTACCACCAGGGGACATGGCCCAGCAGAGACACAGACA
CTGGGGAGCCTCCCTGATATAAATCTAACACAAATATCCACATTGGCCAATGAGTTACGGGACT
CTAGATTGGCCAATTGTCCAAGTCCCCTATTTCCCGGACCTTCTAAGCCCTTTTGGGTGCTGGT
GGTGGTTGGTGGAGTCCTGGCTTGCTATAGCTTGCTAGTAACAGTGGCCTTTATTATTTTCTGGG
TGAGGAGTAAGAGGAGCAGGCTCCTGCACAGTGACTACATGAACATGACTCCCCGCCGCCCG
GGCCCACCCGCAAGCATTACCAGCCCTATGCCCCACCACGCGACTTCGCAGCCTATCGCTCCT
GA

11.2.8 Sequence of 19_BB_3z_TIM-3 CAR

GCCGCCACCATGCTTCTCCTGGTGACAAGCCTTCTGCTCTGTGAGTTACCACACCCAGCATTCC
TCCTGATCCCAGACATCCAGATGACACAGACTACATCCTCCCTGTCTGCCTCTCTGGGAGACAG
AGTCACCATCAGTTGCAGGGCAAGTCAGGACATTAGTAAATATTTAAATTGGTATCAGCAGAAAC
CAGATGGAAGTGTAAACTCCTGATCTACCATACATCAAGATTACACTCAGGAGTCCCATCAAGG
TTCAGTGGCAGTGGGTCTGGAACAGATTATTCTCTCACCATTAGCAACCTGGAGCAAGAAGATA
TTGCCACTTACTTTTGCCAACAGGGTAATACGCTTCCGTACACGTTCCGGAGGGGGGACTAAGTT
GGAAATAACAGGCTCCACCTCTGGATCCGGCAAGCCCGGATCTGGCGAGGGATCCACCAAGG
GCGAGGTGAAACTGCAGGAGTCAGGACCTGGCCTGGTGGCGCCCTCACAGAGCCTGTCCGTC
ACATGCACTGTCTCAGGGGTCTCATTACCCGACTATGGTGTAAGCTGGATTCCGCCAGCCTCCAC
GAAAGGGTCTGGAGTGGCTGGGAGTAATATGGGGTAGTGAAACCACATACTATAATTCAGCTCT
CAAATCCAGACTGACCATCATCAAGGACAACCTCAAGAGCCAAGTTTTCTTAAAAATGAACAGTC
TGCAAAGTATGACACAGCCATTTACTACTGTGCCAAACATTATTACTACGGTGGTAGCTATGCT
ATGGACTACTGGGGTCAAGGAACCTCAGTCACCGTCTCCTCAGAGCAAAGCTCATTCTGAAG
AGGACTTGTTTCGTGCCGGTCTTCCCTGCCAGCGAAGCCACCACGACGCCAGCGCCGCGACCAC
CAACACCGGCGCCACCATCGCGTCGCAGCCCCTGTCCCTGCGCCCAGAGGCGTGCCGGCCA
GCGGGCGGGGGCGCAGTGCACACGAGGGGGCTGGACTTCGCCTGTGATATCTACATCTGGGC
GCCCTTGCCGGGACTTGTGGGGTCTTCTCCTGTCACTGGTTATCACCCTTTACTGCAACCAC
AGGAACAAACGGGGCAGAAAGAAACTCCTGTATATATTCAAACAACCATTTATGAGACCAGTACA
AACTACTCAAGAGGAAGATGGCTGTAGCTGCCGATTTCCAGAAGAAGAAGAAGGAGGATGTGAA
CTGAGAGTGAAGTTCAGCAGGAGCGCAGACGCCCCCGGTACCAGCAGGGCCAGAACCAGCT
CTATAACGAGCTCAATCTAGGACGAAGAGAGGAGTACGATGTTTTGGACAAGAGACGTGGCCG
GGACCCTGAGATGGGGGAAAGCCGAGAAGGAAGAACCCTCAGGAAGGCCTGTACAATGAACT
GCAGAAAGATAAGATGGCGGAGGCCTACAGTGAGATTGGGATGAAAGGCGAGCGCCGGAGGG
GCAAGGGGCACGATGGCCTTTACCAGGGTCTCAGTACAGCCACCAAGGACACCTACGACGCC

TTCACATGCAGGCCCTGCCCCCTCGCGTGAAACAGACTTTGAATTTTGACCTTCTCAAGTTGGC
GGGAGACGTGGAGTCCAACCCAGGCCCGTTTTACATCTTCCCTTTGACTGTGTCTGCTGCTG
CTGCTGCTACTACTTACAAGGTCCTCAGAAGTGGAATACAGAGCGGAGGTTCGGTCAGAATGCCT
ATCTGCCCTGCTTCTACACCCAGCCGCCCCAGGGAACCTCGTGCCCGTCTGCTGGGGCAAAG
GAGCCTGTCTGTGTTTGAATGTGGCAACGTGGTGCTCAGGACTGATGAAAGGGATGTGAATTA
TTGGACATCCAGATACTGGCTAAATGGGGATTTCCGCAAAGGAGATGTGTCCCTGACCATAGAG
AATGTGACTCTAGCAGACAGTGGGATCTACTGCTGCCGGATCCAAATCCCAGGCATAATGAATG
ATGAAAAATTTAACCTGAAGTTGGTCATCAAACCAGCCAAGGTCACCCCTGCACCGACTCGGCA
GAGAGACTTCACTGCAGCCTTTCCAAGGATGCTTACCACCAGGGGACATGGCCCAGCAGAGAC
ACAGACACTGGGGAGCCTCCCTGATATAAATCTAACACAAATATCCACATTGGCCAATGAGTTAC
GGGACTCTAGATTGGCCAATGACTTACGGGACTCTGGAGCAACCATCAGAATAGGCATCTACAT
CGGAGCAGGGATCTGTGCTGGGCTGGCTCTGGCTCTTATCTTCGGCGCTTTAATTTTCAAATGG
TATTCTCATAGCAAAGAGAAGATACAGAATTTAAGCCTCATCTCTTTGGCCAACCTCCCTCCCTC
AGGATTGGCAAATGCAGTAGCAGAGGGGAATTCGCTCAGAAGAAAACATCTATACCATTGAAGAG
AACGTATATGAAGTGGAGGAGCCCAATGAGTATTATTGCTATGTCAGCAGCAGGCAGCAACCCT
CACAACCTTTGGGTTGTGCGCTTTGCAATGCCATAG

11.2.9 Sequence of 19t CAR

ATGCTTCTCCTGGTGACAAGCCTTCTGCTCTGTGAGTTACCACACCCAGCATTCTCCTGATCCC
AGACATCCAGATGACACAGACTACATCCTCCCTGTCTGCCTCTCTGGGAGACAGAGTCACCATC
AGTTGCAGGGCAAGTCAGGACATTAGTAAATATTTAAATTGGTATCAGCAGAAACCAGATGGAAC
TGTTAAACTCCTGATCTACCATAACATCAAGATTACACTCAGGAGTCCCATCAAGGTTTCAGTGGCA
GTGGGTCTGGAACAGATTATTCTCTCACCATTAGCAACCTGGAGCAAGAAGATATTGCCACTTAC
TTTTGCCAACAGGGTAATACGCTTCCGTACACGTTCCGGAGGGGGGACTAAGTTGGAATAACAG
GCTCCACCTCTGGATCCGGCAAGCCCGGATCTGGCGAGGGATCCACCAAGGGCGAGGTGAAA
CTGCAGGAGTCAGGACCTGGCCTGGTGGCGCCCTCACAGAGCCTGTCCGTCACATGCACTGTC
TCAGGGGTCTCATTACCCGACTATGGTGTAAGCTGGATTCGCCAGCCTCCACGAAAGGGTCTG
GAGTGGCTGGGAGTAATATGGGGTAGTGAAACCACATACTATAATTCAGCTCTCAAATCCAGAC
TGACCATCATCAAGGACAACCTCCAAGAGCCAAGTTTTCTTAAAAATGAACAGTCTGCAAACCTGAT
GACACAGCCATTTACTACTGTGCCAAACATTATTACTACGGTGGTAGCTATGCTATGGACTACTG
GGGTCAAGGAACCTCAGTCACCGTCTCCTCAGAGCAAAAGCTCATTTCTGAAGAGGACTTGTTT
GTGCCGGTCTTCTGCCAGCGAAGCCCACCACGACGCCAGCGCCGCGACCACCAACACCCGGC
GCCACCATCGCGTCGCAGCCCTGTCCCTGCGCCAGAGGCGTGCCGGCCAGCGGGCGGGG
GGCGCAGTGACACGAGGGGGCTGGACTTCGCCTGTGATATCTACATCTGGGCGCCCTTGGCC
GGGACTTGTGGGGTCTTCTCCTGTCACTGGTTATCACCCCTTTACTGCAACCACAGGAACTGA

11.2.10 Sequence of 28-TM1 fusion receptor

CAGCATCGTTCTGTGTTGTCTCTGTCTGACTGTGTTTCTGTATTTGTCTGAAAATTAGCTCGACAA
AGTTAAGTAATAGTCCCTCTCTCCAAGCTCACTTACAGGCGGCCGCGCCGCCACCATGTTTTCA
CATCTTCCCTTTGACTGTGTCCTGCTGCTGCTGCTGCTACTACTTACAAGGTCCTCAGAAGTGGA
ATACAGAGCGGAGGTCGGTCAGAATGCCTATCTGCCCTGCTTCTACACCCCAGCCGCCCCAGG
GAACCTCGTGCCCGTCTGCTGGGGCAAAGGAGCCTGTCCTGTGTTTGAATGTGGCAACGTGGT
GCTCAGGACTGATGAAAGGGATGTGAATTATTGGACATCCAGATACTGGCTAAATGGGGATTTC
CGCAAAGGAGATGTGTCCCTGACCATAGAGAATGTGACTCTAGCAGACAGTGGGATCTACTGCT
GCCGGATCCAAATCCCAGGCATAATGAATGATGAAAAATTTAACCTGAAGTTGGTCATCAAACCA
GCCAAGGTCACCCCTGCACCGACTCGGCAGAGAGACTTCACTGCAGCCTTTCCAAGGATGCTT
ACCACCAGGGGACATGGCCCAGCAGAGACACAGACACTGGGGAGCCTCCCTGATATAAATCTA
ACACAAATATCCACATTGGCCAATGAGTTACGGGACTCTAGATTGGCCAATGACTTACGGGACT
CTGGAGCAACCATCAGAATAGGCTTTTGGGTGCTGGTGGTGGTTGGTGGAGTCCTGGCTTGCT
ATAGCTTGCTAGTAACAGTGGCCTTTATTATTTTCTGGGTGAGGAGTAAGAGGAGCAGGCTCCT
GCACAGTGACTACATGAACATGACTCCCCGCCGCCCGGGCCCACCCGCAAGCATTACCAGCC
CTATGCCCCACCACGCGACTTCGCAGCCTATCGTCTCCTGAGAATTCGAGCATCTTACCGCCATT
TATTCCCATATTTGTTCTGTTTTTCTTGATTTGGGTATACATTTAAATG

11.2.11 Sequence of 28-TM2 fusion receptor

CAGCATCGTTCTGTGTTGTCTCTGTCTGACTGTGTTTCTGTATTTGTCTGAAAATTAGCTCGACAA
AGTTAAGTAATAGTCCCTCTCTCCAAGCTCACTTACAGGCGGCCGCATGTTTTCACATCTTCCCT
TTGACTGTGTCCTGCTGCTGCTGCTGCTACTACTTACAAGGTCCTCAGAAGTGGAATACAGAGC
GGAGGTCGGTCAGAATGCCTATCTGCCCTGCTTCTACACCCCAGCCGCCCCAGGGAACCTCGT
GCCCGTCTGCTGGGGCAAAGGAGCCTGTCCTGTGTTTGAATGTGGCAACGTGGTGCTCAGGAC
TGATGAAAGGGATGTGAATTATTGGACATCCAGATACTGGCTAAATGGGGATTTCCGCAAAGGA
GATGTGTCCCTGACCATAGAGAATGTGACTCTAGCAGACAGTGGGATCTACTGCTGCCGGATCC
AAATCCCAGGCATAATGAATGATGAAAAATTTAACCTGAAGTTGGTCATCAAACCAGCCAAGGTC
ACCCCTGCACCGACTCTGCAGAGAGACTTCACTGCAGCCTTTCCAAGGATGCTTACCACCAGGG
GACATGGCCCAGCAGAGACACAGACACTGGGGAGCCTCCCTGATATAAATCTAACACAAATATC
CACATTGGCCAATGAGTTACGGGACTCTAGATTGGCCAATGACTTACGGCCCCTATTTCCCGGA
CCTTCTAAGCCCTTTTGGGTGCTGGTGGTGGTTGGTGGAGTCCTGGCTTGCTATAGCTTGCTAG
TAACAGTGGCCTTTATTATTTTCTGGGTGAGGAGTAAGAGGAGCAGGCTCCTGCACAGTGACTA
CATGAACATGACTCCCCGCCGCCCGGGCCCACCCGCAAGCATTACCAGCCCTATGCCCCACC
ACGCGACTTCGCAGCCTATCGTCTCCTGAGAATTCGAGCATCTTACCGCCATTTATTCCCATATTT
GTTCTGTTTTTCTTGATTTGGGTATACATTTAAATG

11.2.12 Sequence of 28-TM3 fusion receptor

CAGCATCGTTCTGTGTTGTCTCTGTCTGACTGTGTTTCTGTATTTGTCTGAAAATTAGCTCGACAA
AGTTAAGTAATAGTCCCTCTCTCCAAGCTCACTTACAGGCGGCCGCATGTTTTACATCTTCCCT
TTGACTGTGTCCTGCTGCTGCTGCTGCTACTACTTACAAGTCTCAGAAGTGGAATACAGAGC
GGAGGTTCGGTCAGAATGCCTATCTGCCCTGCTTCTACACCCCAGCCGCCCCAGGGAACCTCGT
GCCCCGTCTGCTGGGGCAAAGGAGCCTGTCTGTGTTGAATGTGGCAACGTGGTGCTCAGGAC
TGATGAAAGGGATGTGAATTATTGGACATCCAGATACTGGCTAAATGGGGATTTCCGCAAAGGA
GATGTGTCCCTGACCATAGAGAATGTGACTCTAGCAGACAGTGGGATCTACTGCTGCCGGATCC
AAATCCCAGGCATAATGAATGATGAAAAATTTAACCTGAAGTTGGTCATCAAACCAGCCAAGGTC
ACCCCTGCACCGACTCTGCAGAGAGACTTCACTGCAGCCTTTCCAAGGATGCTTACCACCAGGG
GACATGGCCCAGCAGAGACACAGACACTGGGGAGCCTCCCTGATATAAATCTAACACAAATATC
CACATTGGCCAATGAGTTACGGGACTCTAGATTGGCCAATTGTCCAAGTCCCCTATTTCCCGGA
CCTTCTAAGCCCTTTTGGGTGCTGGTGGTGGTTGGTGGAGTCCGGCTTGCTATAGCTTGCTAG
TAACAGTGGCCTTTATTATTTTCTGGGTGAGGAGTAAGAGGAGCAGGCTCCTGCACAGTACTA
CATGAACATGACTCCCCGCCGCCCGGGCCACCCGCAAGCATTACCAGCCCTATGCCCCACC
ACGCGACTTCGCAGCCTATCGCTCCTGAGAATTGAGCATCTTACCGCCATTTATTCCCATATTT
GTTCTGTTTTTCTTGATTTGGGTATACATTTAAATG

11.2.13 Sequence of 8-TM fusion receptor

CAGCATCGTTCTGTGTTGTCTCTGTCTGACTGTGTTTCTGTATTTGTCTGAAAATTAGCTCGACAA
AGTTAAGTAATAGTCCCTCTCTCCAAGCTCACTTACAGGCGGCCGCATGTTTTACATCTTCCCT
TTGACTGTGTCCTGCTGCTGCTGCTGCTACTACTTACAAGTCTCAGAAGTGGAATACAGAGC
GGAGGTTCGGTCAGAATGCCTATCTGCCCTGCTTCTACACCCCAGCCGCCCCAGGGAACCTCGT
GCCCCGTCTGCTGGGGCAAAGGAGCCTGTCTGTGTTGAATGTGGCAACGTGGTGCTCAGGAC
TGATGAAAGGGATGTGAATTATTGGACATCCAGATACTGGCTAAATGGGGATTTCCGCAAAGGA
GATGTGTCCCTGACCATAGAGAATGTGACTCTAGCAGACAGTGGGATCTACTGCTGCCGGATCC
AAATCCCAGGCATAATGAATGATGAAAAATTTAACCTGAAGTTGGTCATCAAACCAGCCAAGGTC
ACCCCTGCACCGACTCTGCAGAGAGACTTCACTGCAGCCTTTCCAAGGATGCTTACCACCAGGG
GACATGGCCCAGCAGAGACACAGACACTGGGGAGCCTCCCTGATATAAATCTAACACAAATATC
CACATTGGCCAATGAGTTACGGGACTCTAGATTGGCCAATGACTTACGGGACTCTGGAGCAACC
ATCAGAATAGGCATCTACATCTGGGCGCCCTTGGCCGGGACTTGTGGGGTCCCTTCTCCTGTCAC
TGGTTATCACCAGGAGTAAGAGGAGCAGGCTCCTGCACAGTACTACATGAACATGACTCCCCG
CCGCCCCGGGCCACCCGCAAGCATTACCAGCCCTATGCCCCACCACGCGACTTCGCAGCCTA
TCGCTCCTGAGAATTGAGCATCTTACCGCCATTTATTCCCATATTTGTTCTGTTTTTCTTGATTT
GGGTATACATTTAAATG

11.2.14 Sequence of TIM3t construct

ATGTTTTACATCTTCCCTTTGACTGTGTCCTGCTGCTGCTGCTGCTACTACTTACAAGGTCCTC
AGAAGTGAATACAGAGCGGAGGTCGGTCAGAATGCCTATCTGCCCTGCTTCTACACCCCAGC
CGCCCCAGGGAACCTCGTGCCCGTCTGCTGGGGCAAAGGAGCCTGTCCTGTGTTTGAATGTGG
CAACGTGGTGCTCAGGACTGATGAAAGGGATGTGAATTATTGGACATCCAGATACTGGCTAAAT
GGGGATTTCCGCAAAGGAGATGTGTCCCTGACCATAGAGAATGTGACTCTAGCAGACAGTGGG
ATCTACTGCTGCCGGATCCAAATCCCAGGCATAATGAATGATGAAAAATTTAACCTGAAGTTGGT
CATCAAACCAGCCAAGGTCACCCCTGCACCGACTCTGCAGAGAGACTTCACTGCAGCCTTTCCA
AGGATGCTTACCACCAGGGGACATGGCCCAGCAGAGACACAGACACTGGGGAGCCTCCCTGAT
ATAAATCTAACACAAATATCCACATTGGCCAATGAGTTACGGGACTCTAGATTGGCCAATGACTT
ACGGGACTCTGGAGCAACCATCAGAATAGGCATCTACATCGGAGCAGGGATCTGTGCTGGGCT
GGCTCTGGCTCTTATCTTCGGCGCTTTAATT

11.2.15 Sequence of TIM3-TM1 fusion receptor

CAGCATCGTTCTGTGTTGTCTCTGTCTGACTGTGTTTCTGTATTTGTCTGAAAATTAGCTCGACAA
AGTTAAGTAATAGTCCCTCTCTCCAAGCTCACTTACAGGCGGCCGCATGTTTTACATCTTCCCT
TTGACTGTGTCCTGCTGCTGCTGCTGCTACTACTTACAAGTCCCTCAGAAGTGAATACAGAGC
GGAGGTCGGTCAGAATGCCTATCTGCCCTGCTTCTACACCCCAGCCGCCCCAGGGAACCTCGT
GCCCGTCTGCTGGGGCAAAGGAGCCTGTCCTGTGTTTGAATGTGGCAACGTGGTGCTCAGGAC
TGATGAAAGGGATGTGAATTATTGGACATCCAGATACTGGCTAAATGGGGATTTCCGCAAAGGA
GATGTGTCCCTGACCATAGAGAATGTGACTCTAGCAGACAGTGGGATCTACTGCTGCCGGATCC
AAATCCCAGGCATAATGAATGATGAAAAATTTAACCTGAAGTTGGTCATCAAACCAGCCAAGGTC
ACCCCTGCACCGACTCTGCAGAGAGACTTCACTGCAGCCTTTCCAAGGATGCTTACCACCAGGG
GACATGGCCCAGCAGAGACACAGACACTGGGGAGCCTCCCTGATATAAATCTAACACAAATATC
CACATTGGCCAATGAGTTACGGGACTCTAGATTGGCCAATGACTTACGGGACTCTGGAGCAACC
ATCAGAATAGGCATCTACATCGGAGCAGGGATCTGTGCTGGGCTGGCTCTGGCTCTTATCTTCG
GCGCTTTAATTTTCAAATGGTATTCTCATAGCAAAGAGAGTGACTACATGAACATGACTCCCCGC
CGCCCCGGGCCACCCGCAAGCATTACCAGCCCTATGCCCCACCACGCGACTTCGCAGCCTAT
CGCTCCTGAGAATTCGAGCATCTTACCGCCATTTATTCCCATATTTGTTCTGTTTTTCTTGATTTG
GGTATACATTTAAATG

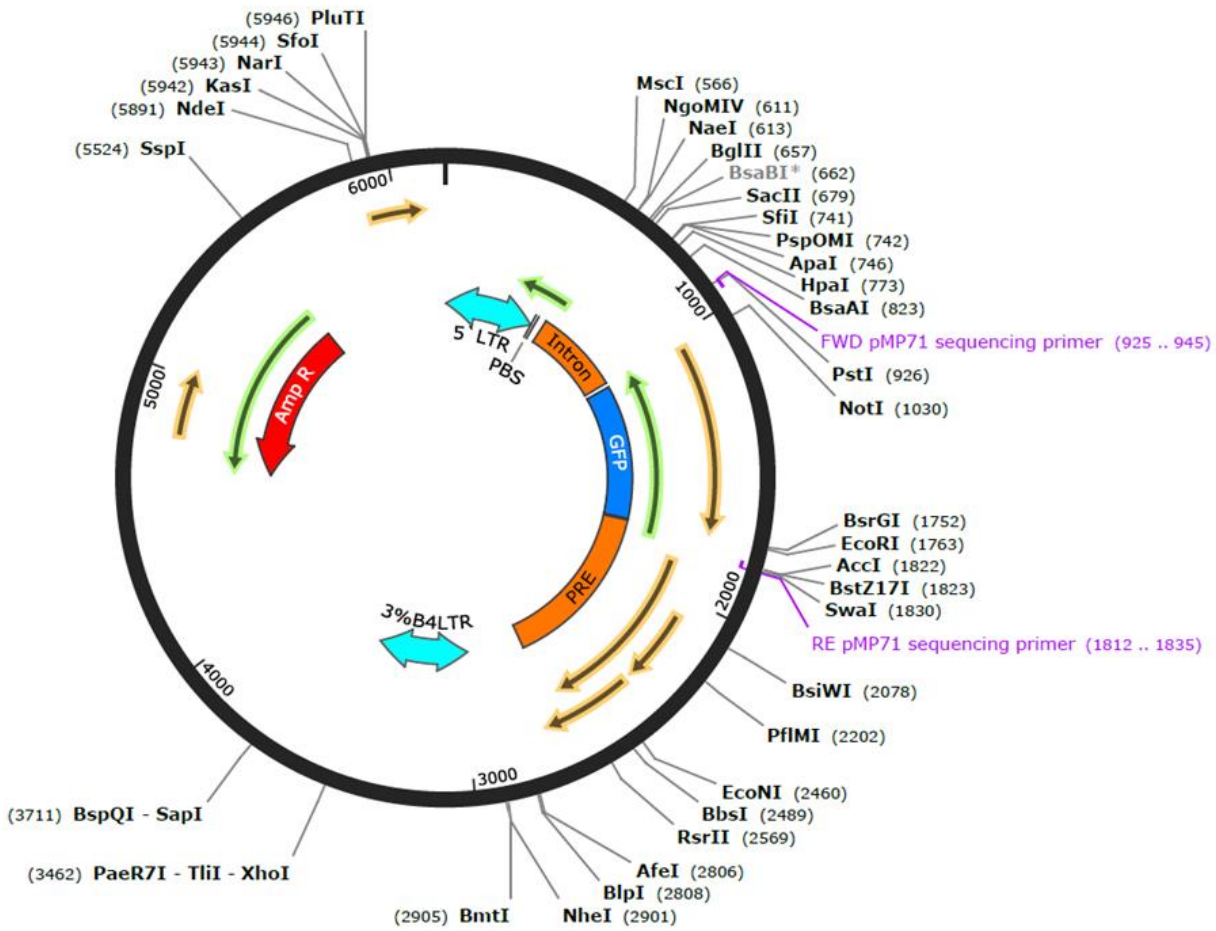
11.2.16 Sequence of TIM3-TM2 fusion receptor

CAGCATCGTTCTGTGTTGTCTCTGTCTGACTGTGTTTCTGTATTTGTCTGAAAATTAGCTCGACAA
AGTTAAGTAATAGTCCCTCTCTCCAAGCTCACTTACAGGCGGCCGCAGCCGCCACCATGTTTTCA
CATCTTCCCTTTGACTGTGTCCTGCTGCTGCTGCTGCTACTACTTACAAGTCCCTCAGAAGTGGA
ATACAGAGCGGAGGTCGGTCAGAATGCCTATCTGCCCTGCTTCTACACCCCAGCCGCCCCAGG
GAACCTCGTGCCCGTCTGCTGGGGCAAAGGAGCCTGTCCTGTGTTTGAATGTGGCAACGTGGT

GCTCAGGACTGATGAAAGGGATGTGAATTATTGGACATCCAGATACTGGCTAAATGGGGATTTC
CGCAAAGGAGATGTGTCCCTGACCATAGAGAATGTGACTCTAGCAGACAGTGGGATCTACTGCT
GCCGGATCCAAATCCCAGGCATAATGAATGATGAAAAATTTAACCTGAAGTTGGTCATCAAACCA
GCCAAGGTCACCCCTGCACCGACTCGGCAGAGAGACTTCACTGCAGCCTTTCCAAGGATGCTT
ACCACCAGGGGACATGGCCCAGCAGAGACACAGACACTGGGGAGCCTCCCTGATATAAATCTA
ACACAAATATCCACATTGGCCAATGAGTTACGGGACTCTAGATTGGCCAATGACTTACGGGACT
CTGGAGCAACCATCAGAATAGGCATCTACATCGGAGCAGGGATCTGTGCTGGGCTGGCTCTGG
CTCTTATCTTCGGCGCTTTAATTAGGAGTAAGAGGAGCAGGCTCCTGCACAGTGACTACATGAA
CATGACTCCCCGCCGCCCGGGCCACCCGCAAGCATTACCAGCCCTATGCCCCACCACGCGA
CTTCGCAGCCTATCGCTCCTGAGAATTCGAGCATCTTACCGCCATTTATTCCCATATTTGTTCTG
TTTTTCTTGATTTGGGTATACATTTAAATG

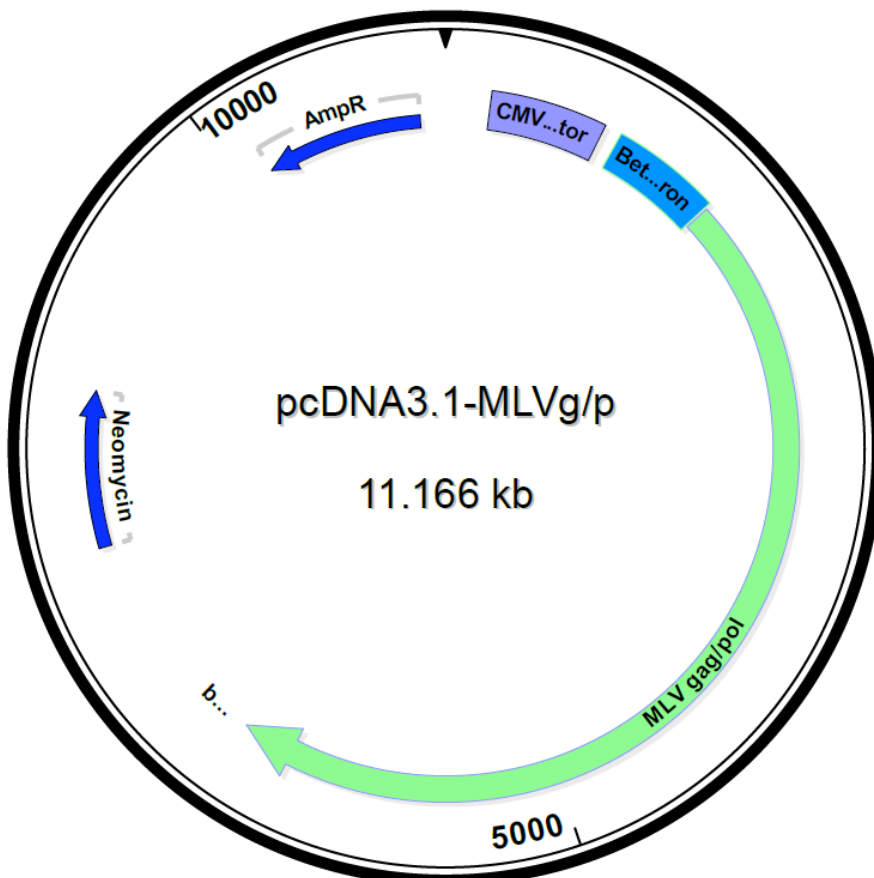
11.3 Vector maps

11.3.1 Vector map of pMP71



CAR constructs were inserted instead of GFP

11.3.2 Vector map of gag/pol (pcDNA3.1-MLV-g/p)



12 Appendix

12.1 Publications

Blaeschke F, Stenger D, Apfelbeck A, Cadilha BL, Benmebarek MR, Mahdawi J, **Ortner E**, Lepenies M, Habjan N, Rataj F, Willier S, Kaeuferle T, Majzner RG, Busch DH, Kobold S, Feuchtinger T. Augmenting anti-CD19 and anti-CD22 CAR T-cell function using PD-1-CD28 checkpoint fusion proteins. *Blood Cancer J.* 11, 108 (2021).

Blaeschke F, **Ortner E**, Stenger D, Mahdawi J, Apfelbeck A, Habjan N, Weißer T, Kaeuferle T, Willier S, Kobold S, Feuchtinger T. Design and Evaluation of TIM-3-CD28 Checkpoint Fusion Proteins to Improve Anti-CD19 CAR T-Cell Function. *Front. Immunol.* 13, (2022).